UNIVERSITÀ
DEGLI STUDI
DI PADOVA

Sede Amministrativa: Università degli Studi di Padova
Dipartimento di Scienze Biomediche

SCUOLA DI DOTTORATO DI RICERCA IN BIOMEDICINA
CICLO XXV

Role of TAZ in cancer stem cells and Wnt signaling

Direttore della Scuola: Ch.mo Prof. Giorgio Palù
Supervisore: Ch.mo Prof. Stefano Piccolo

Dottorando: Dr. Luca Azzolin

INDEX

ABSTRACT

(ENGLISH VERSION)

The transcriptional co-activator TAZ, known Hippo transducer together with his paralogue YAP, has recently emerged as important player in processes like organ growth and tumorigenesis. Here we focused on two aspects of TAZ biology: the first regards the role of TAZ as molecular determinant of breast cancer stem cells (CSCs); the second is the characterization of TAZ as downstream mediator of Wnt signaling.

In part 1, we show and discuss the discovery that more-malignant/CSC-enriched primary breast cancers, compared to well-differentiated/non-metastatic tumors, display an elevated activity of TAZ, and that this correlates with a poorer prognosis. TAZ protein levels and activity are elevated in prospective CSCs and they increase during tumor evolution toward malignancy, both in vitro and in poorly-differentiated primary breast tumors. Moreover, TAZ is required to sustain self-renewal and tumor-initiation capacities of breast cancer cells. These features make TAZ a determinat of several characteristic of breast CSCs and a attractive molecule for therapy (this work was published last year, Cordenonsi et al., Cell 2011).

In part 2, we show that independently of the Hippo pathway, TAZ is regulated and trascriptionally-activated by the Wnt cascade, sheding lights on the modalitites by which cells respond to the Wnt growth factors. We found that, in the absence of Wnt activity, the components of the β-catenin destruction complex - APC, Axin and GSK3 - are also required to keep TAZ at low levels because phosphorylated β-catenin bridges TAZ to its ubiquitin ligase complex. Upon Wnt signaling, escape of β-catenin from the destruction complex impairs TAZ degradation and leads to concomitant accumulation and activation of β-catenin and TAZ (this work was published this year, Azzolin and Zanconato et al., Cell 2012).

ABSTRACT

(ITALIAN VERSION)

Il co-attivatore trascrizionale TAZ, conosciuto per essere un trasduttore della via del segnale Hippo con il suo paralogo YAP, è recentemente emerso come importante fattore in processi quali la crescita degli organi e la tumorigenesi. In questo lavoro ci siamo focalizzati su due aspetti della biologia di TAZ: il primo riguarda il ruolo di TAZ come determinante molecolare delle cellule staminali del tumore al seno; il secondo, la caratterizzazione di TAZ come mediatore a valle della via del segnale Wnt.

Usando un approccio bioinformatico, abbiamo scoperto che i tumori alla mammella più maligni e arricchiti in cellule staminali tumorali mostrano una più elevata attività di TAZ quando comparati ai tumori più differenziati e non metastatici (Parte 1): questo correla inoltre con una prognosi più sfavorevole. I livelli proteici e l'attività di TAZ sono elevati nelle putative cellule staminali tumorali e aumentano durante la progressione dei tumori verso la malignità, sia in vitro che nei tumori primari. In più, TAZ è richiesto per sostenere il rinnovamento e la capacità di formare tumori in vivo da parte delle cellule tumorali mammarie. Queste proprietà rendono TAZ un determinante di parecchie caratteristiche di cellule staminali tumorali mammarie e una molecola interessante dal punto di vista terapeutico.

Abbiamo inoltre studiato i regolatori a monte di TAZ e abbiamo scoperto che, indipendentemente dalla via del segnale Hippo, TAZ è regolato dalla via del segnale Wnt (Parte 2), che ne promuove anche l'attivazione. Questo meccanismo chiarisce una delle modalità attraverso cui le cellule rispondono alle citochine della famiglia Wnt. Dal punto di vista meccanicistico, in assenza del segnale Wnt, i componente del complesso di distruzione di β-catenina - APC, Axin and GSK3 – sono richiesti per mantenere bassi i livelli di TAZ: questo è dovuto al fatto che β-catenina fosforilata fa da ponte tra TAZ e il suo complesso di ubiquitina ligasi. In seguito al segnale Wnt, β-catenina non è più fosforilata nel complesso di distruzione e ciò impedisce la degradazione di TAZ: di conseguenza vi è un contemporaneo accumulo sia di TAZ che di β-catenina.

PUBLICATIONS

Michelangelo Cordenonsi, Francesca Zanconato, Luca Azzolin, Mattia Forcato, Antonio Rosato, Chiara Frasson, Masafumi Inui, Marco Montagner, Anna R. Parenti, Alessandro Poletti, Maria Grazia Daidone, Sirio Dupont, Giuseppe Basso, Silvio Bicciato, and Stefano Piccolo (2011). **The Hippo transducer TAZ confers cancer stem cell-related traits on breast cancer cells.** Cell *147*, 759–772

Luca Azzolin, Francesca Zanconato, Silvia Bresolin, Mattia Forcato, Giuseppe Basso, Silvio Bicciato, Michelangelo Cordenonsi, and Stefano Piccolo (2012). **Role of TAZ as mediator of Wnt signaling.** Cell *151*,1443-1456

This work was realized under the mentorship of Prof. Michelangelo Cordenonsi and in close collaboration with Dr. Francesca Zanconato.

INTRODUCTION

Solid tumors resemble developing organs: they are a complex ensemble of different subtypes of tumor cells, at different degrees of differentiation, mixed with stromal cells and extracellular matrix (ECM); Moreover, solid tumors hijack cell signaling events normally regulating development, tissue repair, remodelling and regeneration (Egeblad et al., 2010). As such, thinking of tumors as complex organs might allow a more profound understanding of the events that governs tumor initiation, evolution toward malignancy and, eventually, metastasis.

Stem cells and cancer

The Cancer Stem Cell (CSC) model of tumor development and progression states that tumors, like normal adult tissues, are organized in cell hierarchy and contain a subset of cells that both self-renew and give rise to differentiated progeny (through symmetric and asymmetric division) (Visvader and Lindeman, 2008). As in other tissues, stem cells are a minority of the whole organ, and are the only cells that can virtually maintain tumor growth indefinitely. The remaining cells, though actively proliferating and making up the bulk of the tumor, are also differentiating and destined to die. The self-renewal properties of the CSCs are thus the real driving force behind tumor growth. Stem cells have become increasingly relevant to cancer research since 1994, when the existence of tumor-initiating cells was demonstrated for human acute myeloid leukaemia (Lapidot et al., 1994): in particular, this small subset of cancerous blood cells, identified on the basis of their phenotypical similaritites to normal hematopoietic stem cells, could propagate the disease in mice. Tumor-initiating cells have then been dubbed CSCs because of their pluripotency - meaning they are able to create all of the other cells in the tumor, much like blood stem cells behave in bone marrow. Even if it has been harder to test whether CSCs fuel the growth of tumors in other tissues, population of cells with stem-like properties have then been described also for breast (Al-Hajj et al., 2003), brain (Singh et al., 2004), prostate (Collins et al., 2005), colon (Ricci-Vitiani et al., 2007) and pancreatic (Li et al., 2007) cancers and others (reviewed in Visvader and Lindeman, 2008 and Baccelli and Trumpp, 2012). The

overall procedure for the isolation of CSCs was rather similar across these studies: fractionation of tumor cells using cell-surface markers characteristic of stem cells, followed by implantation into immunocompromized mice to assess xenograft growth. Very often, CD133 or CD44 cell surface marker were employed to purify CSCs in the previuos studies (Baccelli and Trumpp, 2012).

Located at the top of the tumor hierarch, CSCs divide to create a duplicate copy of themselves that remains undifferentiated (a process called self-renewal) or a daughter cell (called a multipotent progenitor) which subsequently differentiates into the various cells that make up the tumor. These tumor cells then replicate in an erratic and invasive manner. Despite the fact that are relatively rare, CSCs appear to be driving the disease (reviewed in Nguyen et al., 2012). Conventional chemotherapy or radiotherapy are directed against the bulk population of tumor cells, attempting to kill as many cancer cells as possible (Dean et al., 2005). Unfortunately, not only do these treatments often damage healthy tissues in the process, but they may be missing CSCs. Even if the tumor is eliminated, few CSCs that survive can recreate the original tumor over time - the best explanation we have for why relapse can occur after years of remission. CSC resistance might be caused by increased drug efflux capacities, mediated by expression of the multidrug resistance transporters (Dean et al., 2005), or by radiation-induced reactive oxygen species scavenging, as couterbalance mechanism to radiotherapy (Diehn et al., 2009). As such, a combined therapy that target also CSCs would be greatly desirable. It would be therefore auspicable to find the suitable "Achille's heel" of CSCs, particularly in the mechanisms (i.e., signaling pathways) that sustain CSCs themselves, in order to sensitize them to therapy.

Beside these properties, CSCs are operationally defined as cells having some peculiar characteristics. In vitro culture in unattached conditions where cells grow as round spheres is routinely used for enrichment and propagation of stem cells and number of spheres emerging from dissociated tumor samples is used as *bona fide* reflection of their CSC content (Dontu et al., 2003). Xenotransplantation assays have been used to prove cancer stemness: indeed, serial transplantation of CSC-enriched populations into animal models should re-establish the phenotypic heterogeneity evident in the primary tumors and exhibit self-renewing capabilities on serial passages.

However, the definition of CSCs remains largely operational and based on functional assays that register self-renewal in vitro and tumor initiation in vivo. More specifically, we lack molecular mechanisms responsible for the special attributes of CSCs.

Breast tumors

Tumor progression is a chain of cellular and molecular events that occur gradually during the development of neoplasia. During this process, tumors can undergo evolution to overcome organism defense and become more and more aggressive, but how this occurs is only partially understood. Breast cancer is the most common malignant disease in Western women. In these patients, the main cause of death is the metastasis spreading and not the primary tumors, that nowadays can be early diagnosed by mass screening. As a consequence, improving our understanding about the molecular mechanisms of the cells, i.e. CSCs, able to drive tumor formation and metastasis within breast cancers, might provide new prognostic markers or therapeutic targets and also improve clinical management of the disease.

A wide range of histopathological subtypes of breast tumors have been identified, as well as associated prognostic markers or features (Weigelt et al., 2005). Pathologists have classically distinguished three kinds of tumors: grade 1 (G1), grade (G2) and grade 3 (G3) tumors. G1 tumors form tubular structures, like normal mammary gland, and are low proliferating. At contrary, in histological preparations, G3 cancers have lost any sign of differentiation and display a large number of mitotic figures, indicating an active proliferation. Not surprisingly, G3 tumors are associated with malignancy and high risk of metastasis occurrence in breast cancer patients, while patients with G1 tumors have a better clinical outcome. Instead, G2 cancers display intermediate characteristics between G1 and G3.

Many studies have identified subpopulations (Al-Hajj et al., 2003; Sheridan et al., 2006; Grimshaw et al., 2008) of cells within breast tumors that are able to recreate the tumor tissue after injection in immunocompromised mice, and that have been classified as CSCs. In this framework, more recently, it has been shown that G3 breast tumors display a higher content of CSCs with respect to G1, and this could

account to their more aggressive phenotypes (Pece et al., 2010), demonstrating that heterogeneous phenotypical and molecular traits of human breast cancers is a direct reflection of their CSC content. However, how cells can acquire CSC properties is still a matter of debate.

The Hippo pathway

The Hippo pathway (Figure 1) is a tumor suppressor signaling cascade that has emerged as an important regulator of organ growth, tissue regeneration, embryonic development, and stem cell compartment in epitelia (Pan, 2010). It was first identified in *Drosophila melanogaster* (Figure 1A, left panel): indeed, from genetic screenings aimed at finding regulators of tissue growth (Harvey et al., 2003; Jia et al., 2003; Justice et al., 1995; Tapon et al., 2002; Udan et al., 2003; Wu et al., 2003; Xu et al., 1995), it was discovered that loss of the central kinases Hippo (Hpo) and Warts (Wts) results in overgrowth of the imaginal discs and of the corresponding adult organs. The pathway was named Hippo «because of the dark, folded and overgrown cuticle of the mutant [flies] heads» (Udan et al., 2003), that resembled an hippopotamus (Figure 1B). The mechanism of Hpo and Wts action in Drosophila has been then extensively studied (Figure 1A, left panel). When the pathway is active, Hpo in complex with its co-factor Salvador (Sav) phosphorylates Wts and its co-factor Mats (Mob-as-a-tumor-suppressor; Lai et al., 2005), promoting the activation of Wts kinase activity. Activated Wts/Mats complex phosphorylates the trascriptional co-activator Yorkie (Yki), favouring its retention in the cytoplasm by interaction with 14-3-3 proteins (Ren et al., 2010). Conversely, when the pathway is inactive, Yki can freely accumulate in the nucleus and induce the expression of target genes, that promote cell proliferation and survival (reviewed in Halder and Johnson, 2011 and Mauviel et al., 2011). Because Yki lacks an intrinsic DNA-binding activity, its target specificity is dictated by interaction with other factors, mainly Scalloped (Sd). Genetically, overexpression of Yki phenocopies loss of function mutations of Hpo or Wts, including tissue overgrowth in wing imaginal discs (Huang et al., 2005). Thus, Yki is a growth promoter, whereas Hpo, Sav, Wts and Mats act as tumor suppressors by limiting the growth-promoting activity of Yki.

The core Hippo signaling pathway is conserved also in mammals (Figure 1A,

right panel). Aided by the adaptor proteins SAV1/WW45 (Sav in *D. melanogaster*) and MOBKL1A/B (collectively known as MOB1; Mats in *D. melanogaster*), the MST1/2 (Hpo in *D. melanogaster*) kinases phosphorylate and activate the NDR family kinases LATS1/2 (Wts in *D. melanogaster*) (Chan et al., 2005), that in turn phosphorylate the mammalian orthologs of Yki, YAP (Yes-associated protein) (Dong et al, 2007; Zhao et al., 2008) and TAZ (transcriptional coactivator with PDZ-binding motif, also known as Wwtr1) (Lei et al., 2008). LATS1/2-mediated phosphorylation of YAP/TAZ on multiple residues (S61, S109, S127, S164, S381 for human YAP, and S66, S89, S117, S311 for human TAZ) inhibits YAP/TAZ activity through different mechanisms. Phosphorylated YAP on S127 or TAZ on S89 are retained in the cytoplasm by interaction with 14-3-3 proteins (Kanai et al., 2000; Basu et al., 2003). Moreover, phosphorylation of YAP on S381 or TAZ on S311 serves as priming event for successive phosphorylation by Casein Kinase (CK) 1 δ/ε and creation of a phosphodegron motif, that tags the proteins to E3 ubiquitin ligase $SCF^{\beta\text{-}TrCP}$ recognition and subsequent ubiquitin-mediated proteasomal degradation (Liu et al., 2010; Zhao et al., 2010).

When the Hippo cascade is inactive, YAP and TAZ are free to accumulate in the nucleus and activate gene-target transcription. However, because they lack any DNA-binding domain, YAP and TAZ function as transcriptional co-activators and they interact with a range of DNA-binding transcription factors, such as the TEAD/TEF family transcription factors (TEAD1/2/3/4), the p53-family member p73, the Runt family members Runx1 and Runx2, Pax3, Pax8, the thyroid transcription factor-1 (TTF1), TBX5, the peroxisome proliferator-activated receptor γ (PPARγ), and SMAD1/2/3/4 (reviewed in Pan, 2010 and Mauviel et al., 2011). Among these YAP/TAZ interacting transcription factors, TEAD1-4, which represent the orthologs of the *Drosphila* Sd protein, have emerged as the prime mediators of YAP/TAZ function (Zhao et al., 2008; Ota and Sasaki, 2008).

A large number of proteins have been implicated to act upstream of and regulate the Hippo pathway through MST/LATS-dependent mechanisms, both in Drosophila and in mammals (Figure 1A). These include: the FERM domain proteins Merlin (McCartney et al., 2000) and Expanded; the atypical cadherins Fat and Dachsous; the transmembrane polarity-regulator Crumbs (Robinson et al., 2010); the cell polarity factors Lethal giant larvae (Lgl), Discs large (Dlg), Scrib-

ble (Scrib); Jub (Ajuba LIM proteins in mammals); the Ras association family protein RASSF (reviewed in Zhao et al., 2011a). Other regulators have been identified only in mammals: the Crumbs complex-associated protein PALS1 (Varelas et al., 2010), Angiomotin (AMOT) (Zhao et al., 2011b), and the tight junction protein ZO-2 (Oka et al., 2010; Remue et al., 2010). In recent years, however, variations on the classical Hippo view have emerged, including LATS-independent phosphorylation of YAP/TAZ, MST-independent activation of LATS, and phosphorylation-independent modalities of YAP/TAZ controls. These include the regulation by: the adherent juction-associated protein α-catenin (Schlegelmilch et al., 2011; Silvis et al., 2011); KIBRA (Moleirinho et al. 2012) and mechanical cues (Dupont et al., 2011; Halder et al., 2012).

The physiological relevance of the Hippo pathway was supported by genetic studies in mice. In mouse liver, transgenic overexpression of YAP (Dong et al., 2007; Camargo et al., 2007) or liver-specific knockout of Mst1/2 or Sav1 (Zhou et al., 2009; Lee et al., 2010; see Figure 1C) promote organ enlargment, hyperplasia and tumor development. Further confimations come from experiments in mouse heart, where Sav1 (Figure 1D), Mst1/2 or Lats2 conditional depletion leads to heart enlargement or cardiomegaly throught a mechanism that was unlikely to be due to elevated cardiac progenitor number, but rather to an increase in the transcriptional cooperation between YAP and β-catenin to regulate common target gene (Heallen et al., 2011). Similar results are obtained for pancreas and intestine, where transgenic overexpression of YAP leads to a potent expansion of progenitor cells and loss of differentiation (Camargo et al., 2007). However, using a different driver for YAP induction, the same authors have more recently found that YAP suppresses intestinal renewal and overgrowth by inhibiting Wnt signaling pathway (Barry et al., 2012). This is also in contrast with the finding that intestine-specific knockout of Mst1/2 caused marked expansion of an undifferentiated stem cell compartment and loss of secretory cells throughout the small and large intestine in a YAP-dependent manner (Zhou et al., 2011).

The Hippo pathway in tumorigenesis

Consistent with the critical role of Hippo signaling in mammals, deregulation or mutation in the Hippo pathway components have been linked to cancer. Merlin is

a tumor-suppressor protein of the ERM family encoded by the NF2 gene that controls cell growth and contact-dependent inhibition of proliferation and that have been characterized as Hippo regulator (Zhang et al., 2010). Mutations in the NF2 gene are the underlying cause of neurofibromatosis type 2 (NF2), a familial cancer syndrome characterized by the development of sporadic tumors of the nervous system (Bourn et al., 1994). Although mutations in other Hippo pathway components are understudied or not common (Pan, 2010), it is evident the involvement of this pathway in tumorigenesis. Indeed, downregulation or inactivation of MST1/2, MOB1 or LATS1/2 (tumor suppressor components of the pathway) have been shown by many authors in different human cancers. As the most downstream effectors, it is not surprising that YAP and TAZ function as tumor promoters. YAP has been implicated as the candidade oncogene in human chromosome 11q22 amplicon, and indeed amplification of this locus has been identified in human hepatocellular carcinomas (Zender et al., 2006), in breast cancers (Overholtzer et al., 2006) and other cancers (reviewed in Pan, 2010 and Zhao et al., 2010). Moreover, comprehensive survey of the most common solid cancer types revealed widespread and frequent YAP and TAZ overexpression (Pan et al., 2010). Consistent with these findings, overexpression of YAP or TAZ can induce anchorage-independent growth and epithelial-to-mesenchymal transition of mammary cells (Overholtzer et al., 2006; Chan et al., 2008; Lei et al., 2008; Zhao et al., 2008).

YAP/TAZ and Stem Cells

Emerging studies indicate that YAP and TAZ might contribute to the regulation of stem cell and progenitor cell self-renewal and expansion, as well as embryonic development.

In the preimplantation mouse embryo, the inner more-compacted cells display an increased cytoplasmic TAZ/YAP localization, which allow the expression of *Oct4* and inner cell mass (ICM) specification. Conversely, in the less-compacted outer cells TAZ/YAP remain nuclear: this promote *Cdx2* expression, and thereby the trophoblast cell lineage (Nishioka et al., 2009). As proof of principle, disruption of LATS1/2 kinase activity in the ICM favors its conversion to trophoblast (Nishioka et al., 2009). The critical roles of YAP and TAZ are further highlight by the knockout mice. *Yap* deletion causes embryo lethality due to failu-

re in chorioallantoic fusion (Morin-Kenscki et al., 2006), with no significant abnormalities in preimplantation stages or trophoectoderm specification, a phenotype that can be ascribed to TAZ redundant function. Also TAZ knockout mice mainly die in utero in the post-implantation stage and develop polycystic kidney disease (Makita et al., 2008). However, whereas loss of either YAP or TAZ alone does not lead to abnormalities in preimplantation development (Morin-Kenscki et al., 2006; Hossain et al., 2007; Makita et al., 2008), *Yap*$^{-/-}$*Taz*$^{-/-}$ embryos die before the morula stage, prior to the establishment of inside and outside cell populations (Nishioka et al., 2009), confirming their fundamental role in development.

In human embryonic stem cells (ESCs) nuclear TAZ is required to maintain self-renewal markers (Varelas et al., 2008); likewise, YAP is necessary to sustain pluripotency in mouse ESCs (Lian et al., 2010; Qin et al., 2012) and important for reprogrammig of mouse fibroblasts to an induced pluripotent stem cell (IPS) state (Qin et al., 2012).

For instance, YAP expression is generally restricted to the progenitor cells in normal mouse intestine, and transgenic expression of YAP in mouse intestines causes a marked expansion of the progenitor cell compartment (Camargo et al., 2007). Similarly, YAP expression expands basal epidermal undifferentiated stem/progenitor cells in mouse skin (Schlegelmich et al., 2011); moreover it sustain in vitro colony forming capacity of these cells and their ability to seed tumor in grafting experiment (Schlegelmich et al., 2011). Conversely, conditional knockout of YAP in mouse skin leads to decreased proliferation of basal cells, thinner epidermis and failure of skin expansion (Schlegelmich et al., 2011).

In chick embryos, YAP (or TEAD) gain-of-function caused a marked expansion of the neural progenitor population, by increasing their proliferation and inhibiting their differentiation (Cao et al., 2008).

These observations reflect a role of TAZ/YAP in maintaining the balance between stem, progenitor and differentiated cells.

PART 1

Signaling pathways are central events by which cells respond to chemical or physical stimuli (Engeblad et al., 2010). As many of them are often subverted by cancers, we were interested in understanding what pathways were differentially regulated in G3 versus G1 breast tumors, in order to try to explain tumor progression and heterogeneity and the CSCs enrichment in G3 tumors (Pece et al., 2010). This would provide molecular explanation for CSCs origin and maintainance and possible targets for therapy.

RESULTS

TAZ is significantly upregulated in G3 tumors compared to G1

To gain inside the differences between G1 and G3 breast cancers, we decided to use a biostatistics approach in collaboration with the group of prof. Silvio Bicciato, University of Modena. We generated a compendium of data (metadataset) from 7 independent breast cancer gene expression-datasets that also contained information on histological grading and outcome (Table 1; see also Experimental Procedures). This cohort of data, relative to 993 primary tumors, was analyzed by the Significance Analysis of Microarrays (SAM) algorithm to identify a list of genes differentially expressed in G3 versus G1 tumors. Out of these, we found that 78 Affymetrix probesets were specifically up-regulated in G3 tumors compared to G1 (schematic representation of the experiment in Figure 2A; the list of up-regulated probesets in G3 cancers is provided in Table 2). We next tested the statistical association between this list of genes and lists of genes, named signatures, that highlight activation of specific signaling pathways, such as YAP/TAZ, Notch, Ras, STAT3, ErBB2, Wnt/β-catenin, TGF-β, in mammary cell lines (Figure 2A and B). This association was accessed by testing if the proportion of genes of a signature in the list of G3-over-expressed genes was significantly different from what would be expected by chance. Thus, a p-value smaller than 5% indicated a statistically significant enrichment of genes that are target of a specific signaling pathway in G3 tumors. Strikingly, only signatures for the activity of YAP and

TAZ emerged as significantly over-represented among the genes over-expressed in G3 samples (Figure 2B). In other words, G3 breast tumors express a large subset of YAP/TAZ target genes, suggesting the possibility that TAZ and/or YAP get activated more in G3 than in G1 tumors. As previously reported, G3 breast tumors are also characterized by a high expression of embryonic and normal mammary stem cell signatures (Ben-Porath et al., 2008; Pece et al., 2010) (Figures 2B and C), suggesting that TAZ/YAP activity correlates with stemness potential. All together, these findings indicate that tumors classified as poorly differentiated/high grade by histopathological criteria, and as enriched of stemness traits by molecular profiling, in fact display elevated YAP/TAZ activity.

To corroborate the link between YAP/TAZ activation and phenotypic manifestations of CSCs in primary tumors, we decided to examine tumor heterogeneity and metastasis. Indeed, it has been proposed that breast cancer heterogeneity may be explained, at least in part, by the proportion/content of CSCs within each tumor (Pece et al., 2010). In this respect, G2 tumors, whose characteristics in terms of gene-expression and clinical outcome can vary from being similar to G1 to closer to G3 (Ivshina et al., 2006), can be assumed as example of a heterogeneous category of breast cancers. We stratified G2-patients in two categories, with High or Low expression of the YAP/TAZ signature respectively, and tested if these two groups also displayed differential expression of stem cell signatures. Interestingly, G2 tumors stratified by high-YAP/TAZ activity were associated to an enrichment of stem cells' signatures, as proved for G3 cancers, whereas G2 tumors stratified by low-YAP/TAZ activity were more similar to G1 tumors, that is, with a low expression of stem cell signatures (Figure 2C). This at least suggests that YAP/TAZ activity reflects the degree of CSCs representation in G2 tumors.
Metastases are considered the most dramatic manifestation of tumor-initiating capacity of a primary tumor (Chaffer et al., 2011a), because only cells with stem-like capacities are thought to be able to migrate and colonize distant organs. We therefore tested if YAP/TAZ activity was associated to this type of event in our metadataset. By univariate Kaplan-Meier analyses, tumors with high expression of the YAP/TAZ signature displayed a significantly higher probability to develop metastasis and reduced survival than tumors marked by low YAP/TAZ activity (Figure 2D). Taken together, the data support the notion that activation of TAZ and/or YAP specifically parallels with tumor traits previously linked to their CSC

content, such as high histological grade, tumor heterogeneity and metastasis.

Malignant cells express more TAZ than their non-malignant counterparts

We verified the previous conclusions in a cellular context by using two isogenic derivates of the human mammary MCF10A cell line: Ras-transformed MCF10A-T1k cells (hereafter MII) and their malignant derivative, MCF10A-CA1a cells (also known as MIV), derived from in vivo spontaneous evolution of MII cells (Santner et al., 2001) (Figure 3A). To validate MII and MIV cells as model of increased CSC content during malignant evolution of breast cancer (Pece et al., 2010), we compared their self-renewal potential, as assayed by their capacity to form and propagate mammospheres in vitro and to give rise to tumors in vivo when transplanted in the mouse fat pad (Dontu et al., 2003; Visvader and Lindeman, 2008). In the mammosphere assay, we can measure the stem-like properties of cells by evaluating their growth capability in non-adherent non-differentiating culture conditions: indeed, under these conditions, only cells with stem-like properties can initiate the formation of floating spherical colonies, called mammospheres, in which the mammosphere-initiating cells can undergo self-renewal, thus producing other mammosphere-initiating cells, and give rise to differentiated progeny, which instead constitute the bulk of the mammospheres (Dontu et al., 2003). Once cultured in suspension, MIV cells formed more primary and 6-times more secondary mammospheres than MII cells (Figure 3B). The sphere-forming capacity in subsequent serial passages remained stable for MIV cells but declined for MII cells (Figure 3B*)*. Orthotopic transplantations were used to evaluate tumor initiation: in this type of assay, we can assume that only cells endowed with stem-like properties can seed tumors. When injected orthotopically in the fat pad of immunocompromised mice, MII cells are tumorigenic, but non-malignant, and form tumors with "G1-like" characteristics, while MIV cells are metastatic and show properties analogous to G3 cancers (Figure 3C). In order to measure tumorigenicity, we therefore decided to inject orthotopically 10^4 and 10^6 MII or MIV cells. While both concentrations of MIV cells readily formed tumors in all injected mice, MII-derived tumors were detected only in one-third of mice injected with 10^6 cells but not at the lower cell concentration (Figure 3D). Thus, MII and

MIV cells are endowed with significantly different self-renewal and tumorigenic potential, recapitulating the differences in CSC representation previously described also between G1 and G3 tumors. Injection in the mouse mammary fat pad of control and engineered cells was carried out in collaboration with prof. Antonio Rosato; histological examinations were carried out in collaboration with prof. Anna Parenti.

We next asked wheter this difference between MII and MIV could be ascribed to differential expression of TAZ and/or YAP and by western blot analysis we found that TAZ protein levels are higher in MIV cells compared to MII (Figure 3E), with no significant changes in YAP levels. As comparison, we also examined MDA-MB-231 cells, which are human metastatic breast cancer cells, commonly used in breast cancer research (Adorno et al., 2009): this cell line diplayed TAZ levels comparable to those of MIV (Figure 3E), suggesting that an increase in TAZ protein might be characteristic of more malignant cells.

To directly address the role of TAZ as stemness determinant in our model of breast cancer, we knocked down endogenous TAZ by shRNAs in MIV cells. TAZ knockdown downregulated the expression of CTGF, a known TAZ/YAP target gene (Pan, 2010) (Figure 3F), but had no overt effects on cell viability and proliferation in 2D cultures (data not shown). Remarkably, however, MIV-shTAZ formed significantly less primary and secondary mammospheres than control MIV cells (MIV-shControl) (Figure 3G). To exclude possible off-target effects of our RNA interference approach, we co-infected MIV-shTAZ with a shRNA-insensitive mouse TAZ construct, or EGFP as a control: in this experiments, only re-expression of TAZ rescued TAZ-dependent gene responses and mammosphere-forming abilitites (Figure 3H and I).

To assay if TAZ regulates tumor-initiating potential of MIV cells, we compared MIV-shControl and MIV-shTAZ cells for their capacity to seed tumors at limiting dilutions. While shControl cells are able to form tumors in the majority of injected mice, even upon injection of only 20 cells, TAZ depleted cells showed a dramatic decrease of tumor seeding ability, as up to 10^4 cells were required to induce tumors in 100% of the animals (Figure J). Taken together, these in vitro and in vivo results indicate that TAZ is required for self-renewal and tumor initiation of highly-malignant MIV breast cancer cells.

TAZ confers self-renewal capacities to breast cancer cells

A peculiar property of CSCs is the expression of specific cell surface markers that allow their selective isolation by fluorescence-activated cell sorting (FACS). In human, $CD24^{low/-}CD44^{high}$ has been suggested to define a population of cells that contain breast CSCs (Al-Hajj et al, 2003; Sheridan et al., 2006; Grimshaw et al., 2008). Therefore, we decided to examine if these surface markers could identify a CSC population in our cell lines and if manipulating TAZ level we could modify this compartment. First, we analyzed parental MII: we identified and sorted out two different subpopulations, which we called $CD44^{low}$ and $CD44^{high}$, on the basis of CD44 staining, while CD24 staining was uniformly low or negative (Figure 4A). The majority (~65%) of the cells was $CD44^{low}$ (Figure 4A), expressed low level of TAZ and of TAZ-target CTGF (Figure 4B), and after 2-week *in vitro*-culture give rise to the same $CD44^{low}$ cell population (Figure 4A). On the other hand, approximately 30% of the original population was $CD44^{high}$ (Figure 4A), displayed a higher level of TAZ protein and, as a consequence, of CTGF (Figure 4B), and after 15 days of in vitro culture could recapitulate the entire MII population (Figure 4A), indicating that the $CD44^{high}$ cells possess both self-renewal and differentiative capacities. Moreover, the $CD44^{high}$ population included the so-called ‘‘side population (SP)’’ (Figure 4C), which is defined by its ability to exclude the Hoechst vital dye (Dontu et al., 2003). We further confirmed this observation by culturing the two cell population in mammosphere-forming conditions and saw that the $CD44^{high}$-sorted population could give rise to more mammospheres than the $CD24^{low}$ counterpart (Figure 4D). In summary, we identified in MII cells a subpopulation of cells with CSC-like properties that display a higher level and activity of TAZ.

To establish whether TAZ is functionally relevant for the biological traits of the $CD44^{high}CD24^{low}$ population, we knocked down endogenous TAZ in MII cells using three independent shRNAs (Figure 4E). TAZ is required for the maintenance of the $CD44^{high}CD24^{low}$ antigen phenotype (Figure 4F) and for primary and secondary mammosphere formation in MII cells (Figure 4G).

To examine the functional consequences of TAZ overexpression in breast cancer cells, we genetically increased TAZ level in MII cells. We overexpressed a consti-

tutive active TAZ mutant in MII cells, TAZ S89A. This is a LATS phosphomutant, that impairs TAZ interaction with 14-3-3 protein and therefore TAZ retention in the cytoplasm (Kanai et al., 2000). Cells overexpressing TAZ, compared to controls (empty vector), developed a spindle-shaped morphology characteristic of cell transformation and EMT, as reported by others in different mammary cell lines (Chan et al., 2008). Enhancing TAZ caused the activation of TAZ target genes, such as CTGF, Survivin, PAI1 (Figure 5A), loss of E-cadherin expression (Figure 5A), but no differences in cell proliferation (data not shown). Compared to controls, TAZ-overexpressing MII cells were able to form more generations of mammospheres, indicating that they comprise a higher amount of cells with self-renewal capability, i.e. stem cells (Figure 5B). Moreover, we found that the TAZ overexpression caused the conversion of all MII cells into cells with a unique $CD44^{high}$-profile population (Figure 5C), i.e. CSCs. Interestingly, also MDA-MB-231, metastatic cells and therefore highly enriched in CSCs, shared the same $CD44^{high}$ profile (Figure 5C). In conclusion, we believed that TAZ can promote a CSCs phenotype.

Next we wanted to show whether TAZ is per se sufficient to endow CSC-like properties to non-CSCs (i.e. $CD44^{low}CD24^{low}$ cell population). To do this, we first transduced MII with lentiviral vectors encoding for a doxycycline-inducible TAZ(S89A), or EGFP as control. From the transduced MII cells, $CD44^{low}CD24^{low}$ (non-stem) and $CD44^{high}CD24^{low}$ populations were FACS-sorted, cultured in the presence or absence of doxycycline and assayed for mammosphere formation (Figure 5D). As control, induction of EGFP did not modify the mammosphere-forming capacitites of neither $CD44^{low}CD24^{low}$ (Figure 5E, compare lanes 1 and 3) nor $CD44^{high}CD24^{low}$ (compare lanes 2 and 4) subpopulations. Remarkably, induction of TAZ(S89A) in non-stem $CD44^{low}CD24^{low}$ population promoted abundant secondary mammosphere formation (Figure 5E, compare lane 5 and 7). Moreover, TAZ(S89A) activation induced more self-renewal properties also to the putative stem $CD44^{high}CD24^{low}$ population (Figure 5E, compare lanes 6 and 8). These findings suggest that TAZ activity can confer attributes of self-renewal to the more differentiated progeny of prospective CSC populations.

TAZ confers resistance to chemotherapy to breast cancer cells

Another peculiar characteristic of CSCs is their capacity to resist to chemotherapy and, as a consequence, to give rise to recurrence. We noticed that TAZ overexpression in MII cells correlated with an increased in the activity of the multidrug resistance pumps, responsible for the drug elimination from the cell's cytoplasm, as measured by an increase of the SP by FACS (Figure 6A and B), i.e. the population with "Low" Hoestch accumulation due to efficient extrusion. Accordingly, TAZ-expressing cells were more resistant than control cells to Paclitaxel (Figure 6C) and Doxorubicin (Figure 6D), two widely used chemotherapeutic drugs. This is in line with the recently reported dependency of MDA-MB-231 cells on TAZ for Taxol resistance (Lai et al., 2011).

TAZ Promotes High-Grade Breast Cancers

As we show that TAZ protein level correlates with self-renewal and tumorigenic potential in our MII-MIV cellular model and molecularly determines characteristic of CSCs, we used immunohistochemistry to compare TAZ expression in 26 G1 primary breast tumors and 44 G3 invasive ductal carcinomas. In G1 tumors, TAZ expression was typically hardly detectable and only few cells appeared positive (Figures 7A and B). In contrast, the vast majority of G3 tumors (80%) contained a substantial fraction of cells displaying an intense TAZ nuclear staining (Figures 7A and C). Thus, G3 breast cancers are enriched with TAZ-positive cells, a finding that links the increased CSC content of high-grade tumors (Pece et al., 2010) with the present functional characterization of TAZ as a promoter of CSC-like traits.

Moreover, as functional validation of the previous *in vivo* finding, gain-of-TAZ in MII cells not only increased the tumor initiation capacities of our cells when transplanted orthototically in the mouse fat pad (Figure 7 D), but also favoured the formation of more malignant, G3-like tumors (Figure 7E and F). Indeed, while control MII cells formed small tubular carcinomas displaying no nuclear atypia and resembling human G1 tumors (Figure 7E), MII-TAZ(S89A) cells formed invasive less-differentiatied carcinomas that phenocopy several traits of human G3 breast cancers, such as lack of tubular structures, high nuclear pleomorphism, and prominent nucleoli (Figure 7F). Thus, gain of TAZ in MII promotes self-renewal,

tumorigenic potential and the acquisition of more malignant phenotype, all hallmark of CSCs.

DISCUSSION

One of the most important features of neoplasia is the ability to evolve, so that tumors progressively loose the histological characters of the tissues from which they arise and acquire an architecture that resembles less differentiated states of normal tissues (Egeblad et al., 2010). The knowledge of the differentiation status of a tumor plays an important role for deciding the appropriate treatment for a cancer patient: low-differentiated cancer cells frequently develop malignant abilities such as invasive behaviours, resistance to chemotherapy and metastatic proclivity. Indeed, pathologists categorize tumors by criteria that include the morphology of cancer cells and the organization of the neoplastic tissue. A point in case is represented by breast cancer: breast tumors are classified by a composite score, the grade, that integrates assessments of cell de-differentiation and replicative potential. Low-grade breast tumors (G1) are in general benign, while high grade breast cancers (G3) are prone to recur in the primary tumor site after surgery or chemotherapeutic treatment, and to metastatize to distant organs (Elston, 1991). Despite the importance of histological grading for the prognosis of breast cancers, the cellular and molecular basis for the differences between G1 and G3 tumors is poorly understood.

Here we found that TAZ recapitulates some salient traits that have been previously associated with CSCs. The molecular signature of TAZ and its protein level are tightly linked with progression from well-differentiated to high-grade tumors (Figure 8), during which the CSCs content has been shown to dramatically increase (Pece et al., 2010). Indeed, low grade G1 tumors display a low number of TAZ-positive cells that greatly increase in G3 cancers, and in this respect TAZ can be treated as prognostic marker. Moreover, TAZ activity, which we have shown to be associated to molecular signatures of stemness, is a clinical relevant tool to predict the proclivity to develop metastasis, that is another hallmark of CSC activity. In the most heterogeneous breast tumors, the ones catalogued as G2, TAZ activity can distinguish G2 tumors more similar to G1 and those that resem-

ble G3 cancers, in order to prognostically classify also this intermediate class of diseases.

Characterization of CSC purified from in vitro cell cultures have also demostrated an upregulation of the TAZ protein with respect to non-CSCs, that in any case are genetically identical.

At the functional level, by loss of function we demonstrated that TAZ is required for self-renewal and for tumor-initiation properties of breast cancer cells of MIV cells and also for the maintanance of the $CD44^{high}$ subpopulation in MII cells. Raising TAZ level and activity is sufficient for converting otherwise benign experimental tumors into a more aggressive G3-like histopatological phenotype. Thus, TAZ expression and activity embody characteristics that have been classicaly linked to CSCs in breast tumors, that is, tumor heterogeneity, reduced differentiation, self-renewal potential, immonological phenotype, and tumor-seeding abilities. Moreover, a similar function of TAZ have also emerged in malignant gliomas (Bhat et al., 2011).

An unsettled issue in the cancer stem cell field is whether the potential of self-renewal is an exclusive property of CSCs, or whether plasticity exists in these hierarchical lineages, such that any cell, even a non-CSC, could acquire self-renewal potential under appropriate intrinsic or extrinsic cues (Chaffer et al., 2011b; Gupta et al., 2009). Interestingly, this type of plasticity has been recently demonstrated in mammary epithelial cells, where, in a seemingly stochastic manner, non-CSCs and even non-transformed cells, could be spontaneously reverted to a stem-like state without genetic manipulations (Chaffer et al., 2011). Here we showed a similar type of transition but in a molecularly controlled manner, as conditional activation of TAZ in putative non-CSCs could reactivate their self-renewal potential. Thus, in breast cancer, TAZ levels appear to regulate phenotypic plasticity in both the prospetictive stem and non-stem compartments.

Control of proliferation and self-renewal are clearly related events in CSC biology and YAP and TAZ have been previously described both as oncogenes and tumor suppressors (Pan, 2010). It is worth noting, however, that the link between TAZ and CSC traits appears to be independent of regulation of proliferative capacity, as TAZ levels do not significantly impact on proliferation of 2D cultures or mammospheres growth. That said, proliferation may require a threshold of TAZ (or of combined YAP/TAZ) lower than that one required for self-renewal.

A mechanism that links cell polarity and TAZ in breast cancer cells

We also investigated the mechanism that induce TAZ stabilization in CSCs. This is extensively treated in the PhD thesis of Dr. Francesca Zanconato.

Epithelial-to-Mesenchymal Transition (EMT) (Thiery et al., 2009) has been shown to endow stem-cell properties (Mani et al., 2008) and we demonstrated that EMT induces TAZ, and that TAZ is required for EMT-induced self-renewal. As EMT entails loss of cell polarity, we found that a critical event for TAZ activation is deregulation of the cell polarity determinant Scribble. Scribble is also frequently disabled during mammary tumorigenesis (Zhan et al., 2008); it also serves as tumor suppressor in Drosophila (Humbert et al., 2008) and participates in Hippo signaling (Skouloudaki et al., 2009). Biochemically, TAZ and Scribble form a complex at endogenous protein levels in nontransformed and tumoral mammary epithelial cells. Remarkably, loss-of-Scribble - or EMT - disrupts the association of TAZ with the core Hippo kinases and prevent inhibitory phosphorylation and association of TAZ to β-TrCP.

PART 2

Wnt signaling pathway has prominent and widespread roles in development, tissue homeostasis and cancer (Moon et al., 2004; Clevers, 2006; MacDonald et al., 2009). For example, Wnts coordinate proliferation and differentiation during organ growth, and serve as extrinsic factors to regulate stem cells for tissue maintenance and regeneration (Clevers, 2006; Niehrs and Acebron, 2012). A key step in this pathway is the regulation of cytosolic β-catenin levels (MacDonald et al., 2009) by a dedicated "destruction" complex. This complex consists of core components: the scaffold proteins Axin and adenomatous polyposis coli (APC) and the glycogen synthase kinase-3 (GSK3). Mutations in components of the β-catenin destruction complex (mainly APC) result in cancer, most notably of the colon (Clevers, 2006).

In cells not experiencing Wnt signaling (Figure 14A, left panel), the pool of cytosolic free β-catenin is efficiently captured by the destruction complex and phosphorylated by CK1 at S45, which in turn primes GSK3 phosphorylation of β-catenin on the N-terminal T41, S37 and S33 residues (Liu et al., 2002). This phosphomotif, called phosphodegron, is recognized by the F-box-containing protein β-TrCP ubiquitin E3 ligase and targeted to ubiquitination and proteasomal degradation (Aberle et al., 1997; Kitagawa et al., 1999).

Wnt ligands are a large family of secreted glycoproteins. They bind the frizzled (FZD) and low-density-lipoprotein-related protein 5/6 (LRP5/6) coreceptor complex to activate the canonical Wnt signaling pathway. Through an incompletely resolved mechanism, the activated receptor complex disrupts or functionally inactivates the destruction complex, leading to the accumulation and nuclear translocation of β-catenin (Figure 14A, right panel). Several models have been proposed to follow Wnt receptor activation and as a consequence to cause β-catenin stabilization (reviewed in Li et al., 2012). These include: sequestration of Axin by LRP receptors, degradation of Axin, inactivation/desruption of the destruction complex by Dishevelled, inhibition of GSK3 kinase activity, dephosphorylation of β-catenin, sequestration of GSK3 into multivescicular bodies (Taelman et al., 2010), dissociation of β-TrCP from β-catenin (Li et al., 2012). In the nucleus, β-catenin

engages mainly T-cell factor (TCF)/LEF transcription factors to activate the Wnt transcriptional program. In order to monitor Wnt pathway activation, several laboratories have built reporter constructs containing multimerized TCF binding sites (reviewd in Barolo, 2006), to be used both in cell and in vivo. However, these reporters should be used with careful attention, as they often give different responses and, more importantly, they do not respond to other modalities by which Wnt activate gene transcription (Barolo, 2006).

Independently of Wnt signaling, the transcriptional co-activators TAZ and YAP have recently emerged at the centerpiece of poorly-understood mechanisms that control tissue growth and organ size (Pan, 2010). TAZ and YAP promote cell proliferation and inhibit differentiation, particularly in stem cells and organ-specific progenitors, and therefore their activity must be finely tuned in order to avoid loss of tissue regeneration and, at the other extreme, overgrowth and emergence of tumors (Ramos and Camargo, 2012).

Interestingly, there are - at least superficially - clear elements of overlap between β-catenin and TAZ or YAP: biochemically, all are short lived proteins in the cytoplasm, as they are degraded by the same β-TrCP ubiquitin ligase complex (Liu et al., 2010; MacDonald et al., 2009; Zhao et al., 2010); biologically, they appear to control overlapping processes in a number of epithelial and non-epithelial contexts. Although this hints at some form of joined regulation, the possibility that Wnt could signal through TAZ or YAP stabilization has not been explored.

RESULTS

TAZ is activated by Wnt signaling

We initiated this study by discovering that treatment of HEK293 cells with Wnt3A triggered a remarkable increase of TAZ protein levels (Figure 9A), without affecting TAZ transcript levels (Figure 9B). This suggested that Wnt3A promoted TAZ protein stabilization. As control, Wnt3A activated also β-catenin and β-catenin-dependent transcription (Figure 9C). Importantly, Wnt3A triggered a robust induction of transfected 8xGTIIC-Lux (Figure 9A, compare lanes 1 and 2), a synthetic luciferase sensor containing multimerized responsive elements of TE-

AD, the main DNA-binding cofactor of TAZ (Dupont et al., 2011). This induction was dependent on specific stabilization of TAZ, as revealed by depletion of endogenous TAZ by siRNA (Figure 9A, lane 4),. However, this was not dependent on β-catenin or β-catenin target genes, as β-catenin loss after Wnt3A treatment does not modify TAZ induction (Figure 9D). Taken together, these data suggested that Wnt signaling stabilizes and activates TAZ.

We next asked whether Wnt regulated TAZ through the canonical GSK3-APC-Axin intracellular pathway that controls β-catenin (MacDonald et al., 2009). We therefore reactivated the β-catenin destruction complex in Wnt-treated cells by using XAV939: this small molecule promotes Axin stabilization by inhibiting the poly-ADP-ribosylating enzymes tankyrase 1 and tankyrase 2 that otherwise would triggered Axin to degradation (Huang et al., 2009). As reported for β-catenin, XAV939 inhibited the effects of Wnt3A on TAZ transcriptional activity and stability (Figure 9A, lane 3). Conversely, inactivation of Axin, GSK3 or APC by transfections of corresponding siRNAs induced TAZ stabilization and activity (Figure 9E), phenocopying Wnt stimulation. As a control, these treatments promoted also β-catenin dependent-transcription (Figure 9F). Thus, Wnt signaling regulates TAZ in a way that depends on β-catenin multi-subunit destruction complex.

We also tested the possibility that Wnt might activate TAZ by inhibiting the Hippo kinase cascade. Indeed, according to the classical "Hippo" view, TAZ should get phosphorylated and inactivated by its upstream kinase, LATS1/2. As shown in Figure 9G, treatment with Wnt3A ligand could still induce TAZ in LATS1/2 depleted cells, indicating that LATS activity is not crucial for TAZ regulation by Wnt. We also expressed in HEK239 cells a phosphomutant TAZ protein lacking all LATS phosphorylation sites (TAZ 4SA, in which Serines 66, 89, 117 and 306 have been mutated to Alanines): TAZ 4SA is, as expected, more stable than wild-type TAZ; yet, it remains sensitive to Wnt regulation (Figure 9H), thus concluding that Wnt pathway activates TAZ independently of the Hippo cascade.

To extend our findings to *in vivo* conditions, we obtained Ah-Cre; $Apc^{fl/fl}$ mice in which the induction of the Cre recombinase can be achieved in liver, gut and other

organs by intraperitoneal injection of the drug β-naphtophlavone (Sansom et al., 2004). In this context, we verified that in livers of conditional *Apc* knock-out mice TAZ protein level and activity were increased with respect to control mice, as measured by the induction of two well-established TAZ targets Cyr61 and CTGF (Figures 9I-K). As control, Apc deletion upregulates also β-catenin target Cyclin-D1 (Figure 9L).

Role of GSK3 in TAZ degradation

Next, we sought to determine by which mechanism Wnt signaling promotes TAZ stability and activity. We tested the hypothesis that TAZ might follow the same steps of β-catenin on its route to degradation in the context of the Wnt cascade. Indeed, there are element of overlap between the biochemical regulation of TAZ and β-catenin. As reported, β-TrCP is important, in the Wnt OFF status, for the degradation of both β-catenin and TAZ. This was further confirmed by the fact that β-TrCP inactivation, either by siRNA transfection or interference with a dominant negative form of Cullin1 (an essential adaptor of the β-TrCP E3 ubiquitin ligase complex), stabilized TAZ protein level in both MII (Figure 10A) and HEK293 (Figure 10B) cells.

In the canonical Wnt-OFF view, the recognition and successive degradation of β-catenin by β-TrCP (Aberle et al., 1997; Kitagawa et al., 1999) occurs upon phosphorylation by GSK3 (MacDonald et al., 2009; see Figure 14). We therefore tested the possibility that GSK3 phosphorylation and β-TrCP recognition might also drive TAZ degradation. First, endogenous β-TrCP failed to associate to TAZ in co-immunoprecipitation assays from lysates of GSK3-depleted MII cells (Figure 10C), indicating that TAZ/β-TrCP interaction requires GSK3 or a GSK3-mediated modification. Moreover, in reconstitution experiments, we found that GSK3 kinase activity was essential for TAZ degradation: indeed, knockdown of GSK3 stabilized TAZ in MII cells (Figure 10D, lanes 1 vs. 2 and 4 vs. 5) and reconstitution with wild-type GSK3 (Figure 10D, lane 3), but not with kinase-dead GSK3 (Figure 10D, lane 6), rescued TAZ levels and activity. This was also confirmed in HEK293 cells (Figure 10E).

TAZ has consensus sites (Serines 58 and 62) for GSK3 phoshporylation on a DSGXXS motif, called "phosphodegron" (Figure 10F), that tags a given protein for β-TrCP recognition, ubiquitination and proteosomal degradation, as in the case of other Wnt-regulated proteins, β-catenin being the prototypical example (Kim et al., 2009; Taelman et al., 2010). This raised the simple possibility that, in analogy to β-catenin, GSK3 might promote TAZ degradation by phosphorylating these two sites in the context of the Wnt cascade. Thus, if GSK3 directly phosphorylates TAZ, mutation of these two putative GSK3-target sites from Serine to Alanine should render TAZ resistant to GSK3-mediated degradation and insensitive to Wnt stimulation. However, in stark contrast with this prediction, the stability of TAZ S58/62A was still sensitive to GSK3 inhibition (Figure 10G) and the activity of TAZ S58/62A could still be induced by Wnt3A (Figure 10H). We then conclude that GSK3 keeps TAZ levels low irrespectively of the integrity of these N-terminal TAZ motif.

Role of β-catenin in TAZ degradation

As a mechanism entailing direct GSK3 phosphorylation of TAZ was unlikely, we considered that the effect of GSK3 on TAZ stability was primarily indirect, that is, through modification of an intermediary protein. According to our hypothesis, this intermediary protein has to: i) interact with TAZ; ii) be phosphorylated by GSK3 and, as such, serve as adaptor for β-TrCP-mediated TAZ degradation; iii) activate TAZ when absent. In the context of Wnt signaling, we demonstrated that the most likely culprit protein was β-catenin itself, which was proved to fulfill all the previous requirements (Figure 11). Indeed, by co-immunoprecipitation experiments, β-catenin and TAZ form a complex at endogenous protein levels (Figures 11A and B). Furthermore, depletion of β-catenin by siRNA revealed that β-catenin was required for the endogenous association of TAZ to β-TrCP in MII cells (Figure 11C). In this scenario, by impairing TAZ/β-TrCP interation, the absence of β-catenin should stabilize/activate TAZ. This was confirmed by knockdown experiments of β-catenin that caused a robust stabilization of TAZ protein, induction of TAZ transcriptional activity and TAZ nuclear accumulation (Figures 11D-F). We excluded the possibility that loss of β-catenin was affecting TAZ by

regulating events related to the Hippo pathway (Cordenonsi et al., 2011), because it does not modify the apico-basal polarity (Scribble localization, Figure 11F), the cadherin adherens junctions (Figure 11F), or the levels of active LATS (Figure 11G).

All these experiments bring us to elucidate an interesting scenario for TAZ regulation in the Wnt-OFF world: that is, GSK3 prompts TAZ degradation by modifying/phosphorylating β-catenin and, as consequence, GSK3-modified β-catenin brings TAZ to β-TrCP-mediated degradation. So, is it the GSK3-phosphorylated pool of β-catenin the ultimate mediator of TAZ degradation? For this, we analyzed TAZ stability and CTGF induction in two MII cell lines, depleted of endogenous β-catenin and reconstituted at near-to-endogenous levels with either wild-type β-catenin or a S/A phospho-mutant β-catenin (Figure 11H). This β-catenin mutant harbors N-terminal point-mutations that prevent GSK3 phosphorylation and β-TrCP recognition (Liu et al., 2002). As above, knockdown of β-catenin promoted TAZ stabilization in both MII derivatives (Figure 11H, lanes 1 and 2, and lanes 4 and 5); adding back wild-type β-catenin rescued TAZ degradation (Figure 11H, lane 3). However, reconstitution with S/A phospho-mutant β-catenin had no effect (Figure 11H, lane 6), indicating that TAZ degradation relies on β-catenin phosphorylation by GSK3. In these experiments, changes in TAZ protein levels were consistently paralleled by changes in its activity, as indicated by the expression of its target CTGF (Figure 11H).

Further support to this view was provided by experiments in HepG2 hepatocarcinoma cells. These cells carry two different *β-catenin* alleles: one encoding wild-type β-catenin and the other encoding a constitutively active β-catenin bearing a natural deletion in the N-terminus encompassing the GSK3 phosphorylation sites (Figure 11I). We used a siRNA oligonucleotide (#4) that specifically binds within the deletion and, as such, only targets the wild-type and not the mutated allele. By using this siRNA, we found that the sole wild-type β-catenin, able to be phosphorylted by GSK3, is responsible for TAZ degradation (Figure 11J, compare lanes 1 and 5) as depletion of both isoforms does not further increase TAZ stability (Figure 11J, compare lanes 1, 3 and 5).

Mapping the interaction between TAZ and β-catenin

Since we have established a new role for β-catenin in the Wnt-OFF world, as adaptor for bridging TAZ to the β-TrCP complex, we wanted to map the TAZ domain(s) that is necessary for β-catenin binding and next verified that a TAZ mutant that cannot interact with β-catenin should not bind β-TrCP. For this, we obtained GST-TAZ deletion constructs (Figure 12A), that we expressed in bacteria as recombinant proteins, and *in vitro*-translated ^{35}S-radiolabeled β-catenin. Next, by GST-pulldown, we identified the "WW" domain of TAZ as necessary for the association to *in vitro*-translated β-catenin (Figure 12B). Once expressed in human cells not experiencing Wnt signaling, TAZ deleted of the WW domain (TAZ ΔWW) was more stable and basally more active than wild-type TAZ (Figures 12C and E). Importantly, TAZ ΔWW was incapable to associate to endogenous β-catenin and β-TrCP (Figure 12D). As such, TAZ ΔWW could not be further stabilized nor activated by Wnt stimulation in HEK293 cells (Figure 12E). Critically, the behavior of TAZ ΔWW could not be ascribed to an escape from the Hippo pathway, as TAZ ΔWW is still phosphorylated on the leading LATS target S306 (Figure 12F) and can be further stabilized by LATS1/2 depletion (Figure 12G). This corroborates the independence of the two regulation of TAZ: one by Wnt/β-catenin, and the other by the Hippo pathway.

γ-catenin participates to TAZ regulation

γ-catenin is a homologue of β-catenin, and the two proteins are thought to operate in an overlapping manner in several contexts: they have redundant functions in cell adhesion and share Wnt-dependent regulation through phosphorylation by GSK3 and β-TrCP-mediated degradation (Xu et al., 2009). Importantly, TAZ associates with γ-catenin at endogenous protein levels (Figure A), and, similarly to β-catenin, this interaction is dependent on the integrity of the TAZ WW domain (Figure 13B). This prompted us to test if γ-catenin also shares with β-catenin the capacity to regulate TAZ. To examine this, we monitored TAZ activity in HEK293 cells transfected with siRNAs against β-catenin, γ-catenin or both. Depletion of γ-catenin led to TAZ stabilization (Figure 13C) and TAZ-dependent transcriptional activity (Figures 13D and E). Interestingly, concomitant depletion

of both β- and γ-catenin resulted in even stronger transcriptional activation (Figure 13D and E). This indicates that these factors play independent and additive roles in TAZ inhibition.

DISCUSSION

Inhibition of the β-catenin destruction complex is central to Wnt signaling; this results in β-catenin stabilization, the last biochemical event of the Wnt cascade. Here we reveal the existence of a new downstream function of β-catenin, in regulating the stability of another potent transcriptional co-activator, TAZ (Figure 14).

TAZ as a downstream mediator of Wnt signaling

The results shed new light on the modalities by which the Wnt pathway controls gene expression, not only through the β-catenin/TCF complex, but also through TAZ, which came out as general feature of the Wnt response in a variety of cellular model systems. It is noteworthy that when we challenged by gene expression profiling the relevance of TAZ downstream of Wnt signaling, the regulation of a very significant fraction of Wnt target genes turned out to be TAZ-dependent both in mammary epithelial cells and colorectal cancer cells (PhD Thesis of Dr. Francesca Zanconato). The specific relevance of β-catenin or TAZ responses will likely depend on the cellular con-text. In some cell types, or experimental conditions, the effects of Wnt may primarily depend on TCF-dependent transcription; for example it is possible that mouse embryonic stem (ES) cells may represent one extreme situation, whereby TCF3/β-catenin interaction is central for self-renewal, whereas TAZ stabilization is irrelevant (Varelas et al., 2008). Makita et al., reported that a minor fraction of TAZ mutant mice develop to term, suggesting that TAZ may primarily contribute to Wnt responses in adult tissues. It must be also noticed, however, that the vast ma-jority of TAZ mutants die in utero with an as yet uncharacterized phenotype (Makita et al., 2008); in fact, we have been unable to obtain any $TAZ^{-/-}$ newborn in our colony (unpublished data). This leaves open the potential of an overlap between Wnt and TAZ also in embryonic develo-

pment, perhaps consistently with the phenotype of TAZ-deficient zebrafish embryos that display severe defects in mesodermal derivatives, including massive loss of bone differentiation (Hong et al., 2005).

A new role for β-catenin

β-catenin plays active roles both in the presence and absence of Wnt ligands (Figure 14). In the absence of Wnt signaling (i.e., Wnt OFF state), the pool of phospho-β-catenin is an essential element for continuous TAZ degradation as it serves as critical scaffold for TAZ recognition by the β-TrCP E3 ubiquitin ligase. This configures an unexpected role for cytoplasmic β-catenin: besides being re-cruited to the destruction complex for its own degradation, β-catenin works as yet another intermediary of the Wnt cascade upstream of TAZ. Much evidence support this conclusion, including: 1) TAZ and β-catenin form a complex at endogenous protein levels in unstimulated cells (TAZ/β-catenin interaction was already reported by Imajo et al., 2012); 2) β-catenin phosphorylation is required for TAZ degradation; 3) depletion of both GSK3 and β-catenin impairs TAZ/β-TrCP interaction and has the same effects on TAZ.

One possible interpretation of these results would be that TAZ could only bind the phosphorylated form of β-catenin. However, TAZ and β-catenin proteins can associate in vitro (Figure 12B), arguing against a strict requirement of β-catenin phosphorylation. Another equally plausible interpretation is that, irrespectively of β-catenin phosphorylation, TAZ may effectively associate to β-catenin only after cytoplasmic β-catenin is captured by the destruction complex, a scenario compatible with other proteins of the destruction complex either reinforcing the β-catenin/TAZ interaction or escorting the β-catenin/TAZ/β-TrCP recognition. Clearly, the structural and thermodynamic details by which β-catenin recognizes TAZ and favors its association with β-TrCP remains ground for future investigations. Moreover, the relevance of β-catenin as endogenous inhibitor of TAZ was validated at the genome-wide level in mammary epithelial cells by microarray experiments (PhD Thesis of Dr. Francesca Zanconato).

γ-catenin represents yet another variation on this scenario: this β-catenin-related protein is regulated by the Wnt/GSK3/β-TrCP axis but its relevance for TCF-dependent transcription is still debated (Ben-Ze'ev, 1999). Nevertheless, here we show that γ-catenin is able to regulate TAZ-dependent transcriptional responses

by promoting TAZ instability in concert, or redundantly, with β-catenin. From this "TAZ perspective", γ-catenin may effectively be part of the Wnt response.
We propose that in cells experiencing Wnt activity, β-catenin, per se largely dissociated from β-TrCP, is incapable to carry out any adaptor function for TAZ, and as such is irrelevant for TAZ regulation (Figure 14). In this view, it is the loss of the association of phospho-β-catenin to β-TrCP that causes TAZ stabilization: we found that TAZ is indeed stabilized not only by Wnt signaling, but also by experimentally removing β-catenin from cells lacking Wnt stimulation. It also follows that removing β-catenin from cells where the fraction of phospho-β-catenin is negligible - such as Wnt treated cells - should be inconsequential for TAZ function and not lead to further stabilization of TAZ. In fact, β-catenin knock-down cannot further increase TAZ-dependent transcription in Wnt-stimulated HEK293 cells (Figure 1D, lane 3).
The functions of the two pools of β-catenin could be visualized at the endogenous level and within the same cellular context by using HepG2 cells, containing both wild-type and a non-phosphorylatable mutant β-catenin. In line with our model, only wild type β-catenin is relevant to oppose TAZ; mutant-β-catenin is unable to bring TAZ to degradation, while it mediates the β-catenin/TCF transcriptional responses.

TAZ stability at the crossroad between Wnt and Hippo signaling.

Cell-cell adhesion and polarity cues activate the Hippo/LATS kinases leading to TAZ phosphorylation and sequestration in the cytoplasm (Pan, 2010). Moreover, a largely LATS-independent modality to regulate TAZ stability and activity has been also shown to occur as consequence of changes in cell shape and cytoskeletal reorganization induced by mechanical cues, such as rigidity of the extracellular matrix (Dupont et al., 2011). Here we further expanded the land-scape of TAZ regulation by showing that TAZ is controlled by a major family of secreted growth factors, in a manner largely independent from Hippo signaling.
One point worth discussing is that TAZ is phosphorylated by LATS and CK1 to generate a C-terminal phosphodegron, that has been shown to be relevant for TAZ stability and to promote direct association to β-TrCP, at least under conditions of protein overexpression (Liu et al., 2010). This is apparently at odd with the present findings indicating that, at endogenous protein levels, TAZ and β-TrCP asso-

ciate indirectly through a β-catenin bridge. In fact, these two scenarios are perfectly compatible, as these represent formally independent modalities of regulating TAZ stability by the Hippo and Wnt cascades, respectively. Indeed, here we show that LATS inhibition or mutation of the LATS or CK1 phosphorylation sites are irrelevant for TAZ regulation by Wnt (Figure C-D and data not shown); conversely, a TAZ mutant unable to bind β-catenin is insensitive to Wnt but remains under LATS1/2 control. Taken together, these findings open very intriguing possi-bilities for TAZ as hub integrating different physiological inputs.

This network accommodates self-regulating feedback loops; TAZ was demonstrated to negatively regulate the Wnt pathway by inhibiting Dishevelled, a positive Wnt regulator (Varelas et al., 2010a). This may provide a ceiling to the levels of TAZ activation by Wnts and a mechanism to turn off TAZ-dependent responses.

Finally, having established TAZ as Wnt effector opens up many therapeutic possibilities. Targeting TAZ could curb aberrant Wnt signaling in a variety of cancers and other disorders. Conversely, targeting the Wnt pathway by restoring the integrity of the destruction complex would effectively inhibit, at once, two of the most potent oncogenic drivers of human malignancies.

EXPERIMENTAL PROCEDURES

Reagents and plasmids

Doxorubicin, Paclitaxel, XAV939 and β-naphthoflavone were from Sigma. Doxycycline was from Calbiochem.

The constructs for shControl and shTAZ expression in MIV cells were prepared by cloning the Control and TAZ#2 sequences (see RNAi section) into pLKO.1-puro lentiviral vector (Addgene #8453; Stewart et al., 2003) according to manufacturer's protocol.

pSUPER-RETRO-PURO vectors containing the shGFP or TAZ RNAi sequences were used for stable knockdown in MII.

For stable expression of TAZ variants, TAZ cDNAs were subcloned from pEF-TAZ-N-Flag and pEF-TAZ-N-Flag(S89A) constructs (Addgene #19025 and #19026, Kanai et al., 2000) to pBABEhygro (Addgene #1765). The retroviral constructs coding for Flag-mTAZ S58/62A, Flag-mTAZ S306A, Flag-mTAZ S306/309A and Flag-mTAZ ΔWW (deleted of residues 111-158) were generated by mutagenesis from pBABEhygro mTAZ wt. Flag-mTAZ 4SA (i.e, S66/89/117/306A) was as in Dupont et al. (2011). All TAZ cDNA sequences were also subcloned in pCS2 for transient expression in HEK293 cells. For GST-pull down experiments wild-type full-length mouse TAZ was cloned in pGEX4T1; from this deletion constructs of GST-TAZ were generated by enzymatic digestion and self-ligation. Mouse TAZ cDNA is insensitive to the siRNAs used to target the human transcript.

Doxycycline-inducible lentiviral constructs were obtained by substituting the Oct4 sequence in FUW-tetO-hOCT4 (Addgene #20726; Hockemeyer et al., 2008) with mTAZ wt or S89A cDNAs (see above) or with EGFP sequence from PL-SIN-EOS-C(3+)-EiP plasmid (Addgene #21313, Hotta et al., 2009). In this type of experiments cells were also co-transduced with FUdeltaGW-rtTA (Addgene #19780, Maherali et al., 2008). This strategy was implicated for cells used in Figures 3H-I and 5D-E.

A doxycycline-inducible retroviral vectors-based strategy was implicated for cells used in Figures 10D and 11H. Human myc-tagged GSK3β wt or kinase-dead

(KD) mutant (K85A) cDNAs were subcloned in pCS2 and made insensitive to GSK3β siRNA#1 by introducing silent mutations within the siRNA targeting sequence by PCR. For inducible expression of GSK3β in MII cells (Figure 10D), siRNA-insensitive GSK3β variants were subcloned in a doxycycline-inducible retroviral expression vector (pSTC-Puro), and retroviral particles were used to infect MII cells previously transduced with pBABEhygro rtTA (MII-rtTA cells). cDNAs for human β-catenin, wild-type and phospho-mutant (S/A = S33/37/41A, corresponding to the GSK3 sites and the CK1 priming site S45A), were subcloned in pCSP1 and were made insensitive to β-catenin siRNA#4 by introducing silent mutations within the siRNA targeting sequence by PCR. For inducible expression of β-catenin in MII cells (Figure 11H), both siRNA-insensitive β-catenin variants were subcloned in pSTC-Puro, and retroviral particles were used to transduce MII-rtTA cells.

pcDNA3-DN-hCUL1-FLAG (#15818) was purchased from Addgene (Jin et al., 2005).

All constructs were confirmed by sequencing.

Cell lines

MII and MIV cells were a gift from S. Santner (Santner et al., 2001). MII cells were cultured in DMEM/F12 (Gibco, Life Technologies) with 5% horse serum (HS), glutamine and antibiotics, freshly supplemented with insulin, EGF, hydrocortisone, and cholera toxin. For all experiments, MII were grown for 2 days at high density. MIV and MDA-MB-231 were cultured in DMEM/F12 with 10% FBS, glutamine and antibiotics.

HEK293 cells, Control-L-cells (ATCC #CRL-2648) and Wnt3a-L-cells (ATCC #CRL-2647) were cultured in DMEM (Gibco, Life Technologies) supplemented with 10% fetal bovine serum (FBS), glutamine and antibiotics. Conditioned media from L-cells were harvested according to the ATCC protocol.

HepG2 cells were cultured in MEM (Gibco, Life Technologies) supplemented with 10% FBS, glutamine, antibiotics and non essential aminoacids.

RNA interference

siRNA transfections were done with Lipofectamine RNAi-MAX (Life technolo-

gies) in antibiotics-free medium according to manufacturer instructions. Sequences of siRNAs are provided in Table 3.

For stable knock-down, both lentiviral or retroviral vectors were used. Lentiviral particles were prepared by transiently transfecting HEK293T cells with lentiviral vectors together with packaging vectors (pMD2-VSVG and psPAX2). Retroviral particles were prepared by transiently transfecting HEK293GP cells with retroviral vectors together with an envelope-producing vector (pMD2-Env). Infections were carried out as in Martello et al. (2010).

Western blot

Cells were harvested by sonication and extracts quantified with Bradford method. Proteins were run in 4-12% Nupage MOPS acrylamide gels and transferred onto PVDF membrans by wet electrophoretic transfer. Blots were blocked with non-fat dry milk and incubated overnight at 4°C with primary antibodies. Secondary antibodies were incubated 1 hr at room temperature, and then blots were developed with chemiluminescent reagents.

For Western blot: anti-YAP/TAZ, anti-Survivin, anti-GSK3, anti-β-catenin and anti-γ-catenin monoclonal antibodies and anti-CTGF and anti-Cyr61 polyclonal antibodies were from Santa Cruz. anti-GAPDH monoclonal antibody was from Millipore. Anti-PAI1 was from BD Biosciences. Anti-β-TrCP, anti-LATS1 and anti-phospho-S909 LATS1 polyclonal antibodies were from Cell Signaling, and anti-β-catenin polyclonal antibody was from Sigma. Anti-phospho-S306 TAZ polyclonal antiserum was obtained from one rabbit (out of two) immunized with a synthetic peptide (Covance).

Collection and Processing of Breast Cancer Gene-Expression Data

We started from a collection of 7 datasets (Table 1) containing microarray data of breast cancer samples annotated with histological tumor grade and clinical outcome. All data were measured on Affymetrix HG-U133A arrays and have been downloaded from NCBI Gene Expression Omnibus (GEO, http://www.ncbi.nlm.nih.gov/geo/).

Since raw data (.CEL files) were available for all samples, expression values of the metadataset were generated from fluorescence signals using the robust mul-

tiarray average procedure (RMA, Irizarry et al., 2003). Specifically, intensity levels have been background adjusted, normalized using quantile normalization, and log2 expression values calculated using median polish summarization.

To identify genes upregulated in histological G3, we compared the expression profiles of G3 versus G1 samples using SAM algorithm coded in the samr R package (Tusher et al., 2001). In SAM, we estimated the percentage of false positive predictions with 1000 permutations and set the q-value threshold at $1x10^{3}$. The comparison between 270 G3 and 182 G1 samples of the metadataset enlisted 78 Affymetrix probesets overexpressed more than two times in G3 cancers.

As signaling pathway signatures we used lists of genes activated by signaling pathway components in normal, immortalized or tumor human mammary cells. These signatures are TAZ/YAP (Zhang et al., 2009a), Notch A (Notch signature in Mazzone et al., 2010), Notch B (NICD signature in Mazzone et al., 2010), RAS (Bild et al., 2006), ERBB2 (Mackay et al., 2003), β-catenin (Bild et al., 2006), Wnt (DiMeo et al., 2009), TGF-β-A (Padua et al., 2008), TGF-β-B (Adorno et al., 2009), NF-kB (Park et al., 2007), STAT3 (Alvarez et al., 2005), and Src (Bild et al., 2006). The YAP conserved signature (listed in Cordenonsi et al., 2011) is composed of a selection of genes that have been found activated by YAP overexpression in human mammary cells (MCF10A) (Zhao et al., 2008) and that are also activated upon YAP overexpression in mouse liver tissues (Dong et al., 2007) or in immortalized mouse fibroblasts (Ota et al., 2008). Thus, this signature represents a list of evolutionary conserved YAP target genes. We used the following stem cell signatures: human normal mammary stem cells (hNMSC; Pece et al., 2010), invasiveness gene signature (IGS; Liu et al., 2007), CD44high (Shipitsin et al., 2007), embryonic stem cells 1 (ES1) and embryonic stem cells 2 (ES2) (Ben-Porath et al., 2008), and embryonic stem cells-like (ES-like, Kim et al., 2010). All biostatistical analyses were performed in collaboration with prof. Silvio Bicciato.

Mammosphere assay

Cells were trypsinized, counted, and plated as single-cell suspensions (1000 cells/cm^{2}) on ultra-low attachment plates (Costar). Mammospheres were counted after 5 days; cells were thereafter dissociated to be reseeded for a second round of mammosphere formation. Mammosphere cultures of MII and their derivatives

were performed as described in Dontu et al. (2003); for MIV cells, culture conditions were as in Ponti et al. (2005). Statistical analyses were done with Prism software (GraphPad).

Tumorigenesis Assays

For xenograft tumor-seeding studies, the indicated numbers of MII or MIV cells were suspended in 100 μl Matrigel (BD Biosciences) and injected in the fat pads of immunocompromized female mice. Tumor formation was assayed by palpation. After the indicated periods, mice were sacrificed and tumors were explanted for histological analyses. Tumorigenesis assays were performed in collaboration with prof. Antonio Rosato.

Fluorescence-activated cell sorting

Cells were detached from plates with TrypLE (Invitrogen), resuspended ($5x10^5$ cells/ml), incubated in running buffer (PBS 13, BSA 0.5%, and EDTA 5 mM) with anti-human CD44 (clone G44-26, FITC-conjugated, BD Biosciences) and anti-human CD24 (clone ML5, PE-conjugated, BD Biosciences), and finally analyzed or sorted with MoFlo XDP sorter (Beckman Coulter). FACS experiments were performed in collaboration with Dr. Chiara Frasson, in the group of prof. Giuseppe Basso.

Hoechst Staining for Side Population Identification

Cells were detached from plates with TrypLE (Invitrogen), resuspended at $1x10^6$ cells/ml in staining medium containg 5 mg/ml Hoechst-33342 (Molecular Probes) and incubated at 37°C for 1.5 hr in the dark. When indicated, 100 μM Verapamil was added to the cell suspension. Cells were then washed with cold HBSS supplemented with 2% FBS, incubated with 2 μg/ml PI (to esclude dead PI-permeable cells from the following cytofluorimetric analysis), washed again with cold HBSS + 2% FBS and resuspended in running buffer. FACS profiles were obtained with MoFlo XDP sorter (Beckman Coulter). As optical filters for Hoechst blue and red fluorescence, a 424/44 band pass filter and a 660/20 band pass filter were used, respectively.

Treatments with Chemotherapeutic Drugs

MII cells (5000/well) were plated in 100 μl per well in 96-well plates. One day after seeding, Doxorubicin or Paclitaxel were added in four replicates per concentration for each cell line. Cell viability was measured after 72 hr with the CellTiter96 AQueous Non-radioactive Assay (Promega).

Clinical Samples and Immunohistochemistry

Archival formalin-fixed paraffin-embedded breast cancer specimens were collected at the Istituto Nazionale Tumori (INT) of Milan and at the Ospedale San Bassiano-Bassano del Grappa, Italy. For IHC, 4 μm thick sections were obtained from tumor samples and were processed for immunohistochemistry. Immunohistochemical staining was performed on formalin-fixed, paraffin-embedded tissue sections using a fully automated system (Bond-maX; Leica). In brief, one 4-micron-thick section from each paraffin-embedded block was cut. The sections were deparaffinized in Bond Dewax Solution (Leica) at 72°C, rinsed in ethanol, and rehydrated in distilled water. Antigen retrieval was performed by heating sections for 30 min at 99°C in Bond Epitope Retrieval Solution 1 (Leica). Endogenous peroxidase was blocked by 3% hydrogen peroxide before 30 min of incubation with rabbit polyclonal anti-TAZ (Sigma, HPA007415;1:50 diluted). Specimens were then washed with phosphate-buffered saline (PBS) and incubated with Bond Polymer Refine Detection Kit (Leica) according with the manufacturer's protocols. The staining was visualized with 3,30 -diaminobenzidine (DAB) and the slides were counterstained with Mayer's hematoxylin. The sections were then dehydrated, cleared, and mounted. Formalin-fixed, paraffin-embedded positive and negative controls were included in each run. Tumors were scored as positive when over 10% of cells displayed nuclear TAZ staining similar or stronger to that of the cells of normal ducts included in the same section. Immunohistochemical experiments were performed in collaboration with prof. Anna Parenti.

Luciferase Assays

Luciferase assays were performed in HEK293 cells with the established YAP/TAZ-responsive reporter 8xGTIIC-Lux (Dupont et al., 2011) and with the β-catenin/TCF-responsive reporter BAT-Lux (Maretto et al., 2003). Luciferase re-

porters (50 ng/cm^2) were transfected together with CMV-β-gal (75 ng/cm^2) to normalize for transfection efficiency with CPRG (Roche) colorimetic assay. GSK3β, TAZ and DN-Cul1 plasmids were co-transfected at 100, 50 and 100 ng/cm^2 respectively. DNA transfections were done with TransitLT1 (Mirus Bio) according to manufacturer instructions. DNA content in all samples was kept uniform by adding pBluescript plasmid up to 250 ng/cm^2. For luciferase assays in siRNA-depleted cells, cells were first transfected with the indicated siRNAs and, after 24 hr, washed from transfection media, transfected with plasmid DNA, and harvested 48 hr later. Each sample was transfected in duplicate and each experiment was repeated at least three times independently.

Quantitative Real-Time PCR

Cells or tissues were harvested in Trizol (Invitrogen) for total RNA extraction, and contaminant DNA was removed by DNase treatment. qRT-PCR analyses were carried out on retrotranscribed cDNAs with Rotor-Gene Q (Quiagen) thermal cycler and analyzed with Rotor-Gene Analysis6.1 software. Experiments were performed at least three times, with duplicate replicates. Expression levels are always given relative to GAPDH. PCR oligo sequences are listed in Table 4.

Mice

Ah-Cre mice and *Apc*$^{fl/fl}$ mice were a kind gift of Alan R. Clarke (Sansom et al., 2004). Ah-Cre mice were crossed with mice carrying the Apc floxed allele to yield *Ah-Cre;Apc*$^{fl/fl}$ mice. For induction of the Ah promoter, *Ah-Cre;Apc*$^{+/+}$ control and *Ah-Cre;Apc*$^{fl/fl}$ mice received three intraperitoneal injections of 10 mg/kg each of the cytochrome p450 inducer β-naphthoflavone (Sigma) dissolved in corn oil (10 mg/ml). After 4 days, mice were sacrificed and livers were collected for further analysis. Mice were genotyped by PCR on tail genomic DNA extracted by standard procedures (Morsut et al., 2010). Effective recombination of the *Apc* locus was verified in the livers of mice injected with b-naphthoflavone.

Immunoprecipitations

Immunoprecipitations were carried out as in Adorno et al. (2009), with the following modifications: extracts were diluted to 20 mM HEPES (pH 7.8), 100 mM NaCl, 5% glycerol, 2.5 mM $MgCl_2$, 1% Triton X-100, 0.5% NP40 and incubated

with protein A-sepharose-bound primary antibody.

For immunoprecipitations, primary antibody were: anti-TAZ monoclonal antibody (BD Biosciences), anti-β-catenin monoclonal antibody (Santa Cruz), and anti-Flag-tag monoclonal antibody (M2, Sigma).

Immunofluorescence

Cells were plated on Fibronectin (Sigma)-coated glass chamber slides (Nunc) and fixed 10 min at room temperature (RT) with PFA 4%. Slides were permeabilized 10 min at RT with PBS 0.3% Triton X-100, and processed for immunofluorescence according to the following conditions: blocking in 10% BSA or Goat Serum (GS) in PBST for 1 hr, followed by incubation with primary antibody (diluted in 2% BSA or GS in PBST) for 16 hr at 4°C, four washes in PBST and incubation with secondary antibodies (diluted in 2% BSA or GS in PBST) for 1.5 hr at room temperature. Primary antibodies are: anti-Scribble (Santa Cruz; 1:100, blocking with BSA), anti-E-Cadherin (BD Bioscences, 1:1000, blocking with GS), and anti-TAZ (BD Bioscences, 1:100, blocking with BSA).

Secondary antibodies (Invitrogen) are: chicken anti-goat Alexa488 (1:100, blocking with BSA) and goat anti-mouse Alexa488 (1:200, blocking with GS). After three washes in PBS, nuclei were stained with Hoechst (Sigma) for 30 min in PBS. Confocal images were obtained with a Leica TCS SP5 equipped with a CCD camera.

GST Pull-Down

For GST pull-downs, beads with purified proteins were incubated with ^{35}S-methionine labeled in vitro-translated β-catenin for 3 hr in Binding Buffer (25 mM HEPES (pH 7.9), 0.4 M KCl, 0.4% NP40, 5 mM EDTA, 1 mM DTT, 10% glycerol with protease inhibitors). After 4 washes in binding buffer, copurified proteins were analyzed by SDS-page and autoradiography, using Cyclone Plus Phospho-imager (Perkin Elmer).

REFERENCES

Aberle H, Bauer A, Stappert J, Kispert A, Kemler R. (1997). beta-catenin is a target for the ubiquitin-proteasome pathway. EMBO J 16, 3797-804.

Adorno, M., Cordenonsi, M., Montagner, M., Dupont, S., Wong, C., Hann, B., Solari, A., Bobisse, S., Rondina, M.B., Guzzardo, V., et al. (2009). A Mutant-p53/Smad complex opposes p63 to empower TGFbeta-induced metastasis. Cell 137, 87-98.

Al-Hajj, M., Wicha, M.S., Benito-Hernandez, A., Morrison, S.J., and Clarke, M.F. (2003). Prospective identification of tumorigenic breast cancer cells. Proc Natl Acad Sci U S A 100, 3983-3988.

Alvarez, J.V., Febbo, P.G., Ramaswamy, S., Loda, M., Richardson, A., and Frank, D.A. (2005). Identification of a genetic signature of activated signal transducer and activator of transcription 3 in human tumors. Cancer Res 65, 5054-5062.

Baccelli I, Trumpp A. (2012). The evolving concept of cancer and metastasis stem cells. J Cell Biol. *198*, 281-93

Barolo, S. (2006). Transgenic Wnt/TCF pathway reporters: all you need is Lef? Oncogene 25, 7505-7511.

Barry, E.R. , Morikawa, T., Butler, B.L., Shrestha, K., de la Rosa, R., Yan, K.S., Fuchs, C.S., Magness, S.T., Smits, R., Ogino, S., Kuo, C.J., and Camargo, F.D. (2012). Restriction of intestinal stem cell expansion and the regenerative response by YAP. Nature. doi:10.1038/nature11693.

Basu, S., Totty, N.F., Irwin, M.S., Sudol, M., and Downward J. (2003). Akt phosphorylates the Yes-associated protein, YAP, to induce interaction with 14-3-3 and attenuation of p73-mediated apoptosis. Mol Cell 11, 11-23.

Ben-Porath, I., Thomson, M.W., Carey, V.J., Ge, R., Bell, G.W., Regev, A., and Weinberg, R.A. (2008). An embryonic stem cell-like gene expression signature in poorly differentiated aggressive human tumors. Nat Genet 40, 499-507.

Ben-Ze'ev, A. (1999). The dual role of cytoskeletal anchor proteins in cell adhesion and signal transduction. Ann N Y Acad Sci 886, 37-47.

Bhat, K.P., Salazar, K.L., Balasubramaniyan, V., Wani, K., Heathcock, L., Hollingsworth, F., James, J.D., Gumin, J., Diefes, K.L., Kim, S.H., et al. (2011). The transcriptional coactivator TAZ regulates mesenchymal differentiation in malignant glioma. Genes Dev 25, 2594-2609.

Bild, A.H., Yao, G., Cheng, J.T., Wang, Q., Potti, A., Chasse, D., Joshi, M.B., Harpo-le, D., Lancaster, J. M., Berchuck, A., Olson, J. A., Marks, J. R., Dress-

man, H. K., West, M., and Nevins, J.R. (2006). Oncogenic pathway signatures in human cancers as a guide to targeted therapies. Nature 439, 353-357.

Bourn D, Carter SA, Mason S, Gareth D, Evans R, Strachan T. (1994). Germline mutations in the neurofibromatosis type 2 tumour suppressor gene. Hum Mol Genet. *3*, 813-6.

Camargo, F.D., Gokhale, S., Johnnidis, J.B., Fu, D., Bell., G.W., Jaenisch, R., and Brummelkamp, T.R. (2007). YAP1 increases organ size and expands undifferenziated progenitor cells. Curr Biol 17, 2054-2060.

Cao, X., Pfaff, S.L., Gage, F.H. (2008). YAP regulates neural progenitor cell number via the TEA domain transcription factor. Genes Dev 22, 3320–34.

Chaffer, C.L., and Weinberg, R.A. (2011a). A perspective on cancer cell metastasis. Science 331, 1559-1564.

Chaffer, C.L., Brueckmann, I., Scheel, C., Kaestli, A.J., Wiggins, P.A., Rodrigues, L.O., Brooks, M., Reinhardt, F., Su, Y., Polyak, K., et al. (2011b). Normal and neoplastic nonstem cells can spontaneously convert to a stem-like state. Proc Natl Acad Sci U S A.

Chan, E.H., Nousianen, M., Chalamalasetty, R.B., Schafer, A., Nigg, E.A., and Silljè, H.H. (2005). The Ste20-like kinase Mst2 activates the human large tumor suppressor kinase Lats1. Oncogene 24, 2076-2086.

Chan, S.W., Lim, C.J., Guo, K., Ng, C.P., Lee, I., Hunziker, W., Zeng, Q., and Hong, W. (2008). A role for TAZ in migration, invasion, and tumorigenesis of breast cancer cells. Cancer Res 68, 2592-2598.

Clevers, H. (2006). Wnt/β-catenin signaling in development and disease. Cell 127, 469-480.

Collins, A.T., Berry, P.A., Hyde, C., Stower, M.J., Maitland, N.J. (2005). Prospective identification of tumorigenic prostate cancer stem cells. Cancer Res 65, 10946-10951.

Dean, M., Fojo, T., and Bates, S. (2005). Tumour stem cells and drug resistance. Nat Rev Cancer 5, 275-284.

Desmedt, C., Piette, F., Loi, S., Wang, Y., Lallemand, F., Haibe-Kains, B., Viale, G., Delorenzi, M., Zhang, Y., d'Assignies, M.S., et al. (2007). Strong time dependence of the 76-gene prognostic signature for node-negative breast cancer patients in the TRANSBIG multicenter independent validation series. Clinical cancer research : an official journal of the American Association for Cancer Research 13, 3207-3214.

Diehn M, Cho RW, Lobo NA, Kalisky T, Dorie MJ, Kulp AN, Qian D, Lam JS, Ailles LE, Wong M, Joshua B, Kaplan MJ, Wapnir I, Dirbas FM, Somlo G, Garberoglio C, Paz B, Shen J, Lau SK, Quake SR, Brown JM, Weissman IL, Clarke

MF. (2009). Association of reactive oxygen species levels and radioresistance in cancer stem cells. Nature *458*, 780-3.

DiMeo, T.A., Anderson, K., Phadke, P., Fan, C., Perou, C.M., Naber, S., and Kuper-wasser, C. (2009). A novel lung metastasis signature links Wnt signaling with cancer cell self-renewal and epithelial-mesenchymal transition in basal-like breast cancer. Cancer Res 69, 5364-5373.

Dong, J., Feldmann, G., Huang, J., Wu, S., Zhang, N., Comerford, S.A., Gayyed, M.F., Anders, R.A., Maitra, A., and Pan, D. (2007). Elucidation of a universal size-control mechanism in Drosophila and mammals. Cell 130, 1120-1133.

Dontu, G., Abdallah, W.M., Foley, J.M., Jackson, K.W., Clarke, M.F., Kawamura, M.J., and Wicha, M.S. (2003). In vitro propagation and transcriptional profiling of human mammary stem/progenitor cells. Genes Dev 17, 1253-1270.

Dupont, S., Mamidi, A., Cordenonsi, M., Montagner, M., Zacchigna, L., Adorno, M., Martello, G., Stinchfield, M.J., Soligo, S., Morsut, L., Inui M., Moro, S., Modena, N., Argenton, F., Newfeld, S.J., and Piccolo, S. (2009). FAM/USP9x, a deubiquitinating enzyme essential for TGFbeta signaling, controls Smad4 monoubiquitination. Cell 136, 123-135.

Dupont, S., Morsut, L., Aragona, M., Enzo, E., Giulitti, S., Cordenonsi, M., Zanconato, F., Le Digabel, J., Forcato, M., Bicciato, S., et al. (2011). Role of YAP/TAZ in mechanotransduction. Nature 474, 179-183.

Egeblad M, Nakasone ES, Werb Z. (2010). Tumors as organs: complex tissues that interface with the entire organism. Dev Cell. 2010 *18*, 884-901.

Grimshaw MJ, Cooper L, Papazisis K, Coleman JA, Bohnenkamp HR, Chiapero-Stanke L, Taylor-Papadimitriou J, Burchell JM. (2008). Mammosphere culture of metastatic breast cancer cells enriches for tumorigenic breast cancer cells. Breast Cancer Res. *10*, R52.

Gupta, P.B., Chaffer, C.L., and Weinberg, R.A. (2009). Cancer stem cells: mirage or reality? Nat Med 15, 1010-1012.

Halder, G., and Johnson, R.L. (2011). Hippo signaling: growth control and byond. Development 138, 9-22.

Halder, G., Dupont, S., and Piccolo, S. (2012). Transduction of mechanical and cytoskeletal cues by YAP and TAZ. Nat Rev Mol Cell Biol 13, 591-600.

Harvey, K.F., Pfleger, C.M., and Hariharan, I.K. (2003). The Drosophila Mst ortho-log, hippo, restricts growth and cell proliferation and promotes apoptosis. Cell 114, 457-467.

Heallen, T., Zhang, M., Wang, J., Bonilla-Claudio, M., Klysik, E., Johnson, R.L., and Martin, J.F. (2011). Hippo pathway inhibits Wnt signaling to restrain cardiomyocyte proliferation and heart size. Science 332, 458-61.

Hockemeyer, D., Soldner, F., Cook, E.G., Gao, Q., Mitalipova, M., and Jaenisch, R. (2008). A drug-inducible system for direct reprogramming of human somatic cells to pluripotency. Cell Stem Cell 3, 346-353.

Hong, J.H., Hwang, E.S., McManus, M.T., Amsterdam, A., Tian, Y., Kalmukova, R., Mueller, E., Benjamin, T., Spiegelman, B.M., Sharp, P.A., et al. (2005). TAZ, a transcriptional modulator of mesenchymal stem cell differentiation. Science 309, 1074-1078.

Hossain, Z., Ali, S.M., Ko, H.L., Xu, J., Ng, C.P., Guo, K., Ponniah, S., Hong, W., and Hunziker, W. (2007). Glomerulocystic kidney disease in mice with a targeted inactivation of Wwtr1. Proc Natl Acad Sci USA 104, 1631-1636.

Hotta, A., Cheung, A.Y., Farra, N., Vijayaragavan, K., Seguin, C.A., Draper, J.S., Pasceri, P., Maksakova, I.A., Mager, D.L., Rossant, J., et al. (2009). Isolation of human iPS cells using EOS lentiviral vectors to select for pluripotency. Nat Methods 6, 370-376.

Huang, J., Wu, S., Barrera, J., Matthews, K., and Pan, D. (2005). The Hippo signaling pathway coordinately regulates cell proliferation and apoptosis by inactivating Yorkie, the Drosophila Homolog of YAP. Cell 122, 421-434.

Huang, S.M., Mishina, Y.M., Liu, S., Cheung, A., Stegmeier, F., Michaud, G.A., Charlat, O., Wiellette, E., Zhang, Y., Wiessner, S., et al. (2009). Tankyrase inhibition stabilizes axin and antagonizes Wnt signalling. Nature 461, 614-620.

Huang, W., Lv, X., Liu, C., Zha, Z., Zhang, H., Jiang, Y., Xiong, Y., Lei, Q.Y., and Guan, K.L. (2012). The N-terminal phosphodegron targets TAZ/WWTR1 protein for SCFβ-TrCP-dependent degradation in response to phosphatidylinositol 3-kinase inhibition. J. Biol. Chem. 287, 26245-26253.

Humbert, P.O., Grzeschik, N.A., Brumby, A.M., Galea, R., Elsum, I., and Richardson, H.E. (2008). Control of tumourigenesis by the Scribble/Dlg/Lgl polarity module. Oncogene 27, 6888-6907.

Imajo, M., Miyatake, K., Iimura, A., Miyamoto, A., and Nishida, E. (2012). A molecular mechanism that links Hippo signalling to the inhibition of Wnt/β-catenin signalling. EMBO J 31, 1109-1122.

Irizarry, R.A., Hobbs, B., Collin, F., Beazer-Barclay, Y.D., Antonellis, K.J., Scherf, U., and Speed, T.P. (2003). Exploration, normalization, and summaries of high density oligonucleotide array probe level data. Biostatistics (Oxford, England) 4, 249-264.

Ivshina, A.V., George, J., Senko, O., Mow, B., Putti, T.C., Smeds, J., Lindahl, T., Pawitan, Y., Hall, P., Nordgren, H., et al. (2006). Genetic reclassification of histologic grade delineates new clinical subtypes of breast cancer. Cancer Res 66, 10292-10301.

Jia, J., Zhang, W., Wang, B., Trinko, R. and Jiang, J. (2003). The Drosophila Ste20 family kinase dMST functions as a tumor suppressor by restricting cell proliferation and promoting apoptosis. Genes Dev 17, 2514-2519.

Jin, J., Ang, X.L., Shirogane, T., and Wade Harper, J. (2005). Identification of substrates for F-box proteins. Methods in enzymology 399, 287-309.

Justice, R.W., Zlian, O., Woods, D.F., Noll, M., and Bryant, P.J. (1995). The Droso-phila tumor suppressor gene warts encodes a homolog of human myotonic dystrophy kinase and is required for the control of cell shape and proliferation. Genes Dev 9, 534-546.

Kanai, F., Marignani, P.A., Sarbassova, D., Yagi, R., Hall , R.A., Donowitz, M., Hi-saminato, A., Fujiwara, T., Ito, Y., Cantley, L.C., and Yaffe, M.B. (2000). TAZ: a no-vel transcriptional co-activators regulated by interaction with 14-3-3 and PDZ do-mains protein. Embo J 19, 6778-6791.

Kim, N.G., Xu, C., and Gumbiner, B.M. (2009). Identification of targets of the Wnt pathway destruction complex in addition to β-catenin. Proc. Natl Acad. Sci. USA 106, 5165-5170.

Kim, J., Woo, A.J., Chu, J., Snow, J.W., Fujiwara, Y., Kim, C.G., Cantor, A.B., and Orkin, S.H. (2010). A Myc network accounts for similarities between embryonic stem and cancer cell transcription programs. Cell 143, 313-324.

Kitagawa M, Hatakeyama S, Shirane M, Matsumoto M, Ishida N, Hattori K, Nakamichi I, Kikuchi A, Nakayama K, Nakayama K. (1999). An F-box protein, FWD1, mediates ubiquitin-dependent proteolysis of beta-catenin. EMBO J. 18, 2401-10.

Lai, D., Ho, K.C., Hao, Y., and Yang, X. (2011) Taxol resistance in breast cancer cells is mediated by the hippo pathway component TAZ and its downstream transcriptional targets Cyr61 and CTGF. Cancer Res 71, 2728-2738.

Lai, Z.C., Wei, X., Shimiuz, T., Ramos, E., Rohrbaugh, M., Nikolaidis, N., Ho, L.L., and Li, Y. (2005). Control of cell proliferation and apoptosis by mob as tumor suppressor mats. Cell 120, 675-685.

Lapidot, T., Sirard, C., Vormoor, J., Murdoch, B., Hoang, T., Caceres-Cortes, J., Minden, M., Paterson, B., Caligiuri, M.A., and Dick, J.E. (1994). A cell initiating human acute myeloid leukaemia after transplantation into SCID mice. Nature 367, 458-61.

Lee, K.P., Lee, J.H., Kim, T.S., Kim, T.H., Park, H.D., Byun, J.S., Kim, M.C., Jeong, W.I., Calvisi, D.F., Kim, J.M., and Lim, D.S. (2010). The Hippo-Salvador pathway restrains hepatic oval cell proliferation, liver size, and liver tumorigenesis. Proc Natl Acad Sci USA 107, 8248-8253.

Lei, Q.Y., Zhang, H., Zhao, B., Zha, Z.Y., Bai, F., Pei, X.H., Zhao, S., Xiong, Y., and Guan, K.L. (2008) TAZ promotes cell proliferation and epithelial-

mesenchymal tran-sition and is inhibited by the hippo pathway. Mol Cell Biol 28, 2426-2436.

Li, C., Heidt, D.G., Dalerba, P., Burant, C.F., Zhang, L., Adsay, V., Wicha, M., Clar-ke, M.F., Simeone, D.M. (2007). Identification of pancreatic cancer stem cells. Can-cer Res 67, 1030-1037.

Li, V.S., Ng, S.S., Boersema, P.J., Low, T.Y., Karthaus, W.R., Gerlach, J.P., Mohammed, S., Heck, A.J., Maurice, M.M., Mahmoudi, T., et al. (2012). Wnt Signaling through Inhibition of beta-Catenin Degradation in an Intact Axin1 Complex. Cell 149, 1245-1256.

Lian I, Kim J, Okazawa H, Zhao J, Zhao B, Yu J, Chinnaiyan A, Israel MA, Goldstein LS, Abujarour R, Ding S, Guan KL. (2010). The role of YAP transcription coactivator in regulating stem cell self-renewal and differentiation. Genes Dev. *24*, 1106-18.

Liu, C., Li, Y., Semenov, M., Han, C., Baeg, G.H., Tan, Y., Zhang, Z., Lin, X., and He, X. (2002). Control of β-catenin phosphorylation/degradation by a dual-kinase mechanism. Cell 108, 837-847.

Liu, R., Wang, X., Chen, G.Y., Dalerba, P., Gurney, A., Hoey, T., Sherlock, G., Lewicki, J., Shedden, K., and Clarke, M.F. (2007). The prognostic role of a gene signature from tumorigenic breast-cancer cells. N Engl J Med 356, 217-226.

Liu, C.Y., Zha, Z.Y., Zhou, X., Zhang, H., Huang, W., Zhao, D., Li, T., Chan, S.W., Lim, C.J., Hong, W., et al. (2010). The hippo tumor pathway promotes TAZ degradation by phosphorylating a phosphodegron and recruiting the SCF/β-TrCP E3 ligase. J Biol Chem 285, 37159-37169.

Loi, S., Haibe-Kains, B., Desmedt, C., Lallemand, F., Tutt, A.M., Gillet, C., Ellis, P., Harris, A., Bergh, J., Foekens, J.A., et al. (2007). Definition of clinically distinct molecular subtypes in estrogen receptor-positive breast carcinomas through genomic grade. Journal of clinical oncology : official journal of the American Society of Clinical Oncology 25, 1239-1246.

Loi, S., Haibe-Kains, B., Desmedt, C., Wirapati, P., Lallemand, F., Tutt, A.M., Gillet, C., Ellis, P., Ryder, K., Reid, J.F., et al. (2008). Predicting prognosis using molecular profiling in estrogen receptor-positive breast cancer treated with tamoxifen. BMC genomics 9, 239.

Loi, S., Haibe-Kains, B., Majjaj, S., Lallemand, F., Durbecq, V., Larsimont, D., Gonzalez-Angulo, A.M., Pusztai, L., Symmans, W.F., Bardelli, A., et al. (2010). PIK3CA mutations associated with gene signature of low mTORC1 signaling and better outcomes in estrogen receptor-positive breast cancer. Proc Natl Acad Sci U S A 107, 10208-10213.

MacDonald, B.T., Tamai, K., and He, X. (2009). Wnt/ β-catenin signaling: components, mechanisms, and diseases. Developmental cell 17, 9-26.

Mackay, A., Jones, C., Dexter, T., Silva, R.L., Bulmer, K., Jones, A., Simpson, P., Harris, R.A., Jat, P.S., Neville, A.M., et al. (2003). cDNA microarray analysis of genes associated with ERBB2 (HER2/neu) overexpression in human mammary luminal epithelial cells. Oncogene 22, 2680-2688.

Maherali, N., Ahfeldt, T., Rigamonti, A., Utikal, J., Cowan, C., and Hochedlinger, K. (2008). A high-efficiency system for the generation and study of human induced pluripotent stem cells. Cell stem cell 3, 340-345.

Makita, R., Uchijima, Y., Nishiyama, K., Amano, T., Chen, Q., Takeuchi, T., Mitani, A., Nagase, T., Yatomi, Y., Aburatani, H., et al. (2008). Multiple renal cysts, urinary concentration defects, and pulmonary emphysematous changes in mice lacking TAZ. American journal of physiology Renal physiology 294, F542-553.

Mani, S.A., Guo, W., Liao, M.J., Eaton, E.N., Ayyanan, A., Zhou, A.Y., Brooks, M., Reinhard, F., Zhang, C.C., Shipitsin, M., et al. (2008). The epithelial-mesenchymal transition generates cells with properties of stem cells. Cell 133, 704-715.

Maretto, S., Cordenonsi, M., Dupont, S., Braghetta, P., Broccoli, V., Hassan, A.B., Volpin, D., Bressan, G.M., and Piccolo, S. (2003). Mapping Wnt/beta-catenin signaling during mouse development and in colorectal tumors. Proc Natl Acad Sci U S A 100, 3299-3304.

Martello, G., Rosato, A., Ferrari, F., Manfrin, A., Cordenonsi, M., Dupont, S., Enzo, E., Guzzardo, V., Rondina, M., Spruce, T., et al. (2010). A MicroRNA targeting dicer for metastasis control. Cell 141, 1195-1207.

Mauviel, A., Nallet-Staub, F., and Varelas X. (2011). Integrating developmental signals: a hippo in the (path)way. Oncogene doi:10.1038/onc.2011.363.

Mazzone, M., Selfors, L.M., Albeck, J., Overholtzer, M., Sale, S., Carroll, D.L., Pandya, D., Lu, Y., Mills, G.B., Aster, J.C., et al. (2010). Dose-dependent induction of distinct phenotypic responses to Notch pathway activation in mammary epithelial cells. Proc Natl Acad Sci U S A 107, 5012-5017.
McBeath, R., Pirone, D.M., Nelson, C.M., Bhadriraju, K., and Chen, C.S. (2004). Cell shape, cytoskeletal tension, and RhoA regulate stem cell lineage commitment. Dev Cell 6, 483-495.

McCartney, B.M., Kulikauskas, R.M., LaJeunesse, D.R., and Fehon, R.G. (2000). The neurofibromatosis-2 homologue, Merlin, and the tumor suppressor expanded function together in drosophila to regulate cell proliferation and differentiation. Development 127, 1315-1324.

Miller, L.D., Smeds, J., George, J., Vega, V.B., Vergara, L., Ploner, A., Pawitan, Y., Hall, P., Klaar, S., Liu, E.T., et al. (2005). An expression signature for p53 status in human breast cancer predicts mutation status, transcriptional effects, and patient survival. Proc Natl Acad Sci U S A 102, 13550-13555.

Moleirinho S, Chang N, Sims AH, Tilston-Lünel AM, Angus L, Steele A, Boswell V, Barnett SC, Ormandy C, Faratian D, Gunn-Moore FJ, Reynolds PA. (2012). KIBRA exhibits MST-independent functional regulation of the Hippo signaling pathway in mammals. Oncogene. doi: 10.1038/onc.2012.196

Moon, R.T., Kohn, A.D., De Ferrari, G.V., and Kaykas, A. (2004). WNT and β-catenin signalling: diseases and therapies. Nat Rev Genet 5, 691-701.

Morin-Kensicki, E.M., Boone, B.N., Howell, M., Stonebraker, J.R., Teed, J., Alb, J.G., Magnuson, T.R., O'Neal, W., and Milgram, S.L. (2006). Defects in yolk salc va-sculogenesis, chorioallantoic fusion, and embryonic axis elongation in mice with tar-geted disruption of Yap65. Mol Cell Biol 26, 77-87.

Morsut, L., Yan, K.P., Enzo, E., Aragona, M., Soligo, S.M., Wendling, O., Mark, M., Khetchoumian, K., Bressan, G., Chambon, P., et al. (2010). Negative control of Smad activity by ectodermin/Tif1gamma patterns the mammalian embryo. Development (Cambridge, England) 137, 2571-2578.

Nguyen LV, Vanner R, Dirks P, Eaves CJ. (2012) Cancer stem cells: an evolving concept. Nat Rev Cancer 12, 133-43.

Niehrs, C., and Acebron, S.P. (2012). Mitotic and mitogenic Wnt signalling. EMBO J 31, 2705-2713.

Nishioka, N., Inoue, K., Adachi, K., Kiyonari, H., Ota, M., Ralston, A., Yabuta, N., Hirahara, S., Stephenson, R.O., Ogonuki, N., et al. (2009). The Hippo signaling pathway components Lats and Yap pattern Tead4 activity to distinguish mouse trophectoderm from inner cell mass. Developmental cell 16, 398-410.

Oka, T., Remue, E., Meerschaert, K., Vanloo, B., Boucherie, C., Gfeller, D., Bader, G.D., Sidhu, S.S., Vandekerchove, J., Gettemans, J., and Sudol, M. (2010). Functional complexes between YAP2 and ZO-2 are PDZ domain-dependent, and regulate YAP2 nuclear localization and signalling. Biochem J 432, 461-472.

Ota, M., and Sasaki, H. (2008). Mammalian Tead proteins regulate cell proliferation and contact inhibition as transcriptional mediators of Hippo signaling. Development 135, 4059-4069.

Overholtzer M, Zhang J, Smolen GA, Muir B, Li W, Sgroi DC, Deng CX, Brugge JS, Haber DA. (2006). Transforming properties of YAP, a candidate oncogene on the chromosome 11q22 amplicon. Proc Natl Acad Sci U S A. *103*: 12405-10.

Padua, D., Zhang, X.H., Wang, Q., Nadal, C., Gerald, W.L., Gomis, R.R., and Massague, J. (2008). TGFbeta primes breast tumors for lung metastasis seeding through angiopoietin-like 4. Cell 133, 66-77.

Pan, D. (2010). The hippo signaling pathway in development and cancer. Dev Cell 19, 491-505.

Park, B.K., Zhang, H., Zeng, Q., Dai, J., Keller, E.T., Giordano, T., Gu, K., Shah, V., Pei, L., Zarbo, R.J., et al. (2007). NF-kappaB in breast cancer cells promotes osteolytic bone metastasis by inducing osteoclastogenesis via GM-CSF. Nat Med 13, 62-69.

Pawitan, Y., Bjöhle, J., Amler, L., Borg, A.-L., Egyhazi, S., Hall, P., Han, X., Holmberg, L., Huang, F., Klaar, S., et al. (2005). Gene expression profiling spares early breast cancer patients from adjuvant therapy: derived and validated in two population-based cohorts. Breast cancer research : BCR 7, R953-964.

Pece, S., Tosoni, D., Confalonieri, S., Mazzarol, G., Vecchi, M., Ronzoni, S., Bernard, L., Viale, G., Pelicci, P.G., and Di Fiore, P.P. (2010). Biological and molecular heterogeneity of breast cancers correlates with their cancer stem cell content. Cell 140, 62-73.

Ponti, D., Costa, A., Zaffaroni, N., Pratesi, G., Petrangolini, G., Coradini, D., Pilotti, S., Pierotti, M.A., and Daidone, M.G. (2005). Isolation and in vitro propagation of tumorigenic breast cancer cells with stem/progenitor cell properties. Cancer Res 65, 5506-5511

Qin H, Blaschke K, Wei G, Ohi Y, Blouin L, Qi Z, Yu J, Yeh RF, Hebrok M, Ramalho-Santos M. (2012). Transcriptional analysis of pluripotency reveals the Hippo pathway as a barrier to reprogramming. Hum Mol Genet *21*, 2054-67.

Ramos, A., and Camargo, F.D. (2012). The Hippo signaling pathway and stem cell biology. Trends Cell Biol 22, 339-346.

Remue, E., Meerschaert, K., Oka., T., Boucherie, C., Vandekerckhove, J., Sudol, M., and Gettemans, J. (2010). TAZ interacts with zona occludens-1 and -2 proteins in a PDZ-1 dependent manner. FEBS Lett 584, 4175-4180.

Ren, F., Zhang, L., and Jiang, J. (2010). Hippo signaling regulates Yorkie nuclear localization and activity through 14-3-3 dependent and independent mechanisms. Dev Biol 337, 303-312.

Ricci-Vitiani, L., Lombardi, D.G., Pilozzi, E., Biffoni, M., Todaro, M., Peschle, C., De Maria R. (2007). Identification and expansion of human colon-cancer-initiating cells. Nature 445, 111-115.

Robinson, B.S., Huang, J., Hong, Y., and Moberg, K.H. (2010). Crumbs regulates Salvador/Warts/Hippo signaling in Drosophila via the FERM-domain protein Expanded. Curr Biol 20, 582-590.

Sansom, O.J., Reed, K.R., Hayes, A.J., Ireland, H., Brinkmann, H., Newton, I.P., Batlle, E., Simon-Assmann, P., Clevers, H., Nathke, I.S., et al. (2004). Loss of Apc in vivo immediately perturbs Wnt signaling, differentiation, and migration. Genes & development 18, 1385-1390.

Santner, S.J., Dawson, P.J., Tait, L., Soule, H.D., Eliason, J., Mohamed, A.N., Wolman, S.R., Heppner, G.H., and Miller, F.R. (2001). Malignant MCF10CA1

cell lines derived from premalignant human breast epithelial MCF10AT cells. Breast Cancer Res Treat 65, 101-110.

Savagner, P. (2010). The epithelial-mesenchymal transition (EMT) phenomenon. Ann Oncol 21 Suppl 7, vii89-vii92.

Scheel, C., Eaton, E.N., Li, S.H., Chaffer, C.L., Reinhardt, F., Kah, K.J., Bell, G., Guo, W., Rubin, J., Richardson, A.L., et al. (2011). Paracrine and autocrine signals induce and maintain mesenchymal and stem cell states in the breast. Cell 145, 926-940.

Schlegelmilch, K., Mohseni, M., Kirak, O., Pruszak, J., Rodriguez, J.R., Zhou D., Kreger, B.T., Vasioukhin, V., Avruch, J., Brummelkamp, T.R. and Camargo, F.D. (2011). Yap1 acts downstream of alfa-catenin to control epidermal proliferation. Cell 144, 782-795.

Schmidt, M., Böhm, D., von Törne, C., Steiner, E., Puhl, A., Pilch, H., Lehr, H.-A., Hengstler, J.G., Kölbl, H., and Gehrmann, M. (2008). The humoral immune system has a key prognostic impact in node-negative breast cancer. Cancer Res 68, 5405-5413.

Sheridan C, Kishimoto H, Fuchs RK, Mehrotra S, Bhat-Nakshatri P, Turner CH, Goulet R Jr, Badve S, Nakshatri H. (2006). CD44+/CD24- breast cancer cells exhibit enhanced invasive properties: an early step necessary for metastasis. Breast Cancer Res. *8*, R59.

Shipitsin, M., Campbell, L.L., Argani, P., Weremowicz, S., Bloushtain-Qimron, N., Yao, J., Nikolskaya, T., Serebryiskaya, T., Beroukhim, R., Hu, M., et al. (2007). Molecular definition of breast tumor heterogeneity. Cancer Cell 11, 259-273.

Silvis, M.R., Kreger, B.T., Lien, W.H., Klezovitch, O., Rudakova, G.M., and Camar-go, F.D. (2011). Alfa-catenin is a tumor suppressor that control cell accumulation by regulating the localization and activity of the transcriptional coactivator Yap1. Sci Si-gnal 4, ra33.

Singh, S.K., Hawkins, C., Clarke, I.D., Squire, J.A., Bayani, J., Hide, T., Henkelman, R.M., Cusimano, M.D., Dirks, P.B. (2004). Identification of human brain tumour ini-tiating cells. Nature 432, 396-401.

Skouloudaki, K., Puetz, M., Simons, M., Courbard, J. R., Boehlke, C., Hartleben, B., Engel, C., Moeller, M. J., Englert, C., Bollig, F., Schafer, T., Ramachandran, H., Mlodzik, M., Huber, T. B., Kuehn, E. W., Kim, E., Kramer-Zucker, A. and Walz, G. (2009) Scribble participates in Hippo signaling and is required for normal zebrafish pronephoros development. Proc Natl Acad Sci USA 106, 8579-8584.

Sotiriou, C., Wirapati, P., Loi, S., Harris, A., Fox, S., Smeds, J., Nordgren, H., Farmer, P., Praz, V., Haibe-Kains, B., et al. (2006). Gene expression profiling in

breast cancer: understanding the molecular basis of histologic grade to improve prognosis. Journal of the National Cancer Institute 98, 262-272.

Stewart, S.A., Dykxhoorn, D.M., Palliser, D., Mizuno, H., Yu, E.Y., An, D.S., Sabatini, D.M., Chen, I.S., Hahn, W.C., Sharp, P.A., et al. (2003). Lentivirus-delivered stable gene silencing by RNAi in primary cells. Rna 9, 493-501.

Taelman, V.F., Dobrowolski, R., Plouhinec, J.L., Fuentealba, L.C., Vorwald, P.P., Gumper, I., Sabatini, D.D., and De Robertis, E.M. (2010). Wnt signaling requires sequestration of glycogen synthase kinase 3 inside multivesicular endosomes. Cell 143, 1136-1148.

Tapon, N., Harvey, K.F., Bell, D.W., Wahrer, D.C., Schiripo, T.A., Haber, D.A., Ha-riharan, I.K. (2002). Salvador promotes both cell cycle exit and apoptosis in Droso-phila and is mutated in human cancer cell lines. Cell 110, 467–478.

Thiery, J.P., Acloque, H., Huang, R.Y., and Nieto, M.A. (2009). Epithelial-mesenchymal transition in development and disease. Cell 139, 871-890.

Tusher, V.G., Tibshirani, R., and Chu, G. (2001). Significance analysis of mi-croarrays applied to the ionizing radiation response. Proceedings of the National Academy of Sciences of the United States of America 98, 5116-5121.

Udan, R.S., Kango-Singh, M., Nolo, R., Tao, C., Halder, G. (2003). Hippo pro-motes proliferation arrest and apoptosis in the Salvador/Warts pathway. Nat Cell Biol 5, 914–920.

van de Wetering, M., Sancho, E., Verweij, C., de Lau, W., Oving, I., Hurlstone, A., van der Horn, K., Batlle, E., Coudreuse, D., Haramis, A.P., et al. (2002). The β-catenin/TCF-4 complex imposes a crypt progenitor phenotype on colorectal cancer cells. Cell 111, 241-250.

Varelas, X., Sakuma, R., Samavarchi-Tehrani, P., Peerani, R., Rao, B.M., Dem-bowy, J., Yaffe, M.B., Zandstra, P.W., Wrana, J.L. (2008). TAZ controls Smad nucleocyto-plasmic shuttling and regulates human embryonic stem-cell self-renewal. Nature 10, 837-48

Varelas, X., Miller, B.W., Sopko, R., Song, S., Gregorieff, A., Fellouse, F.A., Sa-kuma, R., Pawson, T., Hunziker, W., McNeill, H., et al. (2010a). The Hippo pathway regulates Wnt/ β-catenin signaling. Developmental cell 18, 579-591.

Varelas, X., Samavarchi-Tehrani, P., Narimatsu, M., Weiss, A., Cockburn, K., Larsen, B.G., Rossant, J., and Wrana, J.L. (2010b). The Crumbs complex couples cell density sensing to Hippo-dependent control of the TGF-β-SMAD pathway. Developmental cell 19, 831-844.

Visvader, J.E., and Lindeman, G.J. (2008). Cancer stem cells in solid tumours: accumulating evidence and unresolved questions. Nat Rev Cancer 8, 755-768.

Weigelt B, Peterse JL, van 't Veer LJ. (2005) Breast cancer metastasis: markers and models. Nat Rev Cancer. *5*, 591-602.

Wu, S., Huang, J., Dong, J., and Pan, D. (2003). Hippo encodes a Ste-20 family pro-tein kinase that restricts cell proliferation and promotes apoptosis in conjuction with salvador and warts. Cell 114, 445-456

Xu, T., Wang, W., Zhang, S., Stewart, R.A., and Yu, W. (1995). Identifying tumor suppressor in genetic mosaics: the Drosophila lats gene encodes a putative protein ki-nase. Development 121, 1053-1063.

Xu, C., Kim, N.G., and Gumbiner, B.M. (2009). Regulation of protein stability by GSK3 mediated phosphorylation. Cell Cycle 8, 4032-4039.

Zender L, Spector MS, Xue W, Flemming P, Cordon-Cardo C, Silke J, Fan ST, Luk JM, Wigler M, Hannon GJ, Mu D, Lucito R, Powers S, Lowe SW. (2006). Identification and validation of oncogenes in liver cancer using an integrative oncogenomic approach. Cell *125*, 1253-67.

Zhan, L., Rosenberg, A., Bergami, K.C., Yu, M., Xuan, Z., Jaffe, A.B., Allred, C., and Muthuswamy, S.K. (2008). Deregulation of scribble promotes mammary tumorigenesis and reveals a role for cell polarity in carcinoma. Cell 135, 865-878.

Zhang, H., Liu, C.Y., Zha, Z.Y., Zhao, B., Yao, J., Zhao, S., Xiong, Y., Lei, Q.Y., and Guan, K.L. (2009a). TEAD transcription factors mediate the function of TAZ in cell growth and epithelial-mesenchymal transition. J Biol Chem 284, 13355-13362.

Zhang N, Bai H, David KK, Dong J, Zheng Y, Cai J, Giovannini M, Liu P, Anders RA, Pan D. (2010). The Merlin/NF2 tumor suppressor functions through the YAP oncoprotein to regulate tissue homeostasis in mammals. Dev Cell. 19, 27-38.

Zhao, B., Ye, X., Yu, J., Li, L., Li, W., Li, S., Lin, J.D., Wang, C.Y., Chinnaiyan, A.M., Lai, Z.C., et al. (2008). TEAD mediates YAP-dependent gene induction and growth control. Genes Dev 22, 1962-1971.

Zhao, B., Li, L., Tumaneg, K., Wang, C.Y., and Guan, K.L. (2010). A coordinated phosphorilation by Lats and CK1 regulates YAP stability through SCF(beta-TRCP). Genes Dev 25, 51-63.

Zhao, B., Tumaneng, K., and Guan, K.L. (2011a). The Hippo pathway in organ size control, tissue regeneration and stem cell self-renewal. Nat Cell Biol 13, 877-883.

Zhao, B., Li, L., Lu, Q., Wang, L.H., Liu, C.Y., Lei, Q., and Guan, K.L.(2011b) Angiomotin is a novel Hippo pathway component that inhibits YAP oncoprotein. Genes Dev 25, 51-63.

Zhou, D., Conrad, C., Xia, F., Park, J. S., Payer, B., Yin, Y., Lauwers, G. Y., Thasier, W., Lee, J. T., Avruch, J. and Bardeesy, N. (2009) Mst1 and Mst2 maintain

hepatocyte quiescence and suppress hepatocellular carcinoma development through inactivation of the Yap1 oncogene. Cancer Cell 16, 425-438.

Zhou, D., Zhang, Y., Wu, H., Barry, E., Yin, Y., Lawrence, E., Dawson, D., Willis, J.E., Markowitz, S.D., Camargo, F.D., and Avruch, J. (2011). Mst1 and Mst2 protein kinases restrain intestinal stem cell proliferation and colonic tumorigenesis by inhibition of Yes-associated protein (Yap) overabundance. Proc Natl Acad Sci U S A. 108, E1312-20.

TABLES

Table 1. Breast cancer datasets used in this study to build the metadataset.

Study	Affymetrix platform	Samples	Data source	References
Stockholm	HG-U133A	159	GEO GSE1456	(Pawitan et al., 2005)
Uppsala-Miller	HG-U133A	236	GEO GSE3494	(Miller et al., 2005)
Ivshina-Miller	HG-U133A	249	GEO GSE4922	(Ivshina et al., 2006)
Loi	HG-U133A	327	GEO GSE6532	(Loi et al., 2007; Loi et al., 2008; Loi et al., 2010)
Sotiriou	HG-U133A	187	GEO GSE2990	(Sotiriou et al., 2006)
Desmedt	HG-U133A	198	GEO GSE7390	(Desmedt et al., 2007)
Schmidt	HG-U133A	200	GEO GSE11121	(Schmidt et al., 2008)

Table 2. Affymetrix probesets over-expressed more than two times in G3 as compared to G1 cancers of the metadataset.

Probeset	Gene Symbol	Fold Change
202870_s_at	CDC20	3.17
209773_s_at	RRM2	3.26
204825_at	MELK	2.50
202954_at	UBE2C	2.46
202705_at	CCNB2	2.34
210052_s_at	TPX2	2.39
208079_s_at	AURKA	2.60
218542_at	CEP55	2.54
202095_s_at	BIRC5	2.64
218355_at	KIF4A	2.12
204033_at	TRIP13	2.31
204962_s_at	CENPA	2.57
209408_at	KIF2C	2.04
222077_s_at	RACGAP1	2.19
218009_s_at	PRC1	2.56
201088_at	KPNA2	2.08
203764_at	DLGAP5	2.45
203418_at	CCNA2	2.09
218039_at	NUSAP1	2.50
209714_s_at	CDKN3	2.39
204822_at	TTK	2.57
203755_at	BUB1B	2.00
209642_at	BUB1	2.20
202580_x_at	FOXM1	2.24
201890_at	RRM2	2.93
206102_at	GINS1	2.35
203362_s_at	MAD2L1	2.36
210559_s_at	CDC2	2.42
203554_x_at	PTTG1	2.12
219918_s_at	ASPM	2.61
214710_s_at	CCNB1	2.46
202779_s_at	UBE2S	2.35
203213_at	CDC2	2.38
204641_at	NEK2	2.23
211762_s_at	KPNA2	2.17
203358_s_at	EZH2	2.14
204444_at	KIF11	2.04
220651_s_at	MCM10	2.04
217755_at	HN1	2.16
204170_s_at	CKS2	2.43
201195_s_at	SLC7A5	2.44
204026_s_at	ZWINT	2.10
207828_s_at	CENPF	2.26
201292_at	TOP2A	2.67
204162_at	NDC80	2.12
203214_x_at	CDC2	2.05
218662_s_at	NCAPG	2.00
201291_s_at	TOP2A	3.00
202589_at	TYMS	2.16
202503_s_at	KIAA0101	2.10
218883_s_at	MLF1IP	2.33
218585_s_at	DTL	2.19
219010_at	C1orf106	2.29
204533_at	CXCL10	2.76
219148_at	PBK	2.18
203560_at	GGH	2.20
202270_at	GBP1	2.28
215223_s_at	SOD2	2.06
204475_at	MMP1	3.87
203126_at	IMPA2	2.04
211122_s_at	CXCL11	2.81
210163_at	CXCL11	2.78
202269_x_at	GBP1	2.41
206632_s_at	APOBEC3B	2.08
202917_s_at	S100A8	4.25
204913_s_at	SOX11	2.43
206134_at	ADAMDEC1	2.17
203915_at	CXCL9	2.53
213975_s_at	LYZ	2.03
204914_s_at	SOX11	2.09
205347_s_at	TMSB15A	2.05
217388_s_at	KYNU	2.21
206392_s_at	RARRES1	2.16
220414_at	CALML5	2.28
216491_x_at	IGHM	2.07
203535_at	S100A9	2.18
204351_at	S100P	2.37
214777_at	IGKV4-1	2.01

Table 3. RNAi sequences. Related to Experimental Procedures.

siRNA/ shRNA	**Interfering sequence** (target)	**Notes**
Control	TTCTCCGAACGTGTCACGT	
GFP	CAAGCTGACCCTGAAGTTC	
human		
TAZ#1	ACGTTGACTTAGGAACTTT	A mix of the three TAZ siRNAs was used, unless otherwise specified.
TAZ#2	AGAGGTACTTCCTCAATCA	
TAZ#3	AGGTACTTCCTCAATCACA	
GSK3#1	CAGGGAACTAGTCGCCATC (GSK3α) CCCAAATGTCAAACTACCA (GSK3β)	GSK3 siRNA#1 was used, unless otherwise specified.
GSK3#2	GAAGGTTCTCCAGGACAAG (GSK3α) AGTTGGTAGAAATAATCAA (GSK3β)	
APC#1	GACGTTGCGAGAAGTTGGA	APC siRNA#1 was used, unless otherwise specified.
APC#2	TAATGAACACTACAGATAG	
Axin	GGGCATATCTGGATACCTG (Axin1) GGATACCTGCCGACCTTAA (Axin1) GAGTAGCCAAAGCGATCTA (Axin2) CGATCCTGTTAATCCTTAT (Axin2)	
β-catenin#1	AGGTGCTATCTGTCTGCTC	A mix of β-catenin siRNAs #3 and #4 was used, unless otherwise specified.
β-catenin#2	AACAGTCTTACCTGGACTC	
β-catenin#3	GTAGCTGATATTGATGGAC	
β-catenin#4	GCTTGGAATGAGACTGCTG	
β-TrCP#1	GTGGAATTTGTGGAACATC (β-TrCP1 and β-TrCP2)	β-TrCP siRNA#1 was used, unless otherwise specified.
β-TrCP#2	GCGTTGTATTCGATTTGATAA (β-TrCP1) AAATGTCGGTACTTGAAGAGT (β-TrCP2)	
γ−catenin#1	AGTCGGCCATTGTGCATCT	γ−catenin siRNA#1 was used, unless otherwise specified.
γ−catenin#2	GGGCATCATGGAGGAGGAT	
LATS	Dharmacon siGenome smart pool M-004632-00 (LATS1) Dharmacon siGenome smart pool M-003865-02 (LATS2)	
mouse		
TAZ	TCATTGCGAGATTCGGCTG	

Table 4. PCR oligo sequences. Related to Experimental Procedures.

Gene	Forward primer	Reverse primer
human		
GAPDH	AGCCACATCGCTCAGACAC	GCCCAATACGACCAAATCC
TAZ	GGCTGGGAGATGACCTTCAC	CTGAGTGGGGTGGTTCTGCT
APC	GCCCCTGACCAAAAAGGAAC	TGGCAGCAACAGTCCCACTA
Axin1	AGCCGTGTCGGACATGGA	AAGTAGTACGCCACAACGATGCT
Axin2	TGTGAGGTCCACGGAAACTG	CGTCAGCGCATCACTGGATA
CTGF	AGGAGTGGGTGTGTGACGA	CCAGGCAGTTGGCTCTAATC
Cyclin-D1	TCAAATGTGTGCAGAAGGAGGT	GACAGGAAGCGGTCCAGGTA
mouse		
GAPDH	ATCCTGCACCACCAACTGCT	GGGCCATCCACAGTCTTCTG
TAZ	ATGAATCCGTCCTCGGTGC	GAGTTGAAGAGGGCTTCGAG
Flag-mTAZ	ATGGACTACAAAGACGATGACG	GAGTTGAAGAGGGCTTCGAG
Cyr61	GCTCAGTCAGAAGGCAGACC	GTTCTTGGGGACACAGAGGA
CTGF	CTGCCTACCGACTGGAAGAC	CATTGGTAACTCGGGTGGAG
Cyclin-D1	GACCTTTGTGGCCCTCTGTG	AAAGTGCGTTGTGCGGTAGC

FIGURES

Figure 1. The Hippo pathway.

(A) Schematic representation of the Hippo pathway components in flies (left panel) and vertebrates (right panel). Modified from Halder and Johnson, 2011.

(B) Hippo mutant phenotype in flies. Images and scanning electron micrographs of a wild-type fly (Hippo wt) and a fly with clones of cells homozygous mutant for Hippo that exhibit overgrowth of the adult cuticle (Hippo mutant). Modified from Udan et al., 2003.

(C-D) Hippo mutant phenotypes in mice. (C) Comparison between a mouse liver at 2 months of age from a wild-type animal and a liver at 2 months of age from a mouse mutant in which both *Mst1* and *Mst2* have been genetically inactivated. Modified from Zhou et al., 2009. (D) Comparison between a mouse heart from a wild-type animal and a heart from a *Sav1* knockout mouse. Modified from Heallen et al., 2011.

A

Drosophila

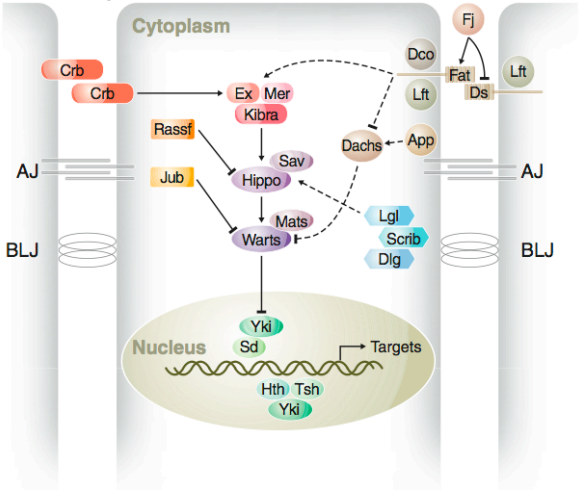

B

Vertebrate

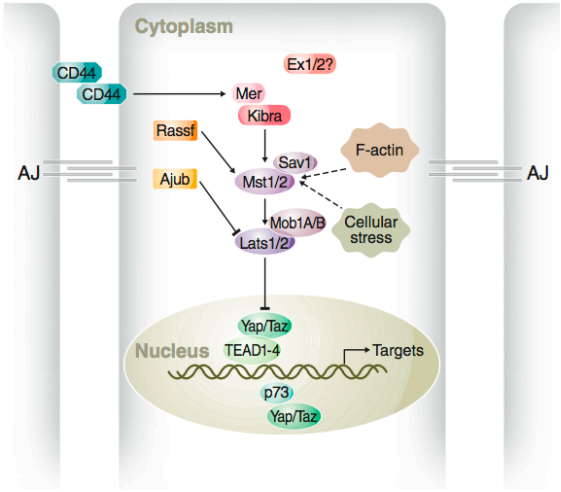

C

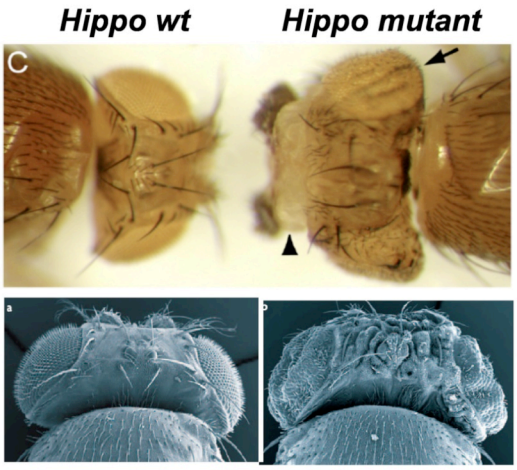

D

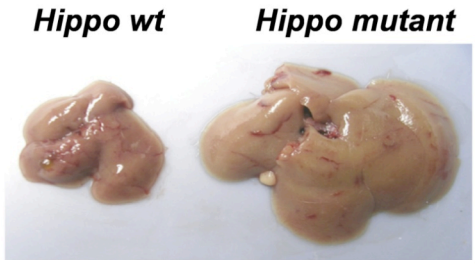

E

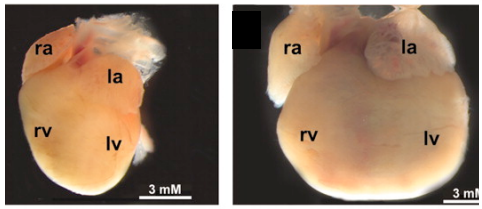

Figure 1

Figure 2. YAP/TAZ signature correlate with high histological grades, stemness and metastasis in breast tumors.

(A-B) Enrichment of gene signatures in the list of genes preferentially expressed in G3 versus G1 tumors in the metadataset. (A) Scheme of the computational procedure used to generate the data reported on the right. (B) Numbers indicate p-values (corrected for multiple tests) for significance of the enrichment. Signatures significantly enriched in G3 tumors (p-value < 0.05) are indicated in bold. ‘‘No overlap’’ indicates the absence of genes in common between the indicated signature and the genes overexpressed in G3 tumors.

(C) Average gene-expression values of signatures for normal mammary (hNMSC), breast cancer (IGS, CD44high), and embryonic (ES1, ES2, ES-like) stem cells in breast tumor samples stratified according to histological grading. G2 tumors were stratified in two groups according to high or low expression of the TAZ/YAP signature. Average gene-expression values of the TAZ/YAP signature (lane 1) are shown as control of the procedure. Data are shown as mean ± SEM.

(D) Kaplan-Meier graphs representing the probability of cumulative metastasis-free survival in breast cancer patients from the metadataset stratified according to the TAZ/YAP signature. The log-rank test p-value reflects the significance of the association between TAZ/YAP signature ‘‘Low’’ and longer survival.

A

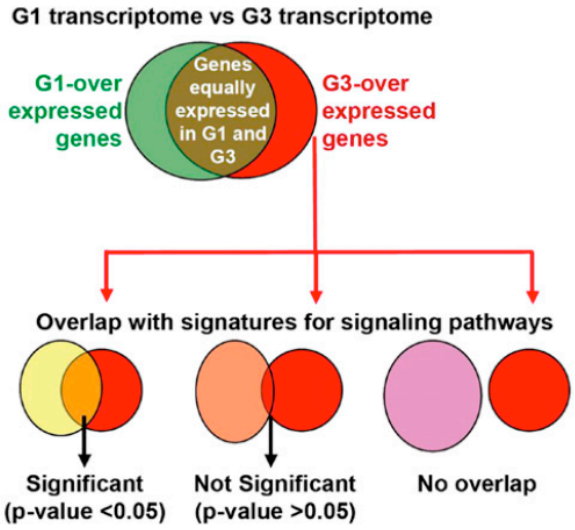

B

metadataset

SIGNATURES	ENRICHMENT IN G3 (p-values)
Normal mammary stem cells	**0.0002**
Embryonic stem cells 1	**<0.0001**
TAZ/YAP	**<0.0001**
YAP conserved	**0.0002**
Notch-A	0.1298
Notch-B	No overlap
Ras	No overlap
ERBB2	0.1499
β-catenin	No overlap
Wnt	No overlap
TGFβ-A	No overlap
TGFβ-B	0.3661
NF-kB	0.5443
STAT3	No overlap
Src	0.1917

C

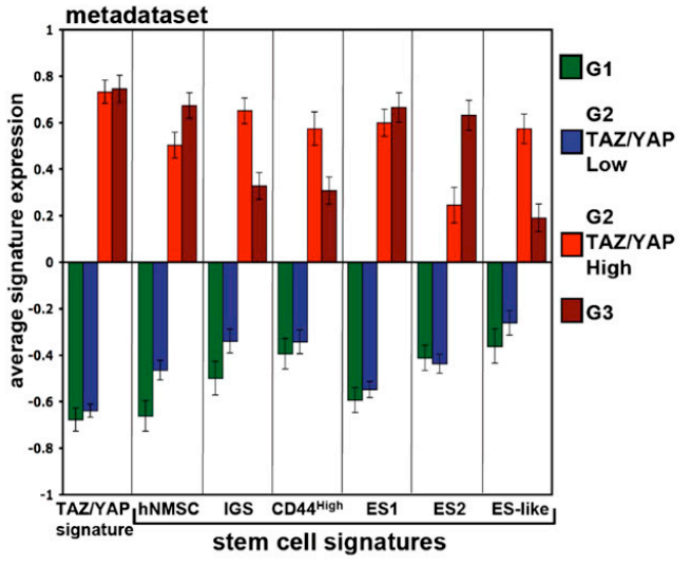

D

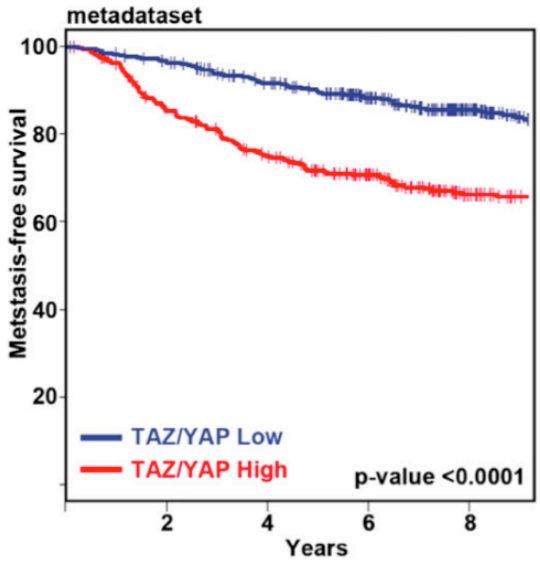

Figure 2

Figure 3. Validation of the MII-MIV cell lines as model for increased CSC content and TAZ level

(A) Schematic representation of the MCF10A-MII-MIV cellular model.

(B) Quantification of primary and secondary mammospheres formed by MII or MIV cells (mean + SEM of six experiments).

(C) Representative hematoxylin and eosin staining of tumors emerging after fat pad injection of $RAG^{-/-}$ mice with MII or MIV cell lines.

(D) Tumor seeding ability of MII and MIV. The indicated number of cells was injected in the fat pad of $RAG^{-/-}$ mice. The table reports data as the number of mice developing palpable tumors after five weeks / the number of injected mice.

(E) Western blot analysis for YAP, TAZ and GAPDH (loading control) in lysates from the MII, MIV and MDA-MB-231 cells.

(F) Western blot analysis for TAZ and CTGF in lysates from control (shControl) and TAZ-depleted (shTAZ) MIV cells.

(G) Quantification of primary and secondary mammospheres formed by shControl or shTAZ MIV cells (mean + SEM of six experiments).

(H-I) Effects of TAZ reconstitution in MIV-shTAZ cells. MIV-shTAZ cells were transduced with a rtTA-encoding lentiviral vector in combination with tetracycline-inducible vectors encoding EGFP or wild-type mouse TAZ (mTAZ). The two resulting cell lines (MIV-shTAZ+EGFP, MIV-shTAZ +mTAZ) were treated with doxycycline (0.1 mg/ml) and compared with shControl and parental shTAZ MIV cells. (H) Western blot analysis for TAZ and CTGF in lysates from the indicated cell lines. (I) Quantification of primary mammospheres formed by the cell lines described above (mean + SEM of six experiments).

(J) Tumor-seeding ability of shControl and shTAZ MIV cells. The indicated number of cells were injected into the fat pads of SCID mice. Palpable tumor formation was evaluated 3 weeks after transplantation. Results are shown as the fraction of mice developing palpable tumors.

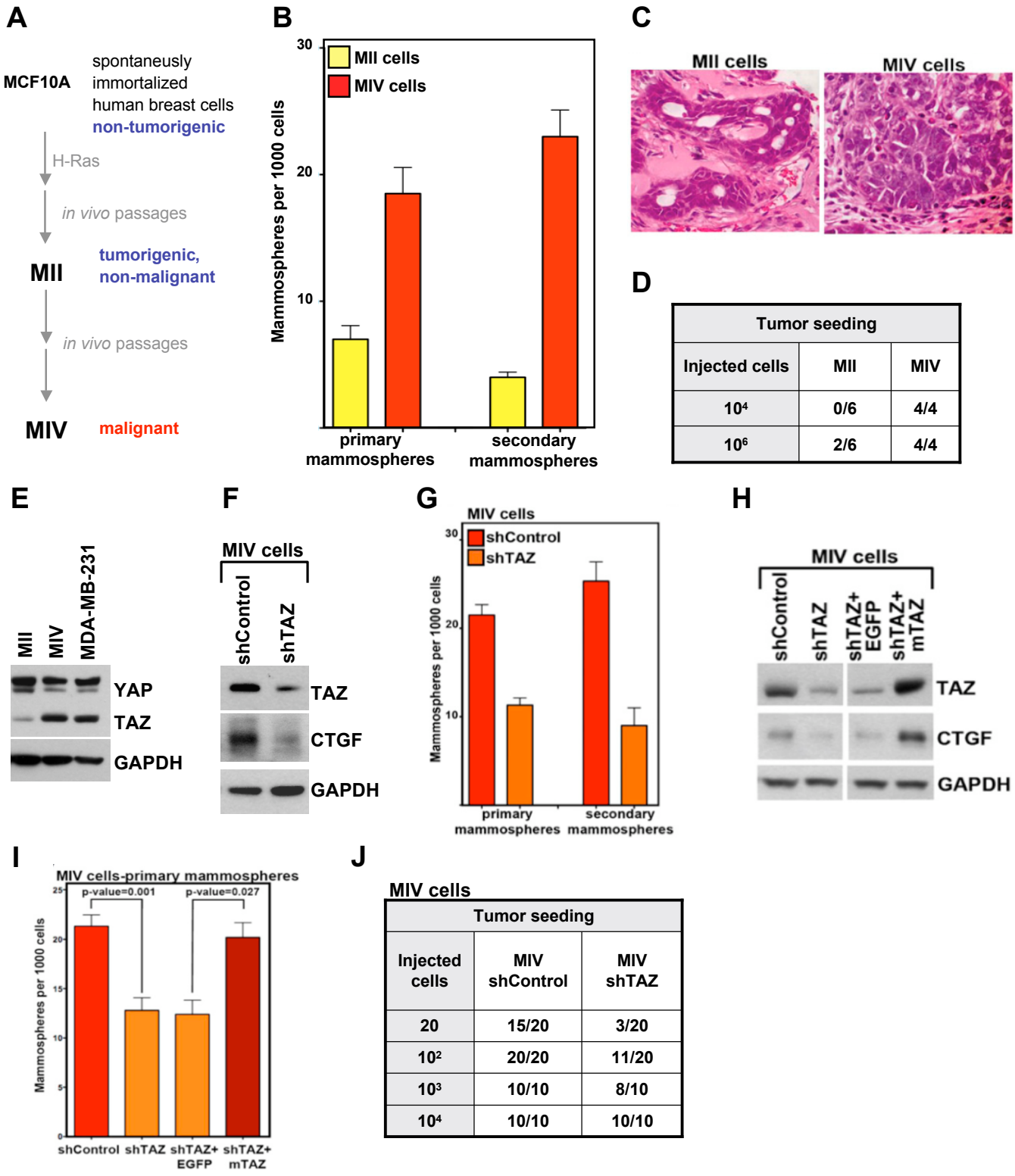
A
MCF10A
spontaneusly immortalized human breast cells
non-tumorigenic
H-Ras
in vivo passages
MII
tumorigenic, non-malignant
in vivo passages
MIV
malignant
B
MII cells
MIV cells
Mammospheres per 1000 cells
30
20
10
primary mammospheres
secondary mammospheres
C
MII cells
MIV cells
D
Tumor seeding
Injected cells
MII
MIV
10⁴
0/6
4/4
10⁶
2/6
4/4
E
MII
MIV
MDA-MB-231
YAP
TAZ
GAPDH
F
MIV cells
shControl
shTAZ
TAZ
CTGF
GAPDH
G
MIV cells
shControl
shTAZ
Mammospheres per 1000 cells
30
20
10
primary mammospheres
secondary mammospheres
H
MIV cells
shControl
shTAZ
shTAZ+ EGFP
shTAZ+ mTAZ
TAZ
CTGF
GAPDH
I
MIV cells-primary mammospheres
p-value=0.001
p-value=0.027
Mammospheres per 1000 cells
25
20
15
10
5
0
shControl
shTAZ
shTAZ+ EGFP
shTAZ+ mTAZ
J
MIV cells
Tumor seeding
Injected cells
MIV shControl
MIV shTAZ
20
15/20
3/20
10²
20/20
11/20
10³
10/10
8/10
10⁴
10/10
10/10

Figure 3

Figure 4. TAZ protein level and activity is elevated in $CD44^{high}$ subpopulation of MII cells and sustain their self-renewal capacities

(A) FACS profile of MII cells with CD24 and CD44 markers. MII cells presented two distinct subpopulation (first panel on the left): $CD44^{Low}CD24^{Low}$ (green) and $CD44^{High}CD24^{Low}$ (red). Once sorted (sorting efficiency is shown in the middle panels) and cultured for a month, the $CD44^{High}CD24^{Low}$ can recreate the entire MII population, whereas the $CD44^{Low}CD24^{Low}$ can not.

(B) Western blot analysis for expression of TAZ, CTGF and Survivin in the $CD44^{Low}CD24^{Low}$ and $CD44^{High}CD24^{Low}$ populations from FACS-sorted MII cells.

(C) Hoechst-33342 staining of MII cells. Left panel: Representative FACS profile of MII cells stained with Hoechst-33342. The SP cells are shown in green. Right panel: Distribution of SP cells according to CD44 expression. The large majority (86%) of the SP is in the $CD44^{High}CD24^{Low}$ population.

(D) Quantification of secondary mammospheres formed by $CD44^{Low}CD24^{Low}$ and $CD44^{High}CD24^{Low}$ MII cells (mean + SEM of six experiments). MII cell populations were purified by FACS, amplified in 2D culture and used for mammosphere formation.

(E) Western blot analysis for TAZ in lysates from control (shGFP) and TAZ-depleted (shTAZ) MII cells.

(F) Effects of TAZ depletion on $CD44^{High}$ subpopulation in MII cells. Left: representative FACS profiles of shGFP or shTAZ#1 MII cells. Right: quantification of $CD44^{High}$ subpopulation in the indicated cell lines.

(G) Quantification of secondary mammospheres formed by shGFP- and shTAZ-MII cells (mean + SEM of six experiments).

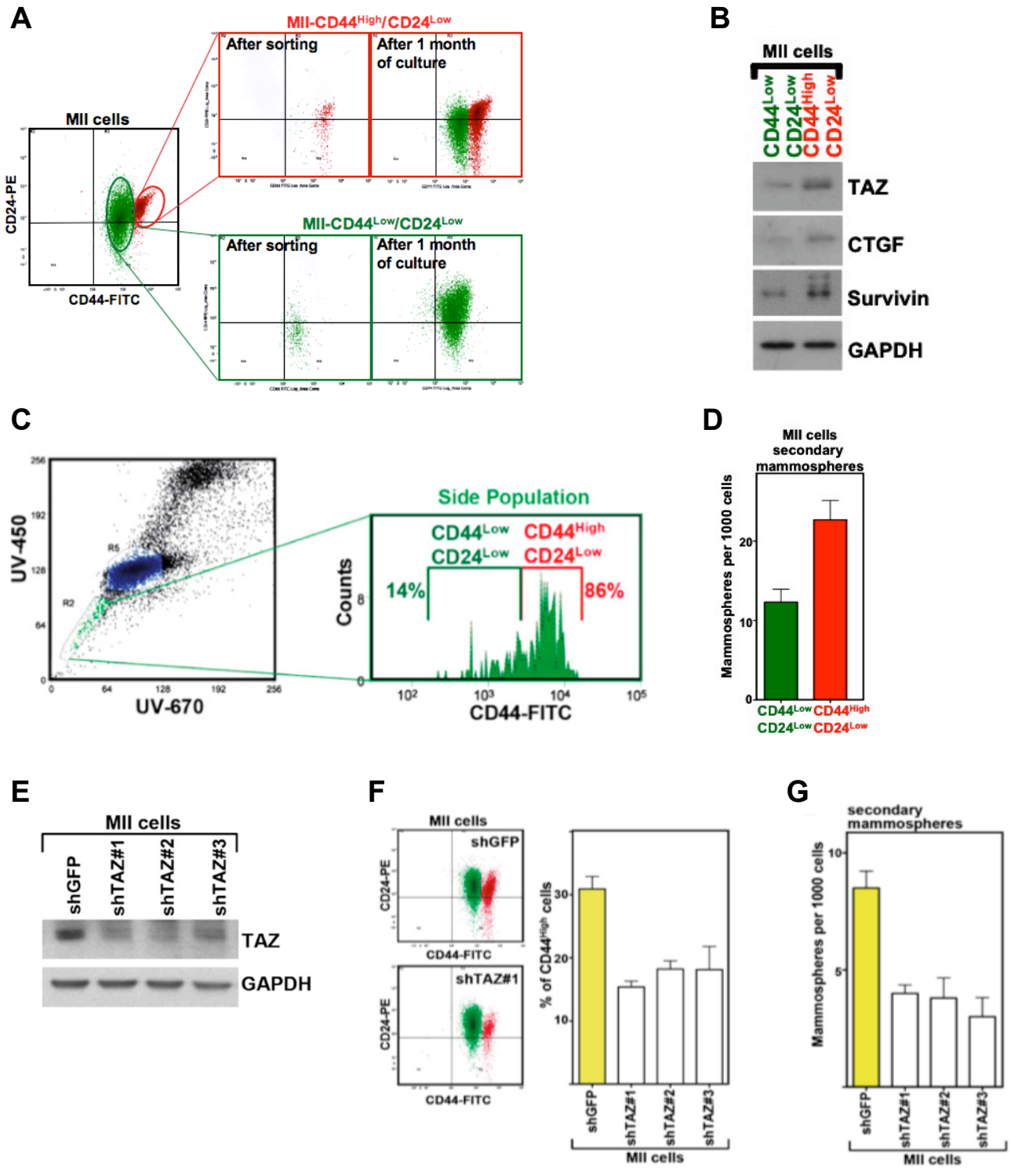
A
MII-CD44High/CD24Low
After sorting
After 1 month of culture
MII cells
CD24-PE
CD44-FITC
MII-CD44Low/CD24Low
After sorting
After 1 month of culture
B
MII cells
CD44Low CD24Low
CD44High CD24Low
TAZ
CTGF
Survivin
GAPDH
C
UV-450
UV-670
R5
R2
Side Population
CD44Low CD24Low
CD44High CD24Low
14%
86%
Counts
CD44-FITC
D
MII cells secondary mammospheres
Mammospheres per 1000 cells
CD44Low CD24Low
CD44High CD24Low
E
MII cells
shGFP
shTAZ#1
shTAZ#2
shTAZ#3
TAZ
GAPDH
F
MII cells
shGFP
shTAZ#1
CD24-PE
CD44-FITC
% of CD44High cells
shGFP
shTAZ#1
shTAZ#2
shTAZ#3
MII cells
G
secondary mammospheres
Mammospheres per 1000 cells
shGFP
shTAZ#1
shTAZ#2
shTAZ#3
MII cells

Figure 4

Figure 5. TAZ confers self-renewal capacities to breast cancer cells

(A) Western blot analysis for TAZ, CTGF, PAI-1 and Survivin in control (Empty vector) and TAZ S89A-expressing MII cells.

(B) Quantification of primary, secondary and tertiary mammospheres formed by MII-empty vector or MII-TAZ S89A cells (mean + SEM of six experiments).

(C) Representative FACS profiles with CD24 and CD44 markers of MII cells transduced with control (empty vector) or TAZ S89A-encoding retroviral vectors, and, as comparison, of MIV and MDA-MB-231 cells

(D-E) Forced expression of TAZ increase mammosphere capacity of $CD44^{Low}CD24^{Low}$. MII cells were transduced with vectors encoding for the reverse tetracycline-dependent transactivator (rtTA) and for a doxycycline-inducible TAZ S89A or EGFP and FACS-sorted according to their $CD44^{Low}CD24^{Low}$ or $CD44^{How}CD24^{Low}$ profile. Each subpopulation was then left untreated or treated with doxycycline (0.5 μg/ml) to induce either TAZ S89A or EGFP, and then tested for mammosphere formation. (D) Schematic representation of the experiment. (E) Quantification of secondary mammospheres formed by the subpopulation of MII cells described above (mean + SEM of six experiments).

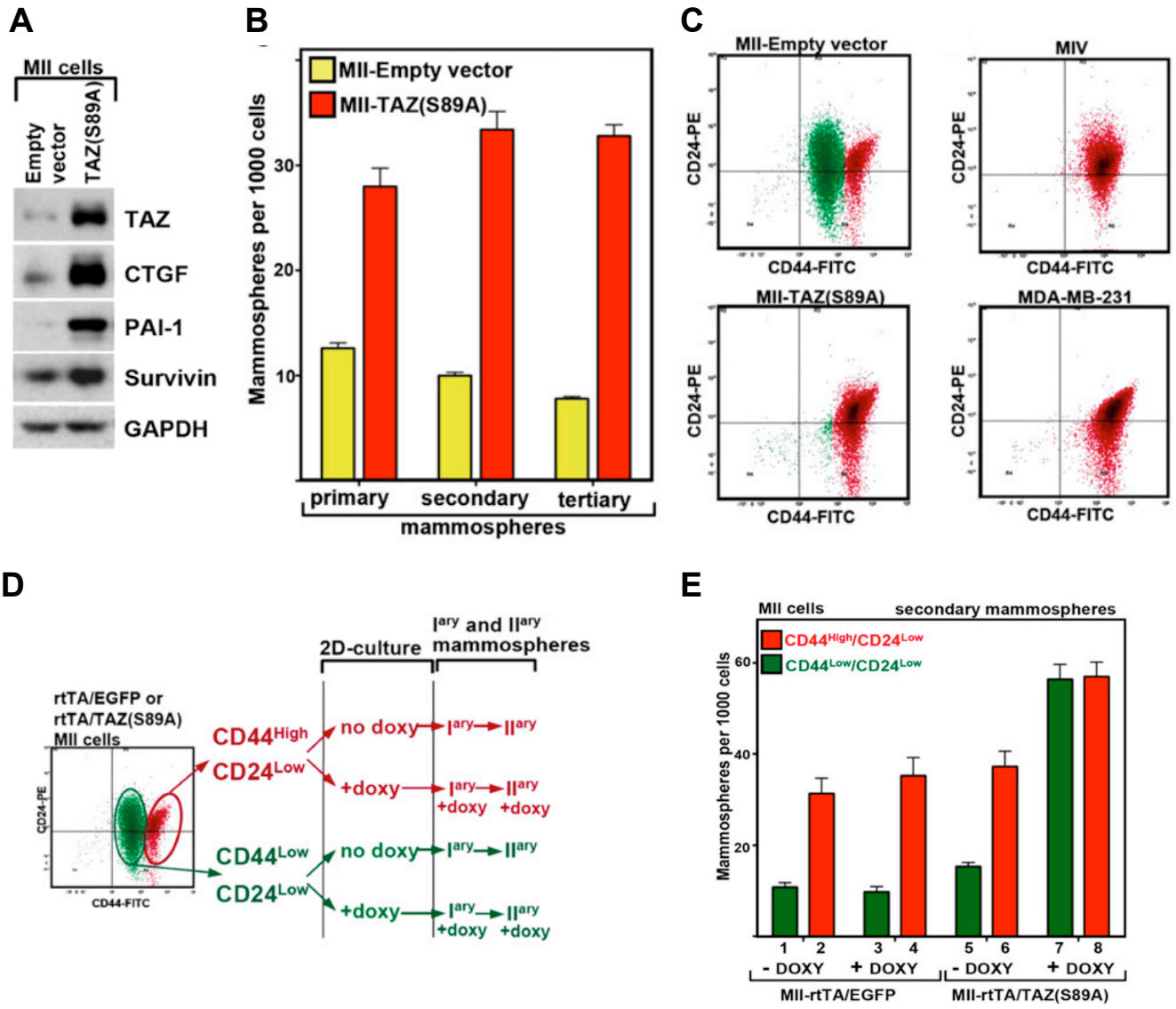
A
MII cells
Empty vector
TAZ(S89A)
TAZ
CTGF
PAI-1
Survivin
GAPDH
B
MII-Empty vector
MII-TAZ(S89A)
Mammospheres per 1000 cells
30
20
10
primary
secondary
tertiary
mammospheres
C
MII-Empty vector
MIV
MII-TAZ(S89A)
MDA-MB-231
CD24-PE
CD44-FITC
D
rtTA/EGFP or
rtTA/TAZ(S89A)
MII cells
CD24-PE
CD44-FITC
2D-culture
I ary and II ary
mammospheres
CD44High
CD24Low
CD44Low
CD24Low
no doxy
+doxy
I ary
II ary
+doxy
E
MII cells
secondary mammospheres
CD44High/CD24Low
CD44Low/CD24Low
Mammospheres per 1000 cells
60
40
20
1 2 3 4 5 6 7 8
- DOXY
+ DOXY
- DOXY
+ DOXY
MII-rtTA/EGFP
MII-rtTA/TAZ(S89A)

Figure 5

Figure 6. TAZ confers resistance to chemotherapy to breast cancer cells

(A) Representative FACS profile of MII-Empty vector and MII-TAZ S89A cells stained with Hoechst-33342. The exclusion of the Hoechst dye in MII-TAZ S89A cells is blocked by Verapamil.

(B) Quantification of the Side population of the cells described in (A).

(C) Dose-response curves of MII-Empty vector and MII-TAZ S89A cells treated with Paclitaxel. Bars denote the standard error (n = 4).

(D) Dose-response curves of MII-Empty vector and MII-TAZ S89A cells treated with Doxorubicin. Bars denote the standard error (n = 4).

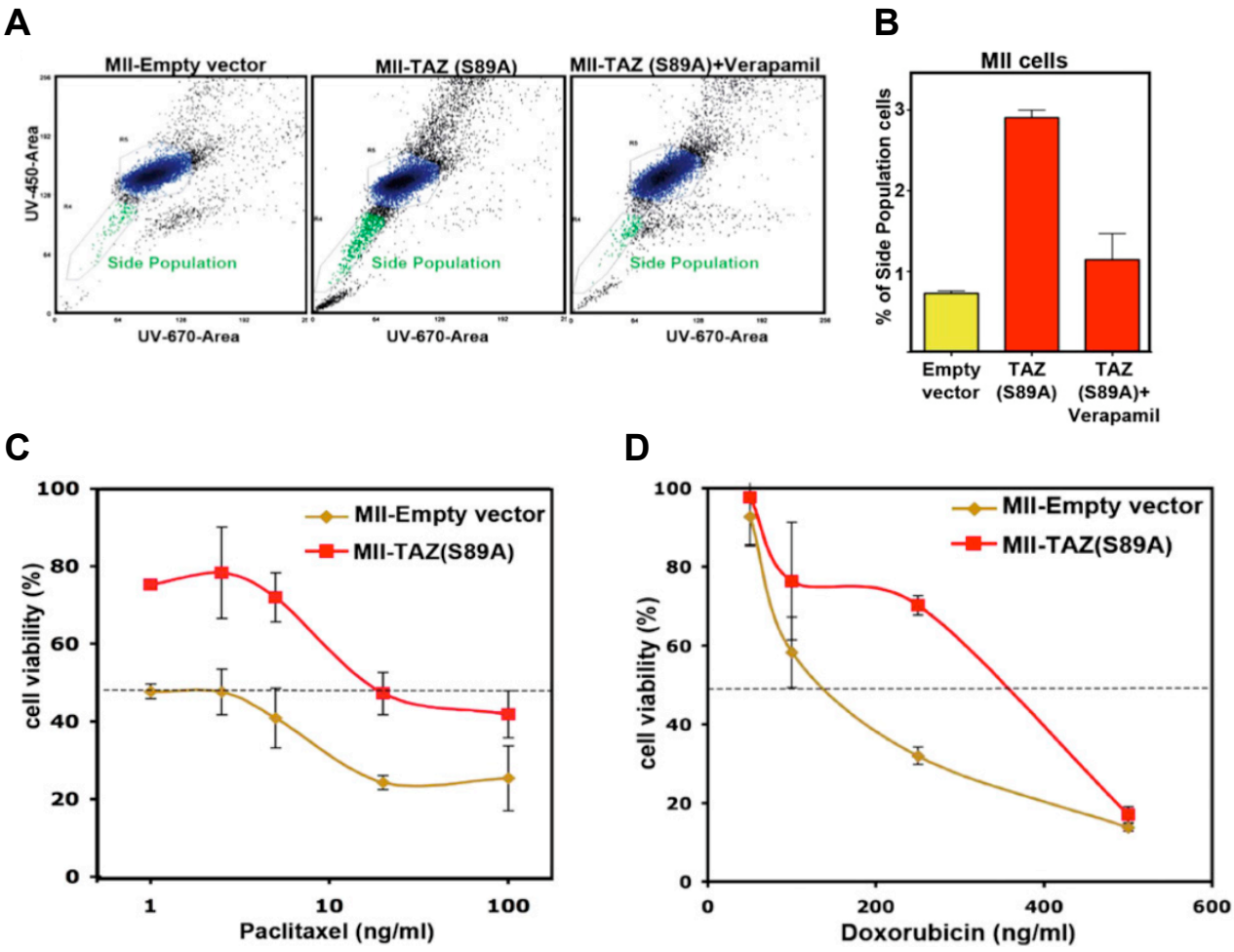
A
MII-Empty vector
MII-TAZ (S89A)
MII-TAZ (S89A)+Verapamil
UV-450-Area
Side Population
UV-670-Area
B
MII cells
% of Side Population cells
Empty vector
TAZ (S89A)
TAZ (S89A)+ Verapamil
C
cell viability (%)
MII-Empty vector
MII-TAZ(S89A)
Paclitaxel (ng/ml)
D
cell viability (%)
MII-Empty vector
MII-TAZ(S89A)
Doxorubicin (ng/ml)

Figure 6

Figure 7. TAZ promotes the formation of high-grade breast cancers

(A) Frequency of TAZ-positive G1 or G3 primary human breast cancers as judged by immunohistochemistry (IHC). Tumors were scored as positive when over 10% of cells displayed nuclear TAZ staining similar to or stronger than that of the cells of normal ducts included in the same section. 35/44 G3 tumors and only 1/26 G1 tumor were found positive for TAZ expression (p value < 0.0001).

(B-C) Representative IHC pictures for TAZ expression in G1 (A) or G3 (B) invasive human breast cancer samples. Nuclei are counterstained with hematoxylin. Black arrowheads in (A) point to the TAZ-positive cells of the normal mammary ductal tissue (NT) included in the same section with G1 tumor structures (G1). Inset in (A) shows (white arrowhead) very rare TAZ-positive cells that are seldom associated with G1 tumors.

(D) Tumor seeding ability of MII-empty vector and MII-TAZ S89A cells. The indicated number of cells was injected in the fat pad of $RAG^{-/-}$ mice. The table reports data as the number of mice developing palpable tumors after five weeks / the number of injected mice.

(E-F) Representative hematoxylin and eosin staining of tumors emerging from fat-pad injection of MII-empty vector (E) and MII-TAZ S89A cells (F).

A

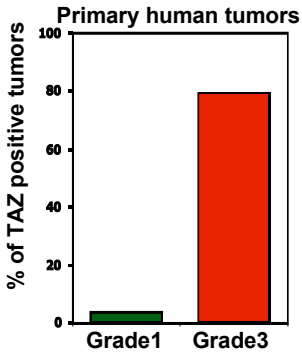

B

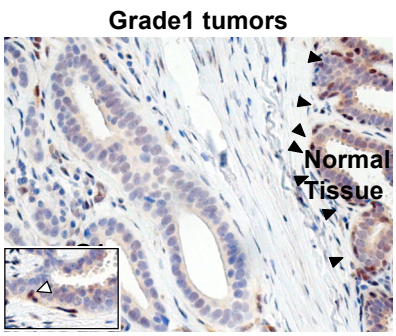

C

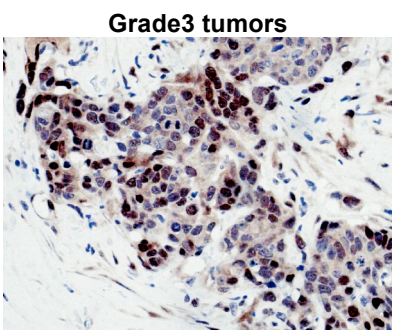

D

Tumor seeding		
Injected cells	MII-Empty vector	MII-TAZ(S89A)
10^4	0/6	2/7
$3x10^5$	1/6	3/6
10^6	1/7	5/7
$3x10^6$	2/6	4/6

E

F

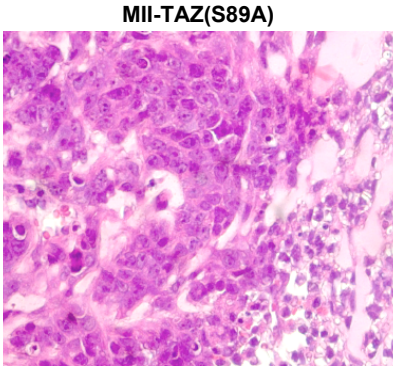

Figure 7

Figure 8. Summary of the results reported in Part 1

Schematic representation of the results presented in Part 1 regarding the role of TAZ in breast tumor as cancer stem cell determinant.

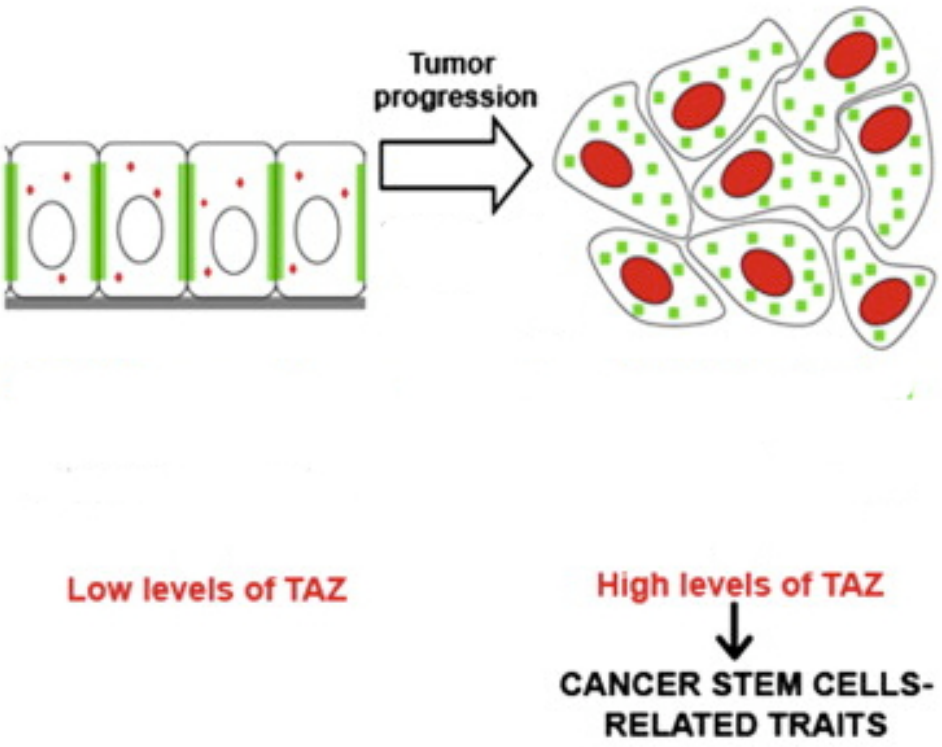
Tumor
progression
Low levels of TAZ
High levels of TAZ
CANCER STEM CELLS-
RELATED TRAITS

Figure 8

Figure 9. Wnt signaling promotes TAZ stabilization and activation

(A) HEK293 cells were transfected with the indicated siRNAs and either left untreated (control conditioned medium, Co) or treated with Wnt3A-conditioned medium for 24 hr. Where indicated, the Wnt inhibitor XAV939 (1 μM) was added to the medium. *Top panel*: Luciferase assay with 8xGTIIC reporter. Bars are mean + SD. *Bottom panel*: western blot for TAZ, YAP, β-catenin and GAPDH (loading control) in the extracts used for the luciferase assay.

(B) qRT-PCR for *TAZ* mRNA expression in HEK293 cells left untreated (control conditioned medium, Co) or treated with Wnt3A-conditioned medium for 24 hr. Data were normalized to control-treated cells; bars are mean + SD.

(C) Validation of Wnt activity using the β-catenin/TCF-luciferase reporter (BAT-Lux). HEK293 cells were transfected with BAT-Lux and with Control or β-catenin siRNAs, and either left untreated (Co) or treated with Wnt3A-conditioned medium for 24 hr. Where indicated, the Wnt inhibitor XAV939 (1 μM) was added to the medium. Data are normalized to lane 1 and are presented as mean + SD.

(D) HEK293 cells were transfected with the indicated siRNAs and used for a luciferase assay on 8xGTIIC reporter (*top panel*). Bars are mean + SD.

(E) HEK293 cells were transfected with Control, GSK3, APC or Axin siRNAs, either alone or with TAZ siRNA, and used for a luciferase assay on 8xGTIIC reporter (*top panel*) or for western blot analysis (*bottom panel*). Bars are mean + SD.

(F) Luciferase assay on BAT-Lux reporter recording the β-catenin transcriptional activity in HEK293 cells transiently transfected with Control, GSK3, APC or Axin siRNAs, either alone or in combination with β-catenin siRNA. Data are normalized to lane 1 and are presented as mean + SD.

(G) HEK293 cells were transfected with Control or LATS siRNAs, and either left untreated (control conditioned medium, Co) or treated with Wnt3A-conditioned medium for 24 hr. *Top panel*: Luciferase reporter assay of the indicated samples. Data are normalized to lane 1 and are presented as mean + SD. *Bottom panel*: western blot for TAZ in the same extracts used above.

(H) Luciferase assay on 8xGTIIC reporter recording the transcriptional activity of mouse wild-type TAZ or TAZ 4SA transiently transfected in HEK293 cells, in the absence (Co) or presence (Wnt3A) of Wnt stimulation. Cells were transfected

with TAZ siRNA to avoid interference from regulations of endogenous TAZ. *Top panel*: Luciferase reporter assay of the indicated samples. Data are normalized to lane 1 and are presented as mean + SD. *Bottom panel*: representative western blot for TAZ in the same extracts used for the luciferase assay.

(I-J) TAZ levels and expression of *Cyr61*, *CTGF* and *Cyclin-D1* in control and APC deficient mouse livers, as evaluated by western blot or qRT-PCR.

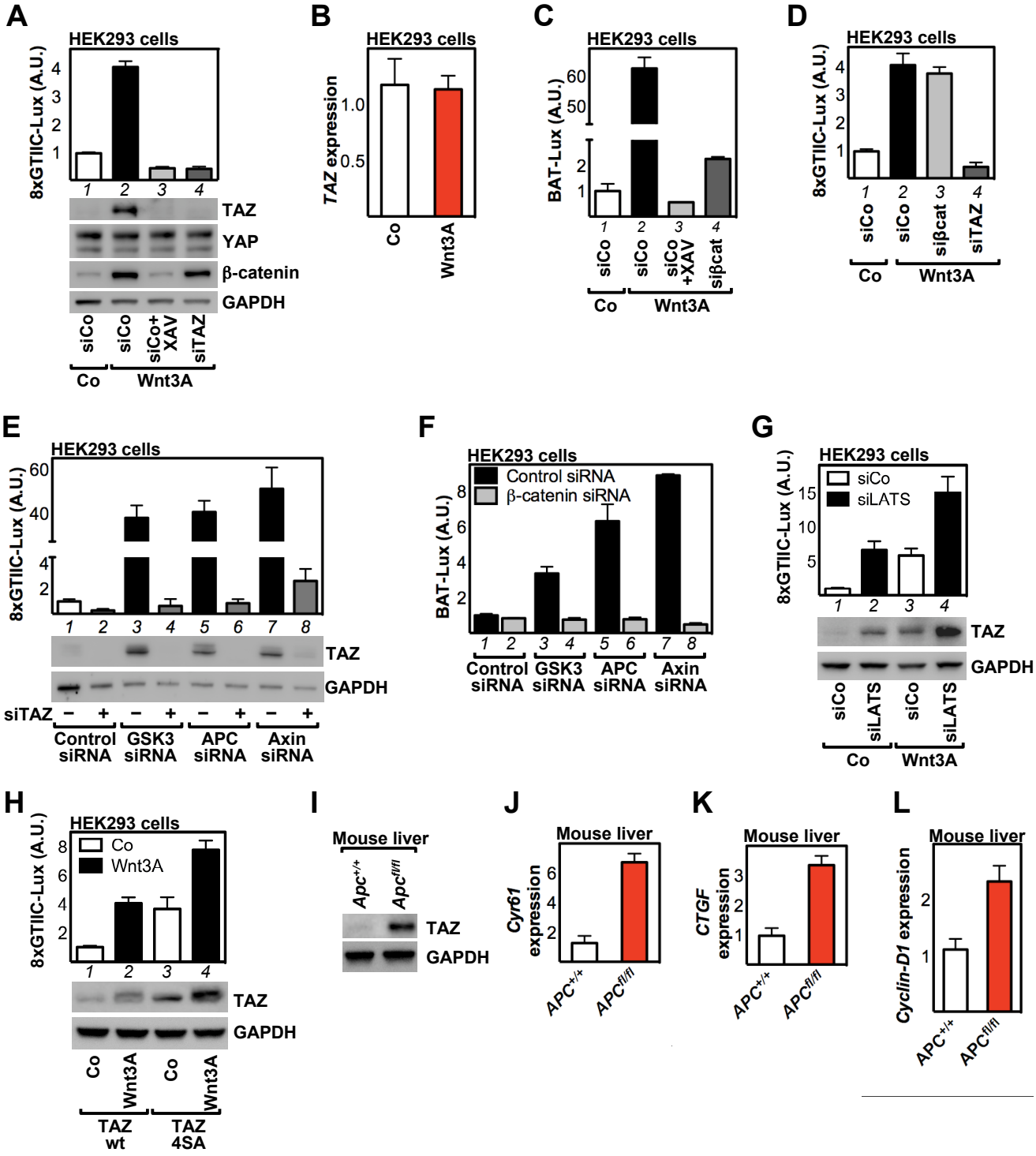
A
HEK293 cells
8xGTIIC-Lux (A.U.)
TAZ
YAP
β-catenin
GAPDH
siCo
siCo
siCo+ XAV
siTAZ
Co
Wnt3A
B
HEK293 cells
TAZ expression
Co
Wnt3A
C
HEK293 cells
BAT-Lux (A.U.)
siCo
siCo
siCo +XAV
siβcat
Co
Wnt3A
D
HEK293 cells
8xGTIIC-Lux (A.U.)
siCo
siCo
siβcat
siTAZ
Co
Wnt3A
E
HEK293 cells
8xGTIIC-Lux (A.U.)
TAZ
GAPDH
siTAZ
Control siRNA
GSK3 siRNA
APC siRNA
Axin siRNA
F
HEK293 cells
Control siRNA
β-catenin siRNA
BAT-Lux (A.U.)
Control siRNA
GSK3 siRNA
APC siRNA
Axin siRNA
G
HEK293 cells
siCo
siLATS
8xGTIIC-Lux (A.U.)
TAZ
GAPDH
siCo
siLATS
siCo
siLATS
Co
Wnt3A
H
HEK293 cells
Co
Wnt3A
8xGTIIC-Lux (A.U.)
TAZ
GAPDH
Co
Wnt3A
Co
Wnt3A
TAZ wt
TAZ 4SA
I
Mouse liver
Apc+/+
Apcfl/fl
TAZ
GAPDH
J
Mouse liver
Cyr61 expression
APC+/+
APCfl/fl
K
Mouse liver
CTGF expression
APC+/+
APCfl/fl
L
Mouse liver
Cyclin-D1 expression
APC+/+
APCfl/fl

Figure 9

Figure 10. GSK3 mediates TAZ degradation

(A) β-TrCP depletion leads to TAZ stabilization in MII cells, as revealed by western blot.

(B) Top panel: Luciferase assay on 8xGTIIC reporter recording TAZ transcriptional activity in HEK293 cells transfected with Control siRNA or two independent siRNAs targeting β-TrCP, with or without TAZ siRNA. Where indicated, a construct encoding a dominant-negative version of human Cullin1 was transfected together with the reporter (lanes 7 and 8). Data are normalized to lane 1 and bars are mean + SD. Bottom panel: western blot for TAZ expression in the same extracts used for the luciferase assay.

(C) Endogenous TAZ binds to β-TrCP in a GSK3-dependent manner. Co-immunoprecipitation and western blot analysis of MII cell lysates shows that endogenous β-TrCP is pulled-down specifically by TAZ (lane 1 vs 2), only in the presence of GSK3 (lane 2 vs 3).

(D) GSK3 kinase activity is essential to dampen TAZ protein levels and function. MII cells were engineered to express doxycycline-inducible/siRNA-insensitive human GSK3b, either wild-type (wt; lanes 1-3) or kinase-dead mutant (KD; lanes 4-6). After depletion of endogenous GSK3 by siRNA transfection (lanes 2, 3, 5 and 6), cells were exposed to 0.5 μg/ml doxycycline to induce the expression of either wt GSK3β (lane 3) or KD GSK3β (lane 6). Lanes 1 and 4 are cells transfected with Control siRNA. *Top panel*: qRT-PCRs for *CTGF* (mean + SD). *Bottom panels*: western blots for TAZ and GSK3. Lane 1 vs. 2 and Lane 4 vs. 5: TAZ is stabilized and activated (CTGF induction) upon GSK3 depletion; lane 3: reconstitution with wt GSK3β rescues the effect of GSK3 depletion; lane 6: reconstitution with KD GSK3β has no effect.

(E) *Top panel*: luciferase assay on 8xGTIIC reporter in HEK293 cells transiently transfected with Control siRNA (lanes 1) or with siRNAs targeting GSK3 (lanes 2-4). Where indicated, constructs encoding siRNA-insensitive GSK3β wt (lane 3) or GSK3β KD (lane 4) were transfected together with the reporter. Data are normalized to lane 1 and bars are mean + SD. *Bottom panel*: western blots for TAZ and GSK3 expression in the same extracts used for the luciferase assay.

(F) Comparison of the GSK3-dependent phosphodegrons of TAZ, β-catenin and other proteins known to be regulated by GSK3 and β-TrCP. Aminoacids essential

for binding to β-TrCP are indicated in red.

(G) GSK3 regulates TAZ independently of its phosphodegron. Lanes 1-2: Western blot for endogenous TAZ shows its stabilization upon GSK3 depletion. Lanes 3-6: MII cells were transfected with TAZ siRNA (to avoid interference from regulations of endogenous TAZ) and reconstituted with siRNA-insensitive mouse TAZ, either wild-type (wt, lanes 3-4) or S58/62A mutant (lanes 5-6). Both wt and S58/62A TAZ are sensitive to GSK3 siRNA.

(H) Wnt activates TAZ independently of its GSK3-phosphodegron. HEK293 cells were transfected with the synthetic 8xGTIIC-Lux reporter. Lanes 1-2: Wnt3A conditioned medium activates the reporter. Lanes 3-4: knockdown of endogenous TAZ abolishes the effect of Wnt. Lanes 5-8: cells were transfected with TAZ siRNA to avoid interference from regulations of endogenous TAZ and reconstituted with either mouse wild-type TAZ (wt, lanes 5-6) or TAZ S58/62A (lanes 7-8). The phosphodegron is irrelevant for TAZ activation by Wnt (lanes 6 and 8). Bars are mean + SD.

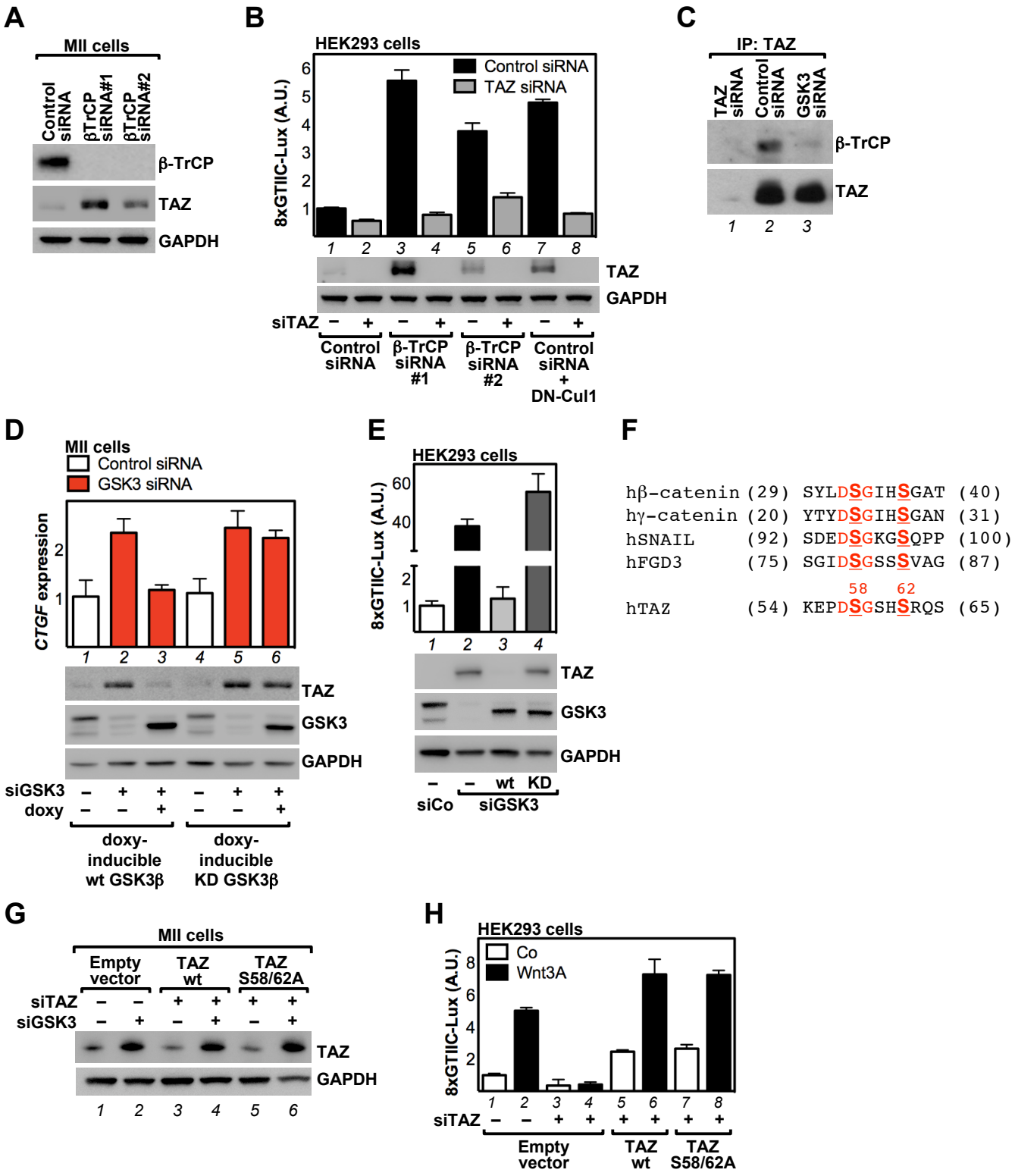
A
MII cells
Control siRNA
βTrCP siRNA#1
βTrCP siRNA#2
β-TrCP
TAZ
GAPDH
B
HEK293 cells
8xGTIIC-Lux (A.U.)
Control siRNA
TAZ siRNA
TAZ
GAPDH
siTAZ
Control siRNA
β-TrCP siRNA #1
β-TrCP siRNA #2
Control siRNA + DN-Cul1
C
IP: TAZ
TAZ siRNA
Control siRNA
GSK3 siRNA
β-TrCP
TAZ
D
MII cells
Control siRNA
GSK3 siRNA
CTGF expression
TAZ
GSK3
GAPDH
siGSK3
doxy
doxy-inducible wt GSK3β
doxy-inducible KD GSK3β
E
HEK293 cells
8xGTIIC-Lux (A.U.)
TAZ
GSK3
GAPDH
siCo
siGSK3
wt
KD
F
hβ-catenin (29) SYLDSGIHSGAT (40)
hγ-catenin (20) YTYDSGIHSGAN (31)
hSNAIL (92) SDEDSGKGSQPP (100)
hFGD3 (75) SGIDSGSSSVAG (87)
58 62
hTAZ (54) KEPDSGSHSRQS (65)
G
MII cells
Empty vector
TAZ wt
TAZ S58/62A
siTAZ
siGSK3
TAZ
GAPDH
H
HEK293 cells
8xGTIIC-Lux (A.U.)
Co
Wnt3A
siTAZ
Empty vector
TAZ wt
TAZ S58/62A

Figure 10

Figure 11. β-catenin mediates TAZ degradation

(A-B) β-catenin associates with TAZ at endogenous protein levels.

(C) β-catenin is required for TAZ interaction with β-TrCP. Endogenous TAZ was immunoprecipitated from lysates of MII cells transfected with Control, β-catenin or TAZ siRNAs, using anti-TAZ antibody, and co-precipitating proteins were detected by western blot.

(D) Endogenous β-catenin is required for TAZ degradation. MII cells were transfected with Control or β-catenin siRNAs. *Top panel*: qRT-PCRs for TAZ target *CTGF*. Bars are mean + SD, normalized to lane 1. *Bottom panels*: western blots for TAZ and β-catenin. GAPDH serves as loading control. *TAZ* mRNA expression wasn't affected by β-catenin depletion (data not shown).

(E) Luciferase assay on 8xGTIIC reporter in HEK293 cells transfected with Control or β-catenin siRNAs, with or without TAZ siRNA. Data are normalized to Control siRNA-transfected cells and bars are mean + SD.

(F) Representative confocal images of TAZ, Scribble and E-cadherin in MII cells transfected with Control or β-catenin siRNAs. Nuclei are stained with Hoechst.

(G) Western blots for total and Serine 909-phosphorylated LATS1 in MII cells transfected with Control or independent β-catenin siRNAs.

(H) Phospho-β-catenin mediates TAZ degradation. MII cells were engineered to express doxycycline-inducible siRNA-insensitive β-catenin, either wild-type (wt; lanes 1-3) or phospho-mutant (S/A, lanes 4-6). After depletion of endogenous β-catenin by siRNA (lanes 2, 3, 5 and 6), cells were treated with 0.5 μg/ml doxycycline to induce the expression of wt (lane 3) or S/A β-catenin (lane 6). Lanes 1 and 4 were cells transfected with Control siRNA. Panels are western blots for TAZ, CTGF and β-catenin. Lane 1 vs. 2, and Lane 4 vs. 5: TAZ is stabilized and activated upon β-catenin depletion; lane 3: reconstitution with wt β-catenin rescues TAZ inhibition; lane 6: S/A β-catenin cannot revert the effect of β-catenin siRNA.

(I) Scheme of the two transcripts (and protein products) encoded by the wild type (wt, black) and exon3/exon4-deleted (del ex3-4, blue) *β-catenin* alleles of HepG2 cells. The phosphodegron site on wild-type β-catenin, missing in the mutant protein, is in orange. The regions of *β-catenin* mRNA targeted by siRNAs are indi-

cated in red: as the sequence targeted by siRNA#4 is within the deletion, this siRNA only hits the wild-type transcripts, whereas siRNA#3 is used to deplete both isoforms.

(J) HepG2 cells were transfected with β-catenin siRNAs indicated in (I), with or without TAZ siRNA. *Top panel*: qRT-PCRs for *CTGF*. Bars are mean + SD, normalized to lane 1. *Bottom panels*: western blots for TAZ and β-catenin.

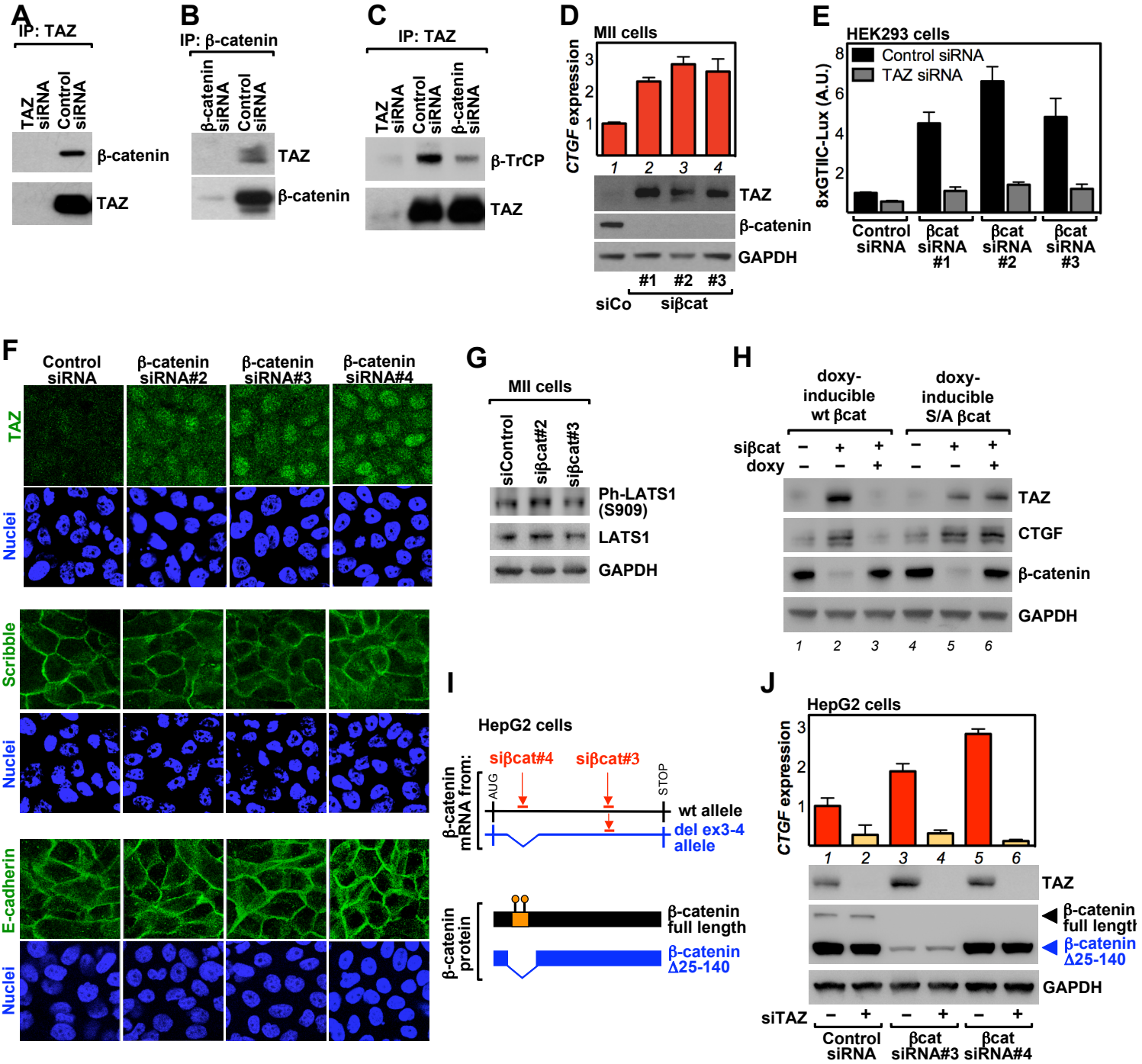
A
IP: TAZ
TAZ siRNA
Control siRNA
β-catenin
TAZ
B
IP: β-catenin
β-catenin siRNA
Control siRNA
TAZ
β-catenin
C
IP: TAZ
TAZ siRNA
Control siRNA
β-catenin siRNA
β-TrCP
TAZ
D
MII cells
CTGF expression
1 2 3 4
TAZ
β-catenin
GAPDH
#1 #2 #3
siCo
siβcat
E
HEK293 cells
Control siRNA
TAZ siRNA
8xGTIIC-Lux (A.U.)
Control siRNA
βcat siRNA #1
βcat siRNA #2
βcat siRNA #3
F
Control siRNA
β-catenin siRNA#2
β-catenin siRNA#3
β-catenin siRNA#4
TAZ
Nuclei
Scribble
Nuclei
E-cadherin
Nuclei
G
MII cells
siControl
siβcat#2
siβcat#3
Ph-LATS1 (S909)
LATS1
GAPDH
H
doxy-inducible wt βcat
doxy-inducible S/A βcat
siβcat
doxy
TAZ
CTGF
β-catenin
GAPDH
1 2 3 4 5 6
I
HepG2 cells
β-catenin mRNA from:
siβcat#4
siβcat#3
AUG
STOP
wt allele
del ex3-4 allele
β-catenin protein
β-catenin full length
β-catenin Δ25-140
J
HepG2 cells
CTGF expression
1 2 3 4 5 6
TAZ
β-catenin full length
β-catenin Δ25-140
GAPDH
siTAZ
Control siRNA
βcat siRNA#3
βcat siRNA#4

Figure 11

Figure 12. The WW domain of TAZ is necessary for the interaction with β-catenin

(A) Schematic representation of GST-TAZ deletion constructs used for the GST-pulldown in (B). TB: TEAD binding domain; TA: Transcriptional Activation domain; PB: PDZ-binding motif.

(B) Autoradiography of *in vitro*-translated ^{35}S-β-catenin pulled-down by the indicated GST-TAZ deletion constructs immobilized on a glutathione-resin. GST protein was used as a negative control. The lane labeled as ''Input'' represents 1/100 of ^{35}S-β-catenin used for the pull down experiments.

(C) Western blot for TAZ in MII cells depleted of endogenous TAZ and transduced with wild-type or ΔWW TAZ. TAZ ΔWW is more stable than the wild-type protein, despite the fact that both the N-terminal (S58 and S62) and the C-terminal (S309) phosphodegrons are not affected by the deletion of the WW domain, as shown in the scheme above the blot (abbreviations are as in A).

(D) The WW domain of TAZ is required for association to β-catenin and β-TrCP. TAZ was immunoprecipitated from lysates of MII cells stably expressing Flag-tagged wild-type or ΔWW TAZ using anti-Flag antibody, and co-precipitating proteins were detected by western blot.

(E) Luciferase assay on 8xGTIIC reporter recording the transcriptional activity of wild-type or ΔWW TAZ transiently transfected in HEK293 cells, in the absence (Co) or presence (Wnt3A) of Wnt stimulation. Cells were transfected with TAZ siRNA to avoid interference from regulations of endogenous TAZ. Data are normalized to lane 1 and are presented as mean + SD. *Bottom panel*: western blots for TAZ in the same extracts used for the luciferase assay.

(F) TAZ ΔWW is phosphorylated at Serine 306. MII cells were depleted of endogenous TAZ and transduced with mouse TAZ (siRNA-insensitive) wild-type, S306A or ΔWW. TAZ was immunoprecipitated with an anti-TAZ antibody and phosphorylation on S306 was detected on the immunoprecipitated protein using a specific antiserum raised in rabbit. TAZ S306A mutant was used as negative control for the antiserum.

(G) TAZ ΔWW is sensitive to LATS inhibition. MII cells depleted of endogenous TAZ were transduced with wild-type, ΔWW or 4SA TAZ, and transfected with Control or LATS siRNAs. TAZ levels were evaluated by western blot.

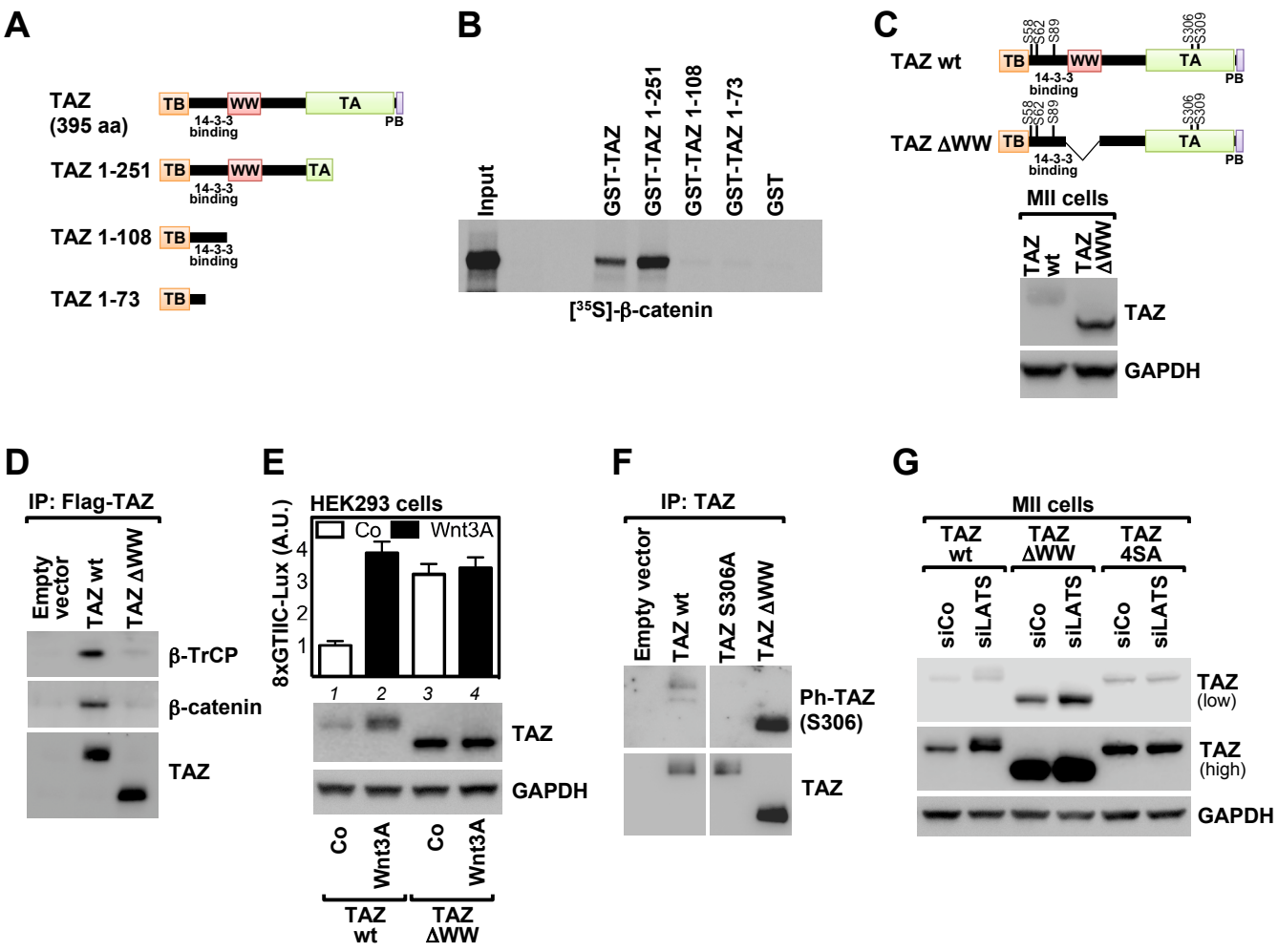
A
TAZ (395 aa)
TB
WW
TA
14-3-3 binding
PB
TAZ 1-251
TAZ 1-108
TAZ 1-73
B
Input
GST-TAZ
GST-TAZ 1-251
GST-TAZ 1-108
GST-TAZ 1-73
GST
[35S]-β-catenin
C
TAZ wt
TAZ ΔWW
S58
S62
S89
S306
S309
MII cells
TAZ wt
TAZ ΔWW
TAZ
GAPDH
D
IP: Flag-TAZ
Empty vector
TAZ wt
TAZ ΔWW
β-TrCP
β-catenin
TAZ
E
HEK293 cells
8xGTIIC-Lux (A.U.)
Co
Wnt3A
1
2
3
4
TAZ
GAPDH
Co
Wnt3A
TAZ wt
TAZ ΔWW
F
IP: TAZ
Empty vector
TAZ wt
TAZ S306A
TAZ ΔWW
Ph-TAZ (S306)
TAZ
G
MII cells
TAZ wt
TAZ ΔWW
TAZ 4SA
siCo
siLATS
TAZ (low)
TAZ (high)
GAPDH

Figure 12

Figure 13. γ-catenin mediates TAZ degradation

(A) Co-immunoprecipitation between endogenous TAZ and γ-catenin in MII cell lysates.

(B) The WW domain of TAZ is required for association to γ-catenin. MII cells stably expressing Flag-tagged wild-type or ΔWW TAZ were cultured at high cell density and then harvested for protein extraction. TAZ was immunoprecipitated from the cell lysates using anti-Flag antibody, and co-precipitating proteins were detected by western blot.

(C) Western blots for TAZ and γ-catenin in extracts from HEK293 cells transfected with Control or γ–catenin siRNA.

(D-E) Luciferase assay on 8xGTIIC reporter in HEK293 cells transfected with Control, β-catenin (siβcat #1 in D or #2 in E) or γ-catenin (siγcat) siRNAs as indicated, with or without TAZ siRNA. Data are normalized to Control siRNA-transfected cells and bars are mean + SD. Similar results were obtained with two different β-catenin or γ-catenin (data not shown) interfering sequences.

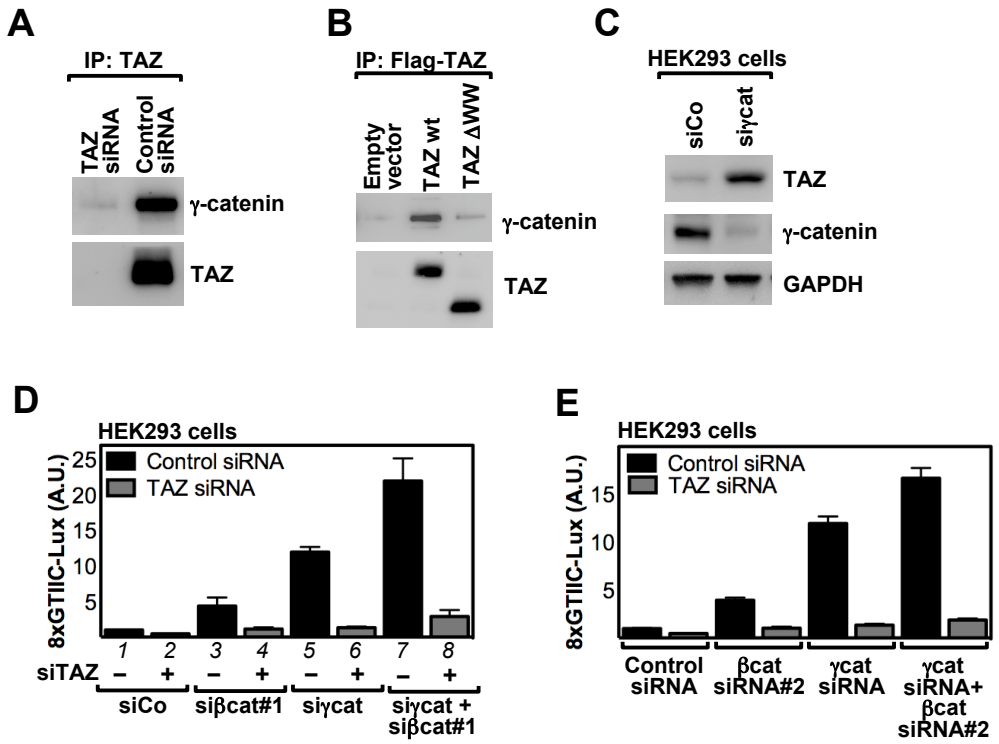
A
IP: TAZ
TAZ siRNA
Control siRNA
γ-catenin
TAZ
B
IP: Flag-TAZ
Empty vector
TAZ wt
TAZ ΔWW
γ-catenin
TAZ
C
HEK293 cells
siCo
siγcat
TAZ
γ-catenin
GAPDH
D
HEK293 cells
Control siRNA
TAZ siRNA
8xGTIIC-Lux (A.U.)
25
20
15
10
5
1 2 3 4 5 6 7 8
siTAZ – + – + – + – +
siCo
siβcat#1
siγcat
siγcat + siβcat#1
E
HEK293 cells
Control siRNA
TAZ siRNA
8xGTIIC-Lux (A.U.)
15
10
5
Control siRNA
βcat siRNA#2
γcat siRNA
γcat siRNA+ βcat siRNA#2

Figure 13

Figure 14. The Wnt pathway and the new perspective on Wnt pathway reported in Part 2

(A) Schematic representation of canonical Wnt pathway.

(B) Schematic representation of the Wnt pathway and the Wnt/TAZ connection that we reported in Part 2.

A

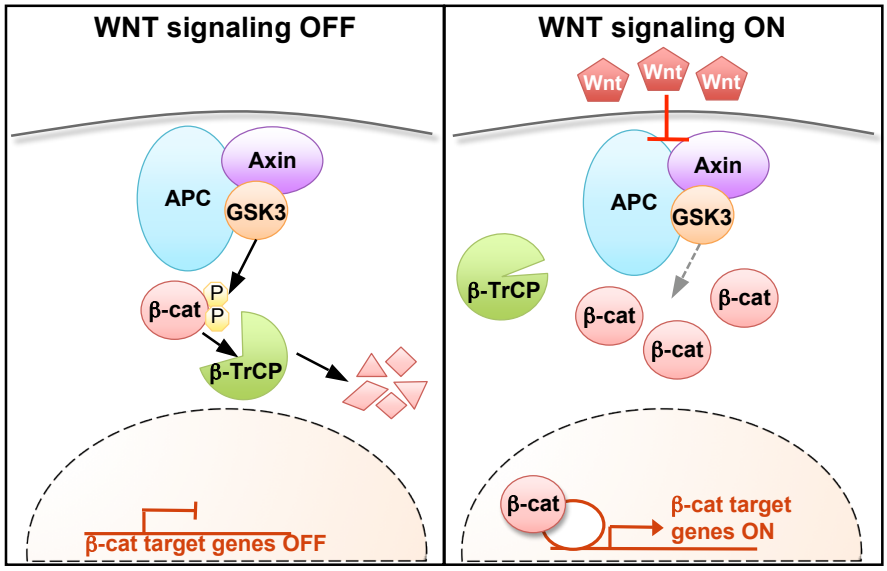
WNT signaling OFF
WNT signaling ON
Axin
APC
GSK3
β-cat
P
P
β-TrCP
Wnt
Wnt
Wnt
β-cat
β-cat
β-cat
β-cat target genes OFF
β-cat
β-cat target genes ON

B

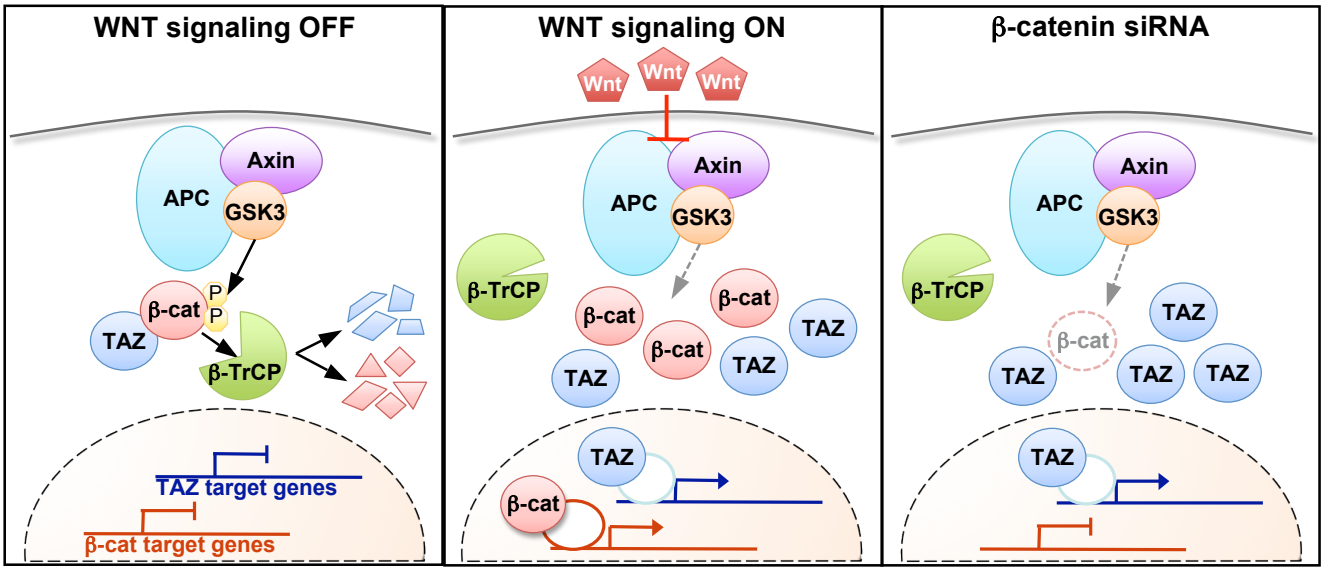
WNT signaling OFF
WNT signaling ON
β-catenin siRNA
Axin
APC
GSK3
β-cat
P
P
TAZ
β-TrCP
Wnt
Wnt
Wnt
β-cat
β-cat
β-cat
TAZ
TAZ
TAZ
TAZ target genes
β-cat target genes
β-cat
TAZ
TAZ
TAZ
TAZ

Figure 14